Ca^{2+} signalling in response to mechanical perturbation and hypo-osmotic shock in *Neurospora crassa*

Peter Marris

Ph.D. Thesis
University of Edinburgh
August 2007

Declaration

This thesis has been composed by myself, and the work of which it is a record has been carried out by myself. All sources of information have been specifically acknowledged by means of reference.

Acknowledgements

I would like to thank my supervisors, Nick Read, for everything that he taught me through the course of this PhD, and Pat Hickey for making this PhD possible.

Most importantly of all I want to thank my parents for their never ending support and for giving me every opportunity I could have ever wished for. To my friends and family, you have helped me through the bad times and made the good times worth remembering for years to come, my deepest and most sincere thanks to you all. Special thanks to Dave, Byron, Robbie and everyone back home, for entertainment, misbehaviour and laughter.

Thanks to everyone from the lab for your friendship and company. In particular I would like to thank Gabriela for her wisdom, Verena for her vibrancy and knowledge, Mari for her encouragement and Kirsten for listening. I must also thank my ipod, a constant companion throughout. For showing me how to use those funny magnifying glasses and for making me laugh when things went wrong I must thank Gray, cheers mate!

Thanks to my collaborators in the defensin work, namely Dilip Shah, Anita Snyder and Rob Spelbrink. For funding, I would like to thank both the BBSRC and Lux Biotechnology. From Lux Biotechnology I want to thank Emma Perfect and Artin Moussavi for their help and for proof reading my thesis.

Finally I would like to thank my undergraduate teachers, Chris Smith and the late John Gallon, for opening my eyes to how fascinating science can be.

Contents

Contents iii

Abstract xi

Abbreviations xiii

Chapter 1 ..... **1**

Introduction 1

1.1 An overview of calcium signalling 3

1.1.1 The calcium transient 3

1.1.2 Induction of the Ca^{2+} transient 3

1.1.3 Removal of Ca^{2+} ions from the cytoplasm 4

1.1.4 Mechanisms by which Ca^{2+} affects a cell 6

1.1.5 Ca^{2+} waves and oscillations 7

1.1.6 Specificity in Ca^{2+} signalling and the Ca^{2+} siganature 8

1.1.6.1 Localization of $[Ca^{2+}]_c$ transients 8

1.1.6.2 The $[Ca^{2+}]_c$ signature 9

1.1.6.3 Input from other signalling systems 9

1.1.6.4 Differentiation of cell types 10
1.2 Fungal Ca^{2+} signalling 10
1.2.1 Ca^{2+} signalling in *Saccharomyces cerevisiae* 10
1.2.1.1 Ca^{2+} permeable channels in *S. cerevisiae* 12
1.2.1.2 Removal of Ca^{2+} from the cytoplasm 14
1.2.1.3 Mediators of Ca^{2+} signalling 15
1.2.1.3.1 Phospholipase C 15
1.2.1.3.2 Calcineurin 16
1.2.2 Ca^{2+} signalling in *Neurospora crassa* 17
1.2.2.1 The roles of Ca^{2+} signalling in *Neurospora crassa* 17
1.2.2.2 The Ca^{2+} signaling machinery of *Neurospora crassa* 20
1.2.3 Ca^{2+} signalling in other filamentous fungi 23
1.3 *Neurospora crassa* as an experimental system 26
1.3.1 Basic characteristics of growth and the cell cycle 26
1.3.2 High throughput generation of *Neurospora crassa* deletion mutants 27
1.4 Measurement of $[Ca^{2+}]_c$ in filamentous fungi 29
1.4.1 Measurment of $[Ca^{2+}]_c$ with Ca^{2+} selective dyes 29
1.4.2 $[Ca^{2+}]_c$ measurement with recombinant aequorin 30
1.5 Involvement of Ca^{2+} signalling in touch sensing and osmotic stress 31
1.5.1 Touch sensing and Ca^{2+} signalling 31
1.5.2 The role of Ca^{2+} in osmotic stress responses 33
1.6 Aims of the work described in the thesis 34

Chapter 2 36

Materials and Methods 36
2.1 Chemicals 36
2.2 Media 36
2.3 Organisms and strains 37
2.4 Plasmids 38
2.5 Culture Media and Growth Conditions 39

2.5.1 Culturing *E. coli* 39
2.5.1.1 Culture media 39
2.5.1.2 Inoculation procedure 39
2.5.1.3 Antibiotics and other selective media 39
2.5.1.4 Types of culture and growth conditions 39
2.5.2 Culturing *N. crassa* 40
2.5.2.1 Culture Media 40
2.5.2.2 Culture Types 40
2.5.2.3 Antibiotics and other selective media 41
2.5.3 Inoculation Procedures 41
2.5.3.1 Stock Cultures 41
2.5.3.2 Microwell Plates set up for 0 h, 6 h and 18 h assays 42
2.5.3.3 Microwell plates set up for aequorin high throughput screen 43
2.6.1 Germination rate determination 43
2.6.2 Measurement of germ tube swelling 44
2.7 In vivo $[Ca^{2+}]_c$ measurement by luminometry 45
2.7.1 Standard luminometry for 0 h, 6 h and 18 h $[Ca^{2+}]_c$ assays 46
2.7.2 Luminometry with chemical treatments 46
2.7.3 Luminometry for high throughput $[Ca^{2+}]_c$ assay 47
2.7.4 Calibration and analysis of luminometer data 47
2.7.4.1 Conversion of luminescence to $[Ca^{2+}]_c$ 47
2.7.4.2 Determining characteristics of the Ca^{2+} response 48
2.8 Transformation and homokaryon purification of *N. crassa* 50
2.8.1 Preparation of conidia for electroporation 50
2.8.2 Electroporation of *N. crassa* 51
2.8.3 Transformant screening and homokaryon purification 52
2.9 Replication, Extraction and Analysis of Plasmid DNA 55
2.9.1 Transforming *E. coli* 55
2.9.2 Extraction of plasmid DNA 55
2.9.3 Determination of DNA concentration 55
2.9.4 Restriction and Analysis of DNA 55

2.9.5 DNA extraction and purification from agarose gels 56
2.9.6 Ethanol Precipitation of DNA 56
2.9.7 Preparation and ligation of DNA 56
2.9.8 *STET* plasmid DNA extraction from *E. coli* 57
2.9.9 Primer design and DNA sequencing 57

Chapter 3 58

Characterization of the $[Ca^{2+}]_c$ and physiological responses to mechanical perturbation 58
3.1 Introduction 58
3.2.1 Refinement of $[Ca^{2+}]_c$ measurement using recombinant codon optimized aequorin 60
3.2.2.1 Dose dependency of the mechanical perturbation response 61
3.2.3 The effects of mechanical perturbation on germ tubes 64
3.2.3.1 Sensitivity of germ tubes to mechanical perturbation 65
3.2.3.2 Measurement of $[Ca^{2+}]_c$ responses at low levels of aequorin expression 67
3.2.3.3 $[Ca^{2+}]_c$ responses of germ tubes to mechanical perturbation, hypo-osmotic shock and high external Ca^{2+} 68
3.2.3.4 Dose-dependency of the $[Ca^{2+}]_c$ response to mechanical perturbation in germ tubes 69
3.2.3.5 Effects of extracellular pH on the $[Ca^{2+}]_c$ response to mechanical perturbation 70
3.2.3.6 Involvement of extracellular Ca^{2+} in the $[Ca^{2+}]_c$ response to mechanical perturbation 71
3.2.3.7 Physiological response of germ tubes to mechanical perturbation – the hyphal swelling assay 74
3.2.5 Conidial response to mechanical perturbation 76
3.3 Discussion 80
3.3.1 Germ tubes provide a sensitive and reliable population for $[Ca^{2+}]_c$ assays 80
3.3.2 $[Ca^{2+}]_c$ responses to mechanical perturbation and hypo-osmotic shock 80

3.3.3 Germ tubes respond to mechanical perturbation by Ca^{2+} dependent apical swelling 81
3.3.4 Summary of results 82

Chapter 4 ..... **83**

Effects of antifungal proteins on the $[Ca^{2+}]_c$ responses to mechanical perturbation and hypo-osmotic shock 83
4.1 Introduction 83
4.2.1 Effects of MsDef1 on the $[Ca^{2+}]_c$ responses to mechanical perturbation and hypo-osmotic shock 86
4.2.3 Effects of MtDef4 on the $[Ca^{2+}]_c$ responses to mechanical perturbation and hypo-osmotic shock 88
4.2.4 Effects of RsAFP2 on the $[Ca^{2+}]_c$ responses to mechanical perturbation and hypo-osmotic shock 89
4.2.5 Effects of KP4 on the $[Ca^{2+}]_c$ responses to mechanical perturbation and hypo-osmotic shock 90
4.2.6 Comparison of defensin effects on the $[Ca^{2+}]_c$ responses to mechanical perturbation and hypo-osmotic shock 91
4.3 Discussion 92
4.3.2 Mechanical perturbation and hypo-osmotic shock 93
4.3.3 Mechanism of antifungal protein action 94
4.4 Summary 95

Chapter 5 ..... **97**

Investigation of the Ca^{2+} signalling machinery involved in the responses to mechanical perturbation and hypo-osmotic shock 97
5.2 Results 99
5.2.1 Transformation of *Neurospora* wt 74A and deletion mutants with pAB19 99
5.2.3 Use of elevated coelenterazine concentrations in deletion mutants transformed with aequorin 99

5.2.4 Involvement of CPCs in the $[Ca^{2+}]_c$ responses to mechanical perturbation and hypo-osmotic shock 101
5.2.4.1 Δ*yvc* caused an increased $[Ca^{2+}]_c$ amplitude in response to mechanical perturbation and hypo-osmotic shock 101
5.2.4.2 MID-1 is involved in the $[Ca^{2+}]_c$ responses to mechanical perturbation and hypo-osmotic shock 102
5.2.4.2 The MID-1 protein is involved in the germ tube swelling response to mechanical perturbation 104
5.2.4.3 L-type Ca^{2+} channel activity may be involved in the $[Ca^{2+}]_c$ responses to mechanical perturbation and hypo-osmotic shock 105
5.2.5 Involvement of cation ATPases in the $[Ca^{2+}]_c$ responses to mechanical perturbation and hypo-osmotic shock 106
5.2.5.3 SERCA type Ca^{2+} ATPase activity is involved in the $[Ca^{2+}]_c$ responses to mechanical perturbation and hypo-osmotic shock 106
5.2.5.1 PH-7 and ENA-1 are involved in the $[Ca^{2+}]_c$ responses to mechanical perturbation and hypo-osmotic shock 108
5.2.6 Role of CAX in the $[Ca^{2+}]_c$ responses to mechanical perturbation and hypo-osmotic shock 109
5.3 Conclusions 111
5.3.1 CPCs are involved in the $[Ca^{2+}]_c$ and swelling responses to mechanical perturbation 111
5.3.1.2 Roles for MID-1 and CCH-1 111
5.3.1.2 Role for YVC 112
5.3.2 Removal of Ca^{2+} from the cytoplasm 113
5.3.2.1 Role for NCA-1 113
5.3.2.2 Roles for ENA-1 and PH-7 113
5.3.3 Specificity of $[Ca^{2+}]_c$ responses to mechanical perturbation and hypo-osmotic shock 114
5.4 Summary 115

Chapter 6 ..... **116**

Development of the aequorin $[Ca^{2+}]_c$ assay for use as a high throughput screen to identify novel antifungal agents 117

6.1 Introduction 117

6.2.1 Optimization of experimental procedure 119

6.2.1.1 Development of assay method 119

6.2.1.2 Discharge calibration for high throughput assay 121

6.2.1.3 The effects of reducing the number of wells per sample for the high throughput assay 123

6.2.1.4 Development of a Microsoft Excel™ worksheet for calibration of $[Ca^{2+}]_c$ ..125

6.2.2 The use of the high through put $[Ca^{2+}]_c$ assay 126

6.2.2.2 Blind testing of unknown compounds using the high throughput assay 130

6.3 Discussion 135

6.3.1 Increase in throughput of the aequorin $[Ca^{2+}]_c$ assay..... 135

6.3.2 Sensitivity of the aequorin high throughput assay 136

6.4 Summary 137

Chapter 7 ..... **138**

Summary and future work 138

Appendix A **143**

Media and Solutions 143

Appendix B **148**

Plasmid Maps 148

Bibliography 151

Abstract

In the natural environment, filamentous fungi respond to a range of mechanical stimuli (e.g. physical surfaces, obstacles, microtopographical features, compression and shaking) and osmotic stresses which elicit various growth and developmental responses. There is a growing body of evidence that the responses of filamentous fungi to both mechanical and osmotic stimuli involve Ca^{2+} signalling.

The aims of this research were to analyze the Ca^{2+} and physiological responses to mechanical perturbation and hypo-osmotic shock in *Neurospora crassa*. Cytosolic free Ca^{2+} concentration ($[Ca^{2+}]_c$) was measured by expression of codon optimized aequorin in wild type and deletion mutants in which genes encoding different components of the Ca^{2+} signalling machinery had been deleted.

The $[Ca^{2+}]_c$ responses of germ tubes, vegetative hyphae and conidia were characterized. Ca^{2+} signatures produced in response to mechanical perturbation or hypo-osmotic shock were analysed to identify which components of the Ca^{2+} signalling machinery were responsible for generating these signatures. The involvement of multiple proteins in the $[Ca^{2+}]_c$ responses to mechanical perturbation and hypo-osmotic shock of germ tubes was identified. The Ca^{2+} signature and germ tube swelling produced in response to

mechanical perturbation were both dependent on the influx of external Ca^{2+} and the MID1 mechanosensory protein.

The plant antifungal proteins (defensins), MsDef1, RsAFP2, MtDef2, and MtDef4, were all found to have distinct, stimulus-specific effects on the $[Ca^{2+}]_c$ responses to mechanical perturbation and hypo-osmotic shock. The mycovirus antifungal protein KP4 exhibited no inhibitory effect on the $[Ca^{2+}]_c$ response to either stimulus. This analysis provided the basis for the development of a high throughput assay for the discovery of antifungal compounds that target Ca^{2+} signalling and homeostasis.

Abbreviations

aeqS	codon optized aequorin gene
bar	ignite resistance gene
$[Ca^{2+}]$	Ca^{2+} concentration
$[Ca^{2+}]_c$	free cytosolic Ca^{2+} concentration
$[Ca^{2+}]_{mit}$	Mitochondrial Ca^{2+} concentration
cADPR	cyclic ADP ribose
CaM	calmodulin
CAMK	Ca^{2+}/calmodulin dependent protein kinase
cAMP	cyclic 3',5'-adenosine monophosphate
CDPK	Ca^{2+} dependent protein kinase
CDRE	Ca^{2+} dependent response element
cGMP	cyclic 3',5'-guanosine monophosphate
CICR	Ca^{2+} induced Ca^{2+} release
CPA	cyclopiazonic acid

CPC	Ca^{2+} permeable channel
CTC	chlortetracycline
DAG	diacylglycerol
dH_2O	distilled water
DMSO	dimethyl sulfoxide
DNA	deoxyribonucleic acid
ER	endoplasmic reticulum
FGSC	Fungal Genetics Stock Centre
FWHM	full width at half maximum amplitude
g	gram
GFP	Green Fluorescent Protein
h	hour
H_2O_2	hydrogen peroxide
HACS	high affinity Ca^{2+} uptake system
HTS	high throughput screen
hygR	hygromycin phosphotransferase gene
Hyg B	hygromcyin B
$InsP_3$	Inositol-1,4,5-trisphosphate
$InsP_3R$	Inositol-1,4,5-trisphosphate receptor
kb	kilo base pairs
l	litre
LACS	low affinity Ca^{2+} uptake system
m	metre
M	molar
MAPK	mitogen activate protein kinase
min	minute
NAADP	nicotinic acid dinucleotide phosphate
ORF	open reading frame
PMCA	plasma membrane Ca^{2+} ATPases
PIP_2	phosphatidyl inositol-4,5-bisphosphate
PKA	protein kinase A

PKC	protein kinase C
PLC	phospholipase C
psi	pounds per square inch
RIP	repeat induced point mutation
RLU	relative light units
rpm	revolutions per minute
RYR	ryanodine receptor
s	second
S1P	sphingosine-1-phosphate
SERCA ATPases	sarco/endoplasmic reticulum Ca^{2+} ATPases
SR	sarcoplasmic reticulum
SV	slowly activating vacuolar channels
TRP	Transient receptor potential
VgS media	Vogel's synthetic media
wt	wild type

Chapter 1

Introduction

In the natural environment organisms are subjected to a wide range of changing conditions and stimuli. To survive and grow successfully they must adapt and respond to these changes in their surroundings. Sensing of and responding to stimuli are mediated by signal transduction cascades. All signal transduction cascades are composed of several key elements. A stimulus is perceived by a receptor which then acts to alter the activity of one or more enzymes responsible for coordination of the response to the stimulus. The activation of a target enzyme by the receptor may occur directly, if they are in close proximity, or commonly the receptors alter the concentration of one or more second messengers. Second messenger molecules then diffuse across the cell to activate target enzymes. The signal transduction cascade must be tightly regulated to prevent unwanted or prolonged activation leading to unnecessary expenditure of resources.

Ca^{2+} ions have been identified to act as a second messenger in a huge range of different organisms from bacteria to higher eukaryotes (Berridge *et al.*, 2000; Michiels *et al.*, 2002; Sanders *et al.*, 2002; Berridge *et al.*, 2003; Dominguez, 2004). In mammalian cells Ca^{2+} is believed to be the most important intracellular messenger discovered so far based on its involvement in, and regulation of almost all known cellular functions and reactions (Brini and Carafoli, 2000; Dominguez, 2004; Petersen *et al.*, 2005). In plants, Ca^{2+} responses are involved in a wide range of environmental, developmental and growth stimuli in a broad range of tissues and cell types (Sanders *et al.*, 2002; Scrase-Field and Knight, 2003; Ng and McAinsh, 2003).

The reasons for calcium acting as a second messenger in so many systems are related to its cellular toxicity. Ca^{2+} ions bind to orthophosphate forming an insoluble product reducing the availability of orthophosphate for cellular energy metabolism (Sanders *et al.*, 1999). In the early stages of evolution organisms living in seawater would have been required to develop mechanisms to maintain free cytosolic Ca^{2+} concentration ($[Ca^{2+}]_c$) at a level far below the millimolar concentrations of their surroundings (Sanders *et al.*, 1999). This strict regulation of concentration is a key requirement for any second messenger. Generation and maintenance of a large concentration gradient facilitates rapid increases in $[Ca^{2+}]_c$, another key feature for a second messenger (Sanders *et al.*, 1999; Brini *et al.*, 2000). The second messenger potential of Ca^{2+} ions is further increased by the capacity of Ca^{2+} to be coordinated to multiple ligands, namely 6 – 8 negatively charged or uncharged oxygen atoms. This enables Ca^{2+} ions to cross link different segments of a protein and induce large conformational changes (Stryer, 1997). The benefits of Ca^{2+} ions compared to a potential competitor, such as Mg^{2+}, are further enhanced by their affinity for oxygen which facilitates highly specific binding. Ca^{2+} ions can form large asymmetric complexes whereas Mg^{2+} ions demand perfectly octahedral cavities not found in proteins (Brini *et al.*, 2000). These properties make Ca^{2+} ions well suited for binding irregularly shaped crevices in proteins and allow it to be selected over Mg^{2+} even when Mg^{2+} is in far greater abundance (Stryer, 1997).

1.1 An overview of calcium signalling

1.1.1 The calcium transient

The basic unit of calcium signalling is a temporary increase in the $[Ca^{2+}]_c$, known as a calcium transient. Calcium transients are composed of two main phases: a period of $[Ca^{2+}]_c$ increase, where influx of Ca^{2+} into the cytoplasm predominates, and a second phase in which the removal of free Ca^{2+} from the cytoplasm exceeds the level of Ca^{2+} influx. Ca^{2+} ions enter the cytoplasm primarily through Ca^{2+} permeable channels (CPCs) resulting in elevated $[Ca^{2+}]_c$. Increased $[Ca^{2+}]_c$ activates Ca^{2+} pumps, Ca^{2+} exchangers, Ca^{2+} binding proteins and this, combined with cytoplasmic buffering, returns $[Ca^{2+}]_c$ to the resting level (Berridge *et al.*, 2000; Sanders *et al.*, 2002; Berridge *et al.*, 2003). The shape, or signature, of the $[Ca^{2+}]_c$ transient is defined by the activities of all factors involved in the response to a specific stimulus. The $[Ca^{2+}]_c$ transient may activate a broad range of enzymes either directly, or indirectly via binding of Ca^{2+} ions to calmodulin (CaM) leading to regulation of a wide range of physiological processes (Berridge *et al.*, 2000; Sanders *et al.*, 2002; Berridge *et al.*, 2003).

1.1.2 Induction of the Ca^{2+} transient

Influx of Ca^{2+} ions into the cytoplasm may originate from either intracellular Ca^{2+} stores or from external sources of Ca^{2+}. Ca^{2+} entry from the external environment is driven by the large electrochemical gradient across the plasma membrane and may occur via many different Ca^{2+} selective channels in animals or non specific CPCs in plants (Sanders *et al.*, 1999; Berridge *et al.*, 2000; Sanders *et al.*, 2002; Berridge *et al.*, 2003; Hetherington and Brownlee, 2004). Plasma membrane Ca^{2+} channels are activated by diverse stimuli including membrane depolarization, binding of hormones or intracellular messengers and mechanical stretching (Berridge *et al.*, 2000; Berridge *et al.*, 2003).

Mammalian intracellular Ca^{2+} stores are contained within the endoplasmic or sarcoplasmic reticulum (ER/SR), the mitochondria and the Golgi (Berridge *et al.*, 2000; Dolman and Tepikin, 2006). Release of Ca^{2+} from endoplasmic or sarcoplasmic reticulum is principally modulated by Ca^{2+} in the process of Ca^{2+} induced Ca^{2+} release (CICR) (Berridge *et al.*, 2000). In CICR $[Ca^{2+}]$ on either side of the ER/SR membrane may alter the sensitivity of different receptors. This sensitivity to activation by Ca^{2+} ions is further modulated by the binding of Ca^{2+} mobilizing second messengers generated by activation of cell surface receptors. The inositol-1,4,5-trisphosphate receptor ($InsP_3R$, activated by Inositol-1,4,5-trisphosphate ($InsP_3$)) and the ryanodine receptor families (RYR, activated by cyclic ADP ribose (cADPR)) are the most studied examples of these channels. Other second messengers acting on, currently unidentified, Ca^{2+} channels are nicotinic acid dinucleotide phosphate (NAADP) and sphingosine-1-phosphate (S1P) (Berridge *et al.*, 2000).

Intracellular Ca^{2+} stores in plant cells include the ER, vacuoles, nucleus, the chloroplasts, and the mitochondria (Sanders *et al.*, 1999; Sanders *et al.*, 2002; Xiong *et al.*, 2006). Vacuolar CPCs may be activated by $InsP_3$, cADPR, membrane hyperpolarization and membrane depolarization. The Ca^{2+} activation of slowly activating vacuolar (SV) channels led to identification of CICR in plants (Sanders *et al.*, 2002). Despite much functional evidence for $InsP_3$, cADPR and NAADP activated Ca^{2+} channels no obvious homologues of the mammalian genes have been identified (Hetherington *et al.*, 2004).

1.1.3 Removal of Ca^{2+} ions from the cytoplasm

The second stage of a $[Ca^{2+}]_c$ transient is the removal of Ca^{2+} ions from the cytoplasm. Ca^{2+} ions entering the cytoplasm are rapidly bound to a large range of cytosolic Ca^{2+} buffers such as parvalbumin, calbindin-D_{28K} and calretinin (Berridge *et al.*, 2000; Berridge *et al.*, 2003). Buffers bind Ca^{2+} ions in the influx phase of a $[Ca^{2+}]_c$ transient and unload Ca^{2+} ions during the efflux phase, and by doing so may shape the $[Ca^{2+}]_c$ transient (Sanders *et al.*, 1999; Berridge *et al.*, 2000; Berridge *et al.*, 2003). These proteins are

important in generating the cytoplasmic Ca^{2+} buffering capacity which varies in activity between different cell types. The small proportion of Ca^{2+} ions that remain unbound increase $[Ca^{2+}]_c$ which activates 5 different pumping mechanisms that remove Ca^{2+} from the cytoplasm of mammalian cells (Berridge *et al.*, 2000; Berridge *et al.*, 2003). These mechanisms include the plasma membrane Ca^{2+} ATPases (PMCA), ER / SR reticulum Ca^{2+} ATPases (SERCA ATPases), Na^+/Ca^{2+} exchangers and Ca^{2+} ATPases present in the Golgi membrane (Berridge *et al.*, 2000; Dolman *et al.*, 2006). The fifth mechanism of Ca^{2+} removal in mammalian cells involves Ca^{2+} uptake by mitochondria. Mitochondria accumulate very large amounts of Ca^{2+} via Ca^{2+} pumps. Buffers in the mitochondrial matrix then prevent large elevation in $[Ca^{2+}]_{mit}$ (Berridge *et al.*, 2000; Pozzan *et al.*, 2000; Berridge *et al.*, 2003). Once resting $[Ca^{2+}]_c$ is restored mitochondria unload the accumulated Ca^{2+} by the action of a Na^+/Ca^{2+} exchanger (Berridge *et al.*, 2000). The diverse range of different Ca^{2+} pumps and exchangers is supplemented by different characteristics of activation by $[Ca^{2+}]_c$ (Berridge *et al.*, 2003). Variations in different Ca^{2+} transporters and buffering give the potential for a huge range of different Ca^{2+} uptake systems.

Ca^{2+} removal in plants is similar to mammalian cells but involves different classes of proteins. A range of ATPases transport Ca^{2+} ions into the ER, the vacuole, mitochondria and chloroplasts, across the plasma membrane and a range of other endomembranes (Sanders *et al.*, 1999; Xiong *et al.*, 2006). Vacuoles are the most prominent Ca^{2+} sink in plant cells due to their size and capacity for Ca^{2+} accumulation. Plant cells do not possess Na^+/Ca^{2+} antiporters, but instead have a range of Ca^{2+}/H^+ antiporters localized primarily to the vacuole (Sanders *et al.*, 2002). Ca^{2+} transporters have been less studied in plant cells than in animal cells. However there is growing evidence that their activity may be regulated (Sanders *et al.*, 2002; Hetherington *et al.*, 2004) and may influence signal transduction (Sanders *et al.*, 1999).

In addition to its role in the termination of $[Ca^{2+}]_c$ transients, sequestration of Ca^{2+} into organellar Ca^{2+} stores provides Ca^{2+} for release in response to external stimuli (Sanders *et al.*, 1999; Sanders *et al.*, 2002). Ca^{2+} is also required to support specific organellar

functions such as protein folding in the ER and the passage of proteins along the secretory pathway (Sanders *et al.*, 1999; Sanders *et al.*, 2002; Dolman *et al.*, 2006).

1.1.4 Mechanisms by which Ca^{2+} affects a cell

Elevated $[Ca^{2+}]_c$ increases binding of Ca^{2+} ions to numerous Ca^{2+} sensor proteins such as troponin C and, most commonly, CaM (Sanders *et al.*, 1999; Berridge *et al.*, 2000). Conformational changes induced by Ca^{2+} binding activate effector proteins directly or via activation of Ca^{2+} sensor proteins. Activation of downstream effectors can then influence a very diverse range of processes in both plant and animal cells (Berridge *et al.*, 2000; Sanders *et al.*, 2002; Petersen *et al.*, 2005).

Ca^{2+} ions affect protein phosphorylation via Ca^{2+}/CaM dependent protein kinases (CAMKs) (Cruzalegui and Bading, 2000). In plants a unique family of Ca^{2+} dependent protein kinases (CDPKs) have been identified which contain Ca^{2+} binding CaM like regulatory domains (Sanders *et al.*, 1999; Sanders *et al.*, 2002). In both animal and plant cells Ca^{2+} has been found to regulate the activity of protein phosphates such as the conserved protein phosphatase calcineurin (Sanders *et al.*, 1999). Activated calcineurin can influence transcription via regulation of numerous Ca^{2+} activated transcription factors. Interaction with other protein phosphorylation cascades such as mitogen activated protein kinase (MAPK) cascades may lead to even more wide ranging effects of a $[Ca^{2+}]_c$ transient (Berridge *et al.*, 2000; Cruzalegui *et al.*, 2000).

The potential influence of $[Ca^{2+}]_c$ transients on signal transduction is enhanced by widespread interactions with other signalling pathways (Berridge *et al.*, 2000). Ca^{2+} activated adenylyl cyclase or cAMP phosphodiesterase may alter [cAMP]. cAMP levels can then feed back to the Ca^{2+} system by modulating the activities of Ca^{2+} channels and pumps. Nitric oxide synthase is activated by the binding of Ca^{2+}. Increased levels of nitric oxide diffuse into local cells activating guanylyl cyclase to increase [cGMP]. cGMP may modulate activity of Ca^{2+} channels and pumps (Berridge *et al.*, 2000).

Phosphatidylinositol-3-OH kinase may influence $[Ca^{2+}]_c$ via modulation of $InsP_3$ levels within a cell. In addition to feed back via cyclic nucleotide signalling, Ca^{2+} ions can alter production and catabolism of $InsP_3$ via phospholipase C (PLC) or $Ins(1,4,5)P_3$ kinase (Berridge *et al.*, 2000). Self feedback of Ca^{2+} signalling also occurs by modulation of Ca^{2+} pump and channel activity by Ca^{2+} binding (Berridge *et al.*, 2000). Another important regulator of Ca^{2+} signalling is the cellular oxidation state which, either directly or indirectly modulates the activity of all the major components of the mammalian Ca^{2+} signalling machinery (Davidson and Duchen, 2006).

1.1.5 Ca^{2+} waves and oscillations

In mammalian cells the versatility of Ca^{2+} signalling is further enhanced by spatial and temporal variation in $[Ca^{2+}]_c$ (Berridge *et al.*, 2000; Berridge, 2006). Ca^{2+} transients may range from influx via a single channel to coordinated opening of clusters of Ca^{2+} channels. These signalling events may function within highly localized regions of a cell or may become part of an intracellular Ca^{2+} wave. When Ca^{2+} channel receptors are sufficiently sensitive, the diffusion of Ca^{2+} from one cluster of activated channels may lead to activation of another cluster of channels. This self propagation can spread to additional clusters of Ca^{2+} channels, potentially leading to generation of a $[Ca^{2+}]_c$ wave. Where cells are connected by gap junctions, intracellular Ca^{2+} waves may spread to neighbouring cells leading to intercellular Ca^{2+} waves capable of coordinating the activity of many cells (Berridge *et al.*, 2000). The unitary $[Ca^{2+}]_c$ signalling events characterized in detail in mammalian systems have recently begun to be revealed in plant Ca^{2+} signalling (Ng *et al.*, 2003). A range of different elemental events that are capable of combining to form Ca^{2+} waves have been observed in plants that are similar to those in mammalian systems (Mahlo *et al.*, 1998; Ng *et al.*, 2003).

Further diversity in $[Ca^{2+}]_c$ signals may arise from repeated oscillations in $[Ca^{2+}]_c$. Although individual $[Ca^{2+}]_c$ transients trigger many cellular responses, longer periods of signalling may involve multiple $[Ca^{2+}]_c$ transients. There is massive variation in the

frequency of these oscillations ranging from 1 – 60 seconds up to 24 hours. To decode signals encoded by multiple oscillations two proteins have been found to have particular importance, namely CAMKII and protein kinase C (PKC). Frequency encoding of Ca^{2+} signals has been identified in various processes including liver metabolism, smooth muscle contractility and differential gene transcription, particularly in developing systems (Berridge *et al.*, 2000). The ability of cells to respond differently to specific oscillations has a key role in the specificity of Ca^{2+} signalling.

1.1.6 Specificity in Ca^{2+} signalling and the Ca^{2+} signature

1.1.6.1 Localization of $[Ca^{2+}]_c$ transients

A fundamental question with regards to Ca^{2+} signalling is how one signalling mechanism can generate a huge range of different responses. Spatial aspects of Ca^{2+} signalling have a significant role in the generation of specificity (Berridge, 2006). Ca^{2+} ions entering the cytoplasm diffuse a small distance from the initial site of influx, thus restricting their influence within a cell (Berridge, 2006). If the presence of different Ca^{2+} sensitive processes varies with subcellular location, localized Ca^{2+} signals may only activate processes within the area of increased $[Ca^{2+}]$. Ca^{2+} signalling components can be organized into macromolecular complexes, known as Ca^{2+} microdomains, that are capable of functioning independently in mammals and possibly in plants too (Berridge *et al.*, 2003; Ng *et al.*, 2003). Where Ca^{2+} microdomains are multiplied or mixed with different Ca^{2+} signalling units more diverse signalling systems may be created. $[Ca^{2+}]_c$ responses over larger scales can be coordinated by Ca^{2+} waves (section 1.1.5) which may spread throughout many cells or be highly localized to specific regions (Berridge *et al.*, 2003).

In plant cells the specificity of Ca^{2+} signalling is intimately linked to generation of specific patterns of Ca^{2+} elevation (Sanders *et al.*, 2002; Ng *et al.*, 2003). Separate cytosolic and distinct nuclear elevations of $[Ca^{2+}]$ may regulate different processes in

plants (Pauly *et al.*, 2001; Sanders *et al.*, 2002) and the multicellular alga *Fucus* (Sanders *et al.*, 2002). The existence of distinct nuclear [Ca^{2+}] elevations that are independent of changes in [Ca^{2+}]$_c$ has received intensive study but is the source of much controversy (Bootman *et al.*, 2000; Brini *et al.*, 2000). Despite this, there is still a large body of evidence indicating differential Ca^{2+} signalling in the nuclei of animal cells (Bootman *et al.*, 2000). [Ca^{2+}]$_c$ waves have also been described in *Fucus* but not in other plant cells (Sanders *et al.*, 2002).

1.1.6.2 The [Ca^{2+}]$_c$ signature

The spatial and temporal characteristics of stimulus specific Ca^{2+} transients are known as their Ca^{2+} signatures (Scrase-Field *et al.*, 2003). In the Ca^{2+} signature hypothesis a particular Ca^{2+} signature will trigger a particular response while a different Ca^{2+} signature will not trigger the same response. This hypothesis has become accepted within animal cell signalling however the existence of this mechanism within all plant cells has been strongly questioned. An alternative hypothesis was proposed in which [Ca^{2+}]$_c$ acts as a switch where elevation of [Ca^{2+}]$_c$ past a threshold level initiates a downstream response (Scrase-Field *et al.*, 2003). However, there is still strong support for the signature hypothesis in plant cells and the mechanisms of interpreting Ca^{2+} signals await resolution (Sanders *et al.*, 1999; Scrase-Field *et al.*, 2003; Ng *et al.*, 2003).

1.1.6.3 Input from other signalling systems

In cells where the calcium switch hypothesis functions, the overall outcome of a stimulus may be determined by the balance and interactions of Ca^{2+} signalling with other signal transduction pathways (Mahlo *et al.*, 1998; Scrase-Field *et al.*, 2003). This idea leads to specificity being defined by signalling cascades other than Ca^{2+}.

1.1.6.4 Differentiation of cell types

Specificity may arise from the presence of the appropriate Ca^{2+} signalling machinery or specific downstream elements. Differentiation in particular, may give rise to cell types expressing different Ca^{2+} modulating, sensing or response elements for interpretation of a Ca^{2+} signal (Berridge *et al.*, 2000; Sanders *et al.*, 2002; Berridge *et al.*, 2003). There is a huge variety of different $[Ca^{2+}]_c$ modulating proteins with different characteristics, such as methods of activation, rates of transport and differential localization. Variation in the characteristics of individual proteins is further expanded by alternative splicing which leads to formation of different isomers with subtly different properties (Berridge *et al.*, 2003). Different proteins may lead to incredible degrees of variation in the properties of a $[Ca^{2+}]_c$ transient potentially facilitating differentiation of separate signals by interpretation of the $[Ca^{2+}]_c$ signature. Differential expression of other pathways in different cell types or locations within a cell may alter the nature and levels of these interactions (Sanders *et al.*, 2002).

The combined features and differences in the Ca^{2+} signalling machinery enable incredible versatility in the processes controlled by this mechanism and contribute to its ever growing significance in the cellular signalling of many organisms.

1.2 Fungal Ca^{2+} signalling

1.2.1 Ca^{2+} signalling in *Saccharomyces cerevisiae*

Of all fungal species, the mechanisms of Ca^{2+} signalling have been studied in the greatest detail in *Saccharomyces cerevisiae* (budding yeast). In *S. cerevisiae* Ca^{2+} signalling is involved in a wide range of important physiological responses Table 1.1.

Table 1.1. Responses involving Ca^{2+} signalling in *S. cerevisiae.*

Stimulus	References
Glucose re-addition to starved cells	Nakajima-Shimada *et al.*, 1991; Cunningham and Fink, 1996; Batiza *et al.*, 1996; Coccetti *et al.*, 1998; Tisi *et al.*, 2002; Tokes-Fuzesi *et al.*, 2002; Yoshimura *et al.*, 2004; Kellermayer *et al.*, 2004; Tropia *et al.*, 2006
Response to mating pheromone	Iida *et al.*, 1994; Fischer *et al.*, 1997; Paidhungat and Garrett, 1997; Locke *et al.*, 2000; Muller *et al.*, 2001; Muller *et al.*, 2003
Hypo-osmotic shock	Batiza *et al.*, 1996; Loukin *et al.*, 2007
Hyper-osmotic shock	Matsumoto *et al.*, 2002; Denis and Cyert, 2002; Zhou *et al.*, 2003
High external calcium	Miseta *et al.*, 1999a; 1999b; Forster and Kane, 2000
Alkaline stress	Serrano *et al.*, 2002; Viladevall *et al.*, 2004
Antifungal treatment	Edlind *et al.*, 2002; Courchesne and Ozturk, 2003
Cold shock	Batiza *et al.*, 1996; Peiter *et al.*, 2005
Iron toxicity	Peiter *et al.*, 2005
Endoplasmic reticulum stress	Cronin *et al.*, 2002; Bonilla and Cunningham, 2003
Salt tolerance	Mendoza *et al.*, 1996; Matheos *et al.*, 1997; Stathopoulos and Cyert, 1997; Matsumoto *et al.*, 2002
Salicylic acid	Mori *et al.*, 1998

Much of the focus of the research into the Ca^{2+} signalling of budding yeast has centred on the proteins that may be responsible for generating the Ca^{2+} transient summarized in Table 1.2.

Table 1.2 Calcium signalling proteins in *S. cerevisiae*

Protein Class	Protein name	References
Ca^{2+} permeable channel	Cch1p	Fischer *et al.*, 1997; Paidhungat *et al.*, 1997
	Mid1p	Iida *et al.*, 1994
	Yvc1p	Palmer *et al.*, 2001
Ca^{2+} ATPase	Pmc1p	Cunningham and Fink, 1994
	Pmr1p	Rudolph *et al.*, 1989
Ca^{2+}/H^{+} exchanger	Vcx1p	Cunningham *et al.*, 1996
Calmodulin	Cmd1p	Davis *et al.*, 1986
Calcineurin A (catalytic subunit)	Cna1p, Cna2p	Cyert *et al.*, 1991
Calcineurin B (regulatory subunit)	Cnb1p	Kuno *et al.*, 1991
Calcineurin activated transcription factor	Crz1p / Tcn1p	Matheos *et al.*, 1997; Stathopoulos *et al.*, 1997
Calcineurin binding protein	Rcn1p	Kingsbury and Cunningham, 2000
CaM dependent protein kinase	Cmk1p, Cmk2p	Cyert, 2001
Calnexin	Cne1p	De Virgilio *et al.*, 1993
Phospholipase C	Plc1p	Flick and Thorner, 1993; Payne and Fitzgerald-Hayes, 1993; Yoko-o *et al.*, 1993

1.2.1.1 Ca^{2+} permeable channels in *S. cerevisiae*

Three CPCs have been identified in *S. cerevisiae* (Table 1.2; Iida *et al.*, 1994; Fischer *et al.*, 1997; Paidhungat *et al.*, 1997; Palmer *et al.*, 2001). The *mid1* and *cch1* genes were both identified by their role in mating pheromone induced Ca^{2+} accumulation (Iida *et al.*,

1994; Fischer *et al.*, 1997; Paidhungat *et al.*, 1997). Although *mid1* has little homology with existing Ca^{2+} channels (Iida *et al.*, 1994), *cch1* has significant levels of similarity to mammalian L-type Ca^{2+} channels (Fischer *et al.*, 1997; Paidhungat *et al.*, 1997). Similarity of *mid1*Δ and *cch1*Δ phenotypes, and the lack of cumulative effects when both were deleted, led to the proposal that they acted as a single CPC (Fischer *et al.*, 1997; Paidhungat *et al.*, 1997). This theory was supported by analysis of their role in a high affinity calcium uptake system (HACS) for Ca^{2+} accumulation upon α factor addition (Locke *et al.*, 2000; Muller *et al.*, 2001). GFP tagging and immunofluorescence microscopy found both Mid1p and Cch1p to be localized to the plasma membrane and that Mid1p also localized to the endoplasmic reticulum (Iida *et al.*, 2004; Yoshimura *et al.*, 2004; Ozeki-Miyawaki *et al.*, 2005). Independent localization of Mid1p suggested it might be capable of Ca^{2+} channel activity without Cch1p. This was supported by generation of stretch activated Ca^{2+} influx when Mid1p was expressed in Chinese hamster ovary cells (Kanzaki *et al.*, 1999). Mid1p may form a homotetrameric CPC (Kanzaki *et al.*, 1999) or may form a complex with other proteins apart from Cch1p (Yoshimura *et al.*, 2004). The $[Ca^{2+}]_c$ response to the amiodarone antifungal agent treatment was specifically inhibited in a *mid1*Δ strain (Courchesne *et al.*, 2003), and deletion of either *cch1* or *mid1* failed to abolish Ca^{2+} influx in response to alkaline stress that was independent of the third yeast Ca^{2+} channel, Yvc1p (Viladevall *et al.*, 2004). The combined evidence suggests that budding yeast may contain a Cch1p/Mid1p CPC in the plasma membrane and an oligomeric Mid1p CPC in the endoplasmic reticulum.

The third CPC channel in *S. cerevisiae* is the vacuolar homolog of mammalian TRP conductance channels, Yvc1p (Palmer *et al.*, 2001). Yvc1p is activated by Ca^{2+} and mechanical stretch applied to vacuolar membranes (Zhou *et al.*, 2003). Yvc1p is responsible for Ca^{2+} influx in response to hyper-osmotic shock where activation results from membrane stretch (Denis and Cyert, 2002; Zhou *et al.*, 2003). Unlike previous examples of transient receptor potential (TRP) conductance channels, Yvc1p was not activated by a range of known Ca^{2+} channel agonists including $InsP_3$, arachidonic acid, linolenic acid and cAMP. The identification of Yvc1p releasing Ca^{2+} from an internal store was the first demonstration of release of Ca^{2+} from intracellular stores by a TRP

channel (Denis and Cyert, 2002). These findings have led to the proposal that the family of fungal TRP channels (Denis and Cyert, 2002) may represent a unique class of TRP channels (Zhou *et al.*, 2003).

In low Ca^{2+} conditions a low affinity Ca^{2+} uptake systems (LACS) was identified that did not involve Cch1p/Mid1p Ca^{2+} channel activity (Muller *et al.*, 2001). The LACS activity was dependent on the Fig1p protein of unknown function (Muller *et al.*, 2001; Muller *et al.*, 2003). When the LACS was active Ca^{2+} uptake was prevented by either direct inhibition by calcineurin (Muller *et al.*, 2001).

1.2.1.2 Removal of Ca^{2+} from the cytoplasm

Intracellular Ca^{2+} storage in *S. cerevisiae* is a flexible system principally involving the vacuoles and Golgi apparatus. Although the Golgi has little role in Ca^{2+} accumulation in wild type (wt) cells, when $[Ca^{2+}]_c$ exceeds the capacity of the vacuolar Ca^{2+} uptake system Golgi Ca^{2+} uptake is increased (Cunningham *et al.*, 1994; Miseta *et al.*, 1999a).

Ca^{2+} accumulation in vacuoles is driven by a pH gradient generated by a vacuolar H^+ ATPase essential for Ca^{2+} accumulation and for Ca^{2+} homeostasis (Ohsumi and Anraku, 1983; Ohya *et al.*, 1991; Forster *et al.*, 2000). Ca^{2+} is sequestered into the vacuole by the Vcx1p Ca^{2+}/H^+ exchanger (Pozos *et al.*, 1996) and the Pmc1p Ca^{2+} ATPase (Cunningham *et al.*, 1994; Cunningham *et al.*, 1996). Rapid sequestration Ca^{2+} ions, after elevation in response to a stimulus, is predominantly the role of Vcx1p whereas Pmc1p is the major determinant in Ca^{2+} homeostasis (Cunningham *et al.*, 1996; Catty *et al.*, 1997; Miseta *et al.*, 1999b; Forster *et al.*, 2000; Denis and Cyert, 2002). Vcx1p is believed to be the only Ca^{2+}/H^+ exchanger in *S. cerevisiae* (Pozos *et al.*, 1996). However Ca^{2+}/H^+ exchange was observed in a *vcx1*Δ strain suggesting the existence of additional Ca^{2+}/H^+ exchangers for which YNL321w may be a possibility (Marchi *et al.*, 1999; Miseta *et al.*, 1999b).

For Ca^{2+} accumulation into the Golgi the Pmr1p Ca^{2+}/Mn^{2+} ATPase was identified and found to be required for secretory protein folding and processing (Rudolph *et al.*, 1989; Antebi and Fink, 1992; Sorin *et al.*, 1997; Durr *et al.*, 1998; Marchi *et al.*, 1999; Strayle *et al.*, 1999; Okorokov *et al.*, 2001; Bonilla *et al.*, 2002). Before the discovery of Pmr1p in the ER (Strayle *et al.*, 1999), ATPase activity was believed to be absent from *S. cerevisiae* ER (Marchi *et al.*, 1999; Strayle *et al.*, 1999). There is also a limited amount of biochemical and genetic evidence that suggests there may be additional, as yet unidentified, Ca^{2+} ATPases in *S. cerevisiae* (Catty and Goffeau, 1996; Sorin *et al.*, 1997). The ER localized Cod1p protein encodes a P-type ATPase whose deletion perturbs Ca^{2+} homeostasis in a similar, and synergistic, fashion to deletion of *pmr1* (Cronin *et al.*, 2002). Biochemical characterization of Cod1p failed to demonstrate Ca^{2+} transport. However, despite this Cod1p has a clear role in $[Ca^{2+}]_c$ homeostasis and ER function (Cronin *et al.*, 2002).

1.2.1.3 Mediators of Ca^{2+} signalling

1.2.1.3.1 Phospholipase C

Saccharomyces cerevisiae contains a single phospholipase C (PLC) gene encoding a phosphatidyl inositol PLC with in vitro Ca^{2+} activation (Flick *et al.*, 1993; Payne *et al.*, 1993; Yoko-o T *et al.*, 1993). Phospholipase C is associated with the plasma membrane and is responsible for converting phosphatidyl inositol-4,5-bis phosphate (PIP_2) into $InsP_3$ and diacylglycerol (DAG). *S. cerevisiae* Plc1p is involved in a diverse range of cellular processes (Flick and Thorner, 1998) including filamentation induced by nitrogen depletion (Ansari *et al.*, 1999) and the activation of glucose catabolism (Coccetti *et al.*, 1998; Tisi *et al.*, 2002; Tisi *et al.*, 2004; Kellermayer *et al.*, 2004). Despite the widespread involvement of Plc1p in different physiological processes, no genes encoding $InsP_3$ receptors have been identified and Plc1p mediated activation of PKC by DAG has not been proven (Wera *et al.*, 2001).

1.2.1.3.2 Calcineurin

The conserved phosphoprotein phosphatase, calcineurin, has a key role in the interpretation and regulation of Ca^{2+} signals in *S. cerevisiae*. Two genes encoding the catalytic subunit (Cyert *et al.*, 1991) and one gene encoding the regulatory subunit of calcineurin were identified in *S. cerevisiae* (Kuno *et al.*, 1991). The activity of the catalytic subunit of calcineurin is dependent upon the regulatory subunit *in vivo* (Mendoza *et al.*, 1996). Calcineurin may exert its effects by altering the phosphorylation state of a protein or by inducing the expression of a wide variety of genes. Calcineurin activity of *S. cerevisiae* is both positively and negatively regulated by direct binding of Rcn1p (Kingsbury *et al.*, 2000; Fox and Heitman, 2002). The interaction between calcineurin and Rcn1p stabilizes Rcn1p, increases calcineurin expression and allows regulation of calcineurin activity by Rcn1p. These features, combined with the requirement of Ca^{2+} signalling via CaM, calcineurin and the transcription factor Crz1p for expression of Rcn1p above basal levels provide a potential negative feedback loop for calcineurin mediated Ca^{2+} signalling in *S. cerevisiae* (Kingsbury *et al.*, 2000).

One major function of calcineurin is the regulation of Ca^{2+} homeostasis. In response to mating pheromone the activity of the Mid1p/Cch1p HACS is inhibited by calcineurin in a mechanism independent from other known targets of calcineurin (Muller *et al.*, 2001). The activities of Pmr1p, Pmc1p and Vcx1p were found to be regulated by calcineurin (Cunningham *et al.*, 1996). Calcineurin inhibited both the *in vivo* activity and also decreased the expression of the *vcx1* gene whereas activation of calcineurin by Ca^{2+}/CaM induced expression the *pmc1* and *pmr1* genes (Cunningham *et al.*, 1996). Despite the modulation of Ca^{2+} transporter activity by calcineurin, all three enzymes appeared to have calcineurin independent activity (Cunningham *et al.*, 1996). These findings were in marked contrast to the regulation of mammalian Ca^{2+} ATPases whose activity is predominantly regulated by direct binding of Ca^{2+}/CaM (Cunningham *et al.*, 1996).

Calcineurin mediates transcription responses of numerous genes to a variety of different stimuli via the Tcn1p/Crz1p transcriptional activator (Matheos *et al.*, 1997; Stathopoulos

et al., 1997; Serrano *et al.*, 2002; Yoshimoto *et al.*, 2002; Matsumoto *et al.*, 2002; Viladevall *et al.*, 2004; Yokoyama *et al.*, 2006). Activated calcineurin dephosphorylates Crz1p resulting in Crz1p localization shifting from the cytosol to the nucleus (Stathopoulos-Gerontides *et al.*, 1999). Crz1p then activates transcription by binding to Ca^{2+} dependent responsive elements (CDREs) in the promotors of target genes leading to changes in their expression (Stathopoulos *et al.*, 1997). Calcineurin and Crz1p are capable of generating distinct expression responses to different stimuli (Matheos *et al.*, 1997; Stathopoulos *et al.*, 1997; Yoshimoto *et al.*, 2002). Crz1p mediated transcription is also inhibited by various protein kinases including Hrr25p and cAMP dependent protein kinase (PKA) which antagonise the shift to nuclear localization induced by calcineurin mediated dephosphorylation (Kafadar *et al.*, 2003; Kafadar and Cyert, 2004). This interaction demonstrates a biochemical mechanism through which different stress signalling pathways may be integrated *in vivo* (Kafadar *et al.*, 2004). The distinct responses may result from different features of $[Ca^{2+}]_c$ responses to a stimuli or a balance between other signalling pathways present in the cell (Matheos *et al.*, 1997; Stathopoulos *et al.*, 1997; Yoshimoto *et al.*, 2002). This mechanism of transcriptional activation is very similar to the effect of calcineurin on the NF-AT transcription factor in mammalian cells suggesting it is a highly conserved mechanism (Stathopoulos-Gerontides *et al.*, 1999).

1.2.2 Ca^{2+} signalling in *Neurospora crassa*

1.2.2.1 The roles of Ca^{2+} signalling in *Neurospora crassa*

Of the filamentous fungi, Ca^{2+} signalling has been best studied in the ascomycete *Neurospora crassa* and is involved in a broad range of physiological processes (Table 1.3).

Table 1.3 Processes involving Ca^{2+} signalling in *N. crassa*

Process	Reference
Hyphal tip growth	Takeuchi *et al.*, 1988; Levina *et al.*, 1995; Rao *et al.*, 1997; Bowman *et al.*, 1997; Prokisch *et al.*, 1997; Silverman-Gavrila and Lew, 2000; 2001; 2002; 2003; Yang *et al.*, 2001b
Hyphal branching	Reissig and Kinney, 1983; Dicker and Turian, 1990; Prokisch *et al.*, 1997; Kothe and Free, 1998; Sone and Griffiths, 1999; Silverman-Gavrila and Lew, 2000; 2001; 2002; Bok *et al.*, 2001
Circadian rhythm	Techel *et al.*, 1990; Sadakane and Nakashima, 1996; Yang *et al.*, 2001b
Conidiation	Rao *et al.*, 1997; Yang *et al.*, 2001b
Germination	Rao *et al.*, 1997; Silverman-Gavrila *et al.*, 2003
Heat shock response	Kallies *et al.*, 1998
Trehalose metabolism	d'Enfert *et al.*, 1999

As with other filamentous fungi an important role of Ca^{2+} signalling in *N. crassa* is in hyphal growth and branching (see references within Table 1.5). A tip high $[Ca^{2+}]_c$ gradient was first reported in growing hyphae of *N. crassa* by the use of Ca^{2+} selective dyes (see section 1.5.1) (Levina *et al.*, 1995). The generation of this gradient did not involve the influx of Ca^{2+} ions from the extracellular medium (Levina *et al.*, 1995; Lew, 1999; Silverman-Gavrila *et al.*, 2000). Disruption of this $[Ca^{2+}]_c$ gradient correlated with a cessation of apical extension (Silverman-Gavrila *et al.*, 2000) and the gradient was never observed in non-growing hyphae (Levina *et al.*, 1995). A model was proposed, based upon extensive inhibitor studies, in which Ca^{2+} containing vesicles are transported to the hyphal tip (Fig 1.1; Silverman-Gavrila *et al.*, 2002). Before fusing with the plasma membrane, Ca^{2+} was proposed to be released via $InsP_3$ activated Ca^{2+} channels. This Ca^{2+}

release then activates fusion of the vesicles with the plasma membrane. As evidence for $InsP_3$ induced Ca^{2+} release in *N. crassa* hyphae was obtained, it was suggested that tip localized, and possibly stretch activated PLC activity was responsible for the localized generation of $InsP_3$.

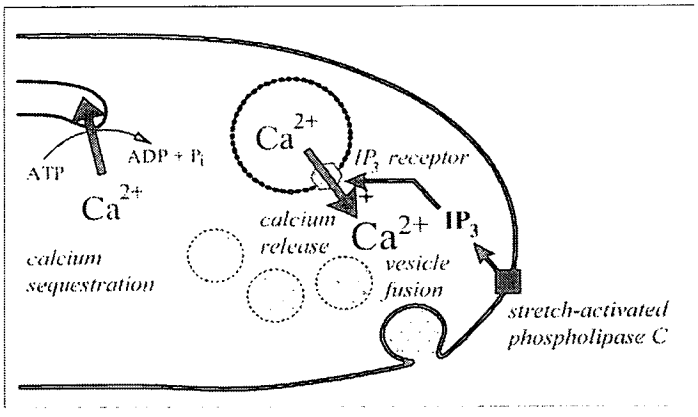

Fig. 1.1 Proposed model for generation of the apical $[Ca^{2+}]_c$ gradient of *N. crassa* (Silverman-Gavrila *et al.*, 2002).

Patch clamping of fractionated membranes identified two distinct, $InsP_3$ activated Ca^{2+} channels of different conductances (Silverman-Gavrila *et al.*, 2002). The large conductance channel, enriched in vacuolar membranes, was believed to be responsible for Ca^{2+} release from isolated vacuoles in response to $InsP_3$ (Cornelius *et al.*, 1989; Schultz *et al.*, 1990). However, evidence was obtained that this Ca^{2+} channel was not involved in the generation of the tip high $[Ca^{2+}]_c$ gradient (Silverman-Gavrila *et al.*, 2002). The second, small conductance, Ca^{2+} channel was enriched in plasma membrane and endoplasmic reticulum fractions and was susceptible to inhibition by a range of compounds which disrupted the apical $[Ca^{2+}]_c$ gradient (Silverman-Gavrila *et al.*, 2002). This work, combined with the identification of an apical gradient of Ca^{2+} containing vesicles (Torralba *et al.*, 2001), implicated the small conductance Ca^{2+} channel as being responsible for generating the $[Ca^{2+}]_c$ gradient (Silverman-Gavrila *et al.*, 2002). As $InsP_3$ activated Ca^{2+} release was not specific for the tip (Silverman-Gavrila *et al.*, 2001) the generation of $InsP_3$ must be tip localized in this model (Silverman-Gavrila *et al.*, 2002). DAG production was found to be stretch activated and it was proposed that expansion of

the plasma membrane could generate membrane tension and therefore stretch activation of PLC (Silverman-Gavrila *et al.*, 2002; 2003).

In *N. crassa*, calcineurin may also act to regulate the tip high Ca^{2+} gradient (Prokisch *et al.*, 1997) possibly involving the *spray* gene product (Bok *et al.*, 2001). Disruption of calcineurin activity was reported to abolish the tip high $[Ca^{2+}]_c$ gradient resulting in increased branching (Prokisch *et al.*, 1997). Inhibition of phosphoinositide turnover inhibits germination, hyphal extension and causes increased branching providing further support for this hypothesis (Hosking *et al.*, 1995). The effects of the Ca^{2+} gradient may be mediated by the actin cytoskeleton potentially via a CaM and actin binding protein (Capelli *et al.*, 1997; Silverman-Gavrila *et al.*, 2001).

1.2.2.2 The Ca^{2+} signaling machinery of *Neurospora crassa*

Efflux of Ca^{2+} across the plasma membrane of *N. crassa* is an energy driven process mediated by Ca^{2+} ATPase activity (Stroobant and Scarborough, 1979; Miller *et al.*, 1990). Vacuolar Ca^{2+} uptake in *N. crassa* involves H^+/Ca^{2+} exchange by the CAX protein (Margolles-Clark *et al.*, 1999) and is dependent upon vacuolar H^+ ATPase activity (Miller *et al.*, 1990). In addition to large scale Ca^{2+} storage the vacuole act as a buffer for short term perturbations in $[Ca^{2+}]_c$ homeostasis (Cornelius and Nakashima, 1987; Miller *et al.*, 1990). Characterization of Ca^{2+} ATPases in *N. crassa* identified the NCA-1 protein as a potential SERCA ATPase, the NCA-2 and NCA-3 homologues of mammalian plasma membrane ATPases, the PMR-1 homolog of the yeast golgi and ER Ca^{2+}/Mn^{2+} ATPase and the PH-7 protein (Benito *et al.*, 2000). With the exception of PMR-1, expression of all of these ATPases was induced by stress conditions. PMR-1 is continually expressed at a low level suggesting an essential role for PMR-1 in *N. crassa* (Benito *et al.*, 2000).

Influx of Ca^{2+} ions into the cytoplasm of *N. crassa* may involve $InsP_3$ activated Ca^{2+} channels (Cornelius *et al.*, 1989; Schultz *et al.*, 1990; Silverman-Gavrila *et al.*, 2002).

Micromolar amounts of $InsP_3$ caused release of Ca^{2+} from isolated vacuoles (Cornelius *et al.*, 1989; Schultz *et al.*, 1990) although the unidentified $InsP_3$ receptor appears to be far less specific for inositol polyphosphates than the mammalian receptor (Schultz *et al.*, 1990).

Ca^{2+} signalling may interact with cAMP signalling in *N. crassa* via modulation of both cAMP phosphodiesterase and adenylyl cyclase activity (Reig *et al.*, 1984; Tellez-Inon *et al.*, 1985). cAMP-mediated protein kinase A dependent protein phosphorylation may also activate Ca^{2+} channels as has been shown in *A. niger* (Bencina *et al.*, 2005). Further interaction between these pathways may be via cAMP induced increases in the levels of inositol polyphosphates in response to heat shock, although increased $[Ca^{2+}]_c$ was not demonstrated in this work (Kallies *et al.*, 1998).

Interpretation of Ca^{2+} signals in *N. crassa* may be mediated by calcineurin. *N. crassa* contains a single gene with homology to the catalytic subunit of other systems (Higuchi *et al.*, 1991) and a gene with homology to the regulatory B subunit (Kothe and Free, 1998). The effects of calcineurin may involve the COT-1 protein kinase which may interact with calcineurin (Gorovits *et al.*, 1999) and its signalling pathway may also involve the *frost* gene product (Sone and Griffiths, 1999). Further interaction between $[Ca^{2+}]_c$ and protein phosphorylation may be mediated by the CAMK-1 Ca^{2+} / CaM dependent protein kinase (Yang *et al.*, 2001b).

The substantial body of functional evidence was further enhanced by a comparative genomic analysis of *N. crassa*, *Magnaporthe grisea* and *S. cerevisiae* (Zelter et al., 2004). This study identified a large number of genes encoding potential Ca^{2+} signalling proteins (see summary in Tables 1.4 and 1.5). These results demonstrate that *N. crassa* may possesses a complex Ca^{2+} signalling machinery capable of generating and interpreting Ca^{2+} signals.

Table 1.4 Predicted $[Ca^{2+}]_c$ modulating proteins in *N. crassa* adapted from (Zelter *et al.*, 2004). [a] Indicates a Na^+ -ATPase. [b] indicates a Ca^{2+}/Na^+ exchanger.

Protein class	**Proteins in *N. crassa***	**Closest *S. cerevisiae* homologue**
Ca^{2+} permable channel	NCU02762.2	Cch1p
	NCU06703.2	Mid1p
	NCU07605.2	Yvc1p
Cation pump	NCA-1	Pmr1p
(Ca^{2+} unless otherwise stated)	NCA-2	Pmc1p
	NCA-3	Pmc1p
	PMR-1	Pmr1p
	PH-7	Ena2p
	ENA-1[b]	Ena2p[a]
	NCU07966.2	none
	NCU04898.2	Spf1p
	NCU03818.2	Neo1p, Ena2p[a]
Ca^{2+}- Transporters	CAX	Vcx1p
(Ca^{2+}/H^+ unless otherwise stated)	NCU00916.2	Vcx1p
	NCU00795.2	Vcx1p
	NCU06366.2	none
	NCU07711.2	Vcx1p
	NCU05360.2	YNL231W
	NCU02826.2[b]	YDL206W[b], Ecm27p[b]
	NCU08490.2[b]	none

Table 1.5 Proteins involved in downstream stages of Ca^{2+} signalling, adapted from (Zelter *et al.*, 2004)

Protein class	**Proteins in *Neurospora***	**Closest *S. cerevisiae* homologue**
Phospholipase C-δ	NCU01266.2	Plc1p
	NCU06245.2	Plc1p
	NCU09655.2	Plc1p
	NCU02175.2	Plc1p
Calmodulin	CMD	Cmd1p
Calcineurin A (catalytic subunit)	CAN-1	Cna1p, Cna2p
Calcineurin B (regulatory subunit)	CNB-1	Cnb1p
Ca^{2+} / CaM dependent protein kinase	CAMK1	Cmk2p
Ca^{2+} and or CaM binding proteins	NCU02283.2	Cmk1p, Cmk2p
	NCU09123.2	Cmk1p, Cmk2p
	NCU06177.2	Pak1p
	NCU09212.2	Rck2p, Rck1p
	NCU00914.2	Kin4p, Arp8p
	NCU02814.2	Dun1p, Rad53p
	NCU06347.2	End3p
Calnexin	NCU09265.2	Cne1p
Calpactin I heavy chain	NCU04421.2	no hit
Calreticulin	NCU09265.2	Cne1p

1.2.3 Ca^{2+} signalling in other filamentous fungi

As with *N. crassa*, Ca^{2+} signalling has been shown to be involved a substantial number of processes in a diverse range of other filamentous fungi (Table 1.6). Many Ca^{2+} signalling

proteins have also been identified in filamentous fungi other than *N. crassa* (Table 1.7).

Table 1.6 Processes involving Ca^{2+} signalling in filamentous fungi other than *N. crassa.*

Process	Fungus	Reference
Hyphal tip growth	*Fusarium graminearum, Zoophthora radicans, Botrytis cinerea, Cryptococcus neoformans*	Magalhaes *et al.*, 1991; Robson *et al.*, 1991a; 1991b; Garrill *et al.*, 1993; Hudecova *et al.*, 1994; Cruz *et al.*, 2001; Fox and Heitman, 2005
Hyphal branching	*Botrytis cinerea, Fusarium graminearum*	Robson *et al.*, 1991a; 1991b; Hudecova *et al.*, 1994
Appressorium formation	*Z. radicans*	Magalhaes *et al.*, 1991
Microtubule stability	*Ustilago maydis*	Adamikova *et al.*, 2004
Virulence (including growth at high temp, alkaline pH and high CO_2)	*C. neoformans*	Odom *et al.*, 1997; Fox *et al.*, 2001; Kraus *et al.*, 2005
Mating	*C. neoformans*	Cruz *et al.*, 2001; Fox *et al.*, 2005
Oxidative stress	*Aspergillus nidulans*	Greene *et al.*, 2002
Touch sensing	*A. awamori, Aspergillus niger, Candida albicans*	Nelson *et al.*, 2004; Bencina *et al.*, 2005; Brand *et al.*, 2007
Cell cycle progression	*A. nidulans*	Rasmussen *et al.*, 1990; Rasmussen *et al.*, 1994; Joseph and Means, 2000

Table 1.7 Ca^{2+} signalling proteins identified in filamentous fungi other than *N. crassa*.

Protein class	Protein name / locus	Fungus	References
Ca^{2+} permeable channel	Mid1p	*C. albicans*	Brand *et al.*, 2007
Ca^{2+} permeable channel	Cch1p	*C. albicans*	Brand *et al.*, 2007
Ca^{2+} ATPase	PMRA	*A. niger*	Yang *et al.*, 2001a
Ca^{2+} ATPase	ECA-1	*Ustilago maydis*	Adamikova *et al.*, 2004
Calcineurin A (catalytic subunit)	CNAA	*A. oryzae*	Juvvadi *et al.*, 2001
Calcineurin A (catalytic subunit)	CNAA	*A. nidulans*	Rasmussen *et al.*, 1994
Calcineurin A (catalytic subunit)	CNA1	*Cryptococcus neoformans*	Odom *et al.*, 1997
Calcineurin B (regulatory subunit)	CNB1	*C. neoformans*	Fox *et al.*, 2001
Calcineurin binding protein	CBP1	*C. neoformans*	Gorlach *et al.*, 2000
Calmodulin	AAK69619	*Fusarium proliferatum*	Kwon *et al.*, 2001
Calmodulin	CAM1	*C. neoformans*	Kraus *et al.*, 2005
Calmodulin	CMDA	*A. nidulans*	Rasmussen *et al.*, 1990
Ca^{2+} / CaM dependent protein kinase	CMKA	*A. nidulans*	Kornstein *et al.*, 1992
Ca^{2+} / CaM dependent protein kinase	CMKB	*A. nidulans*	Joseph *et al.*, 2000
Ca^{2+} / CaM dependent protein kinase	CMKC	*A. nidulans*	Joseph *et al.*, 2000

Protein class	Protein name / locus	Fungus	References
Ca^{2+} / CaM dependent protein kinase	FCaMK	*Arthrobotrys dactyloides*	Tsai *et al.*, 2002
Ca^{2+} / CaM dependent protein kinase	CpkA, CpkB, CpkC	*Stagnospora nodorum*	Solomon *et al.*, 2006
Phospholipase C	ANPLC1	*A. nidulans*	Jung *et al.*, 1997
Phospholipase C	BCPLC1	*Botryotina fuckeliana*	Jung *et al.*, 1997
Phospholipase C	MPLC1	*M. grisea*	Zelter *et al.*, 2004

1.3 *Neurospora crassa* as an experimental system

1.3.1 Basic characteristics of growth and the cell cycle

Neurospora crassa is an extensively studied model filamentous fungus with numerous advantages for experimental research. A principle benefit of *N. crassa* is its ease of culture on defined media with rapid growth and large hyphae making it highly suited for cytological examination. The total genome size of *N. crassa* is about 43 Mbp from which 10082 proteins are predicted. As *N. crassa* is haploid throughout the majority of its life cycle recessive mutant alleles are not masked by dominant alleles on homologous chromosomes (Zelter, 2004). Furthermore, repeat induced point mutation (RIP), in which repeated DNA sequences are subjected to G:C to A:T mutations, has contributed to low levels of gene redundancy. In 2003 *N. crassa* became the first filamentous fungus to have its genome sequenced and annotated (Galagan *et al.*, 2003; Borkovich *et al.*, 2004).

In addition to the experimental advantages of *N. crassa*, an established scientific community exists in which resources and strains are easily and readily shared. A foundation of this community is the Fungal Genetics Stock Centre (FGSC) based at the

University of Kansas, Missouri (http://www.fgsc.net). The FGSC makes many resources, including protocols, strains and plasmid readily available for a range of different filamentous fungi. An important function of the FGSC is to distribute strains, plasmids and other materials produced by the *Neurospora* Genome project (http://www.dartmouth.edu/~neurosporagenome/index.html). The *Neurospora* Genome Project is currently engaged in 4 projects designed to increase understanding and assist research in *N. crassa* (Dunlap et al., 2007). The first of these projects is the creation of deletion mutants for all of the 10082 genes identified in the genome. Once a deletion mutant strain has been created it is then sent to the FGSC for storage and to allow distribution to the *N. crassa* scientific community.

1.3.2 High throughput generation of *Neurospora crassa* deletion mutants

Historically it has proven difficult to produce deletion mutant strains on a large scale in filamentous fungi (Colot *et al.*, 2006). In contrast to *S. cerevisiae*, *N. crassa* wt strains exhibit low levels of homologous recombination after transformation and high levels of non homologous ectopic insertions. The requirements for screening large numbers of transformants, along with the creation of many deletion mutant cassettes by traditional methods, has so far prevented the establishment of large scale gene deletion in *N. crassa*. To increase the speed of deletion cassette creation a method was developed which takes advantage of the recombination machinery of yeast (Fig. 1.2). The automation of both the wet lab work and primer design has allowed this process to be used to generate deletion mutant cassettes far more efficiently than by traditional methods (Colot *et al.*, 2006).

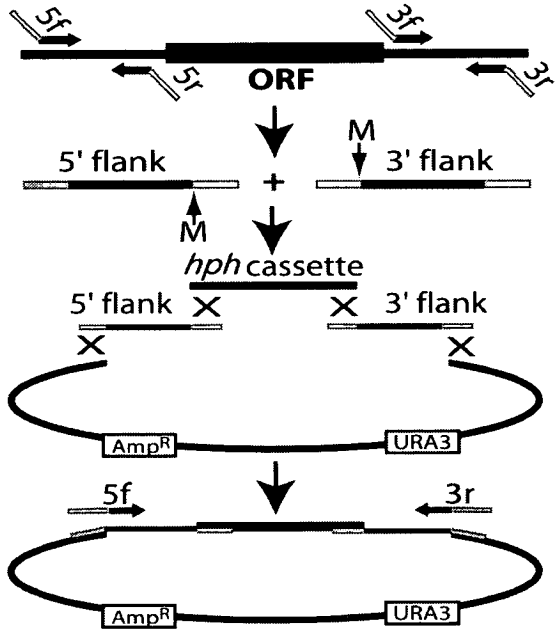

Fig. 1.2 Strategy for creation of deletion mutants used by the *Neurospora* Genome Project (Colot *et al.*, 2006). 5' and 3' flanks are created separately by amplification from genomic DNA using the 5f + 5r and 3f + 3r, primers respectively. Flanking regions and the *hph* cassette are then cotransformed into yeast in which they are assembled by homologous recombination. The completed deletion cassette is then amplified from yeast DNA using the 5f and 3r primers and linearised before transformation into *N. crassa.*

The problem of ectopic insertion was removed by the development of two *N. crassa* strains, Δ*mus-51* and Δ*mus-52* in which non homologous end joining DNA repair was virtually eliminated (Ninomiya *et al.*, 2004). When Δ*mus-51* or Δ*mus-52* were transformed with a deletion mutant cassette (created as described in Fig. 1.2) the target gene was disrupted by insertion of the hygromycin resistance gene. The heterokaryotic knock out mutants, identified by hygromycin resistance screening, were then crossed with *N. crassa* wt after which the ascospores produced are collected and screened again for hygromycin resistance. Successful strains are then verified by examination of ignite resistance and Southern blotting. These protocols are described in full detail on the *Neurospora* Genome project website (http://www/dartmouth.edu/~neurosporagenome/protocols.html).

1.4 Measurement of $[Ca^{2+}]_c$ in filamentous fungi

1.4.1 Measurement of $[Ca^{2+}]_c$ with Ca^{2+} selective dyes

In mammalian and plant systems a variety of methods have been developed for measuring $[Ca^{2+}]_c$. The use of Ca^{2+} sensitive fluourescent dyes has enabled huge advances in the understanding of mammalian Ca^{2+} signalling (Petersen *et al.*, 2005). Despite their success in mammalian cells these dyes have encountered a variety of problems in plants which have since been overcome by careful controls and the use of membrane impermeable dextran conjugated dyes (Read *et al.*, 1993; Knight *et al.*, 1993).

In filamentous fungi there are multiple and serious problems encountered with measurement of $[Ca^{2+}]_c$ by use of Ca^{2+} selective dyes (Hickey *et al.*, 2005). Loading of dyes into the fungal cell by microinjection often results in altered morphology and growth (Silverman-Gavrila *et al.*, 2000; 2001; Zelter, 2004). Once a dye has been introduced it may be cyto-toxic or be rapidly sequestered into organelles. Sequestration of a dye by sub 200 nm vesicles (e.g. secretory vesicles) may be erroneously interpreted as ionic gradients (Hickey *et al.*, 2005). To ensure the accuracy of $[Ca^{2+}]_c$ measurement by Ca^{2+} selective dyes two important controls must be performed. Firstly, membrane impermeable dextran conjugated dyes should be injected into the cells. Second, the sensitivity of the dyes to increased $[Ca^{2+}]_c$ should be confirmed by artificial elevation of $[Ca^{2+}]_c$ by methods such as the use of Ca^{2+} selective ionophores. All of the studies reporting tip high $[Ca^{2+}]_c$ gradients in hyphae using dual dye ratio imaging of Fluo3-AM and Fura-Red-AM dyes (section 1.2.3.1, Silverman-Gavrila *et al.*, 2000; 2001; 2003) lacked these controls (Hickey *et al.*, 2005). Another dye extensively used in *N. crassa* $[Ca^{2+}]_c$ measurement is chlortetracycline (CTC) (Prokisch *et al.*, 1997; Silverman-Gavrila *et al.*, 2002; 2003; Lew and Levina, 2004; Levina and Lew, 2006). CTC fluoresces in response to membrane associated Ca^{2+} and does not report $[Ca^{2+}]_c$. Further more, it has been recently reported that CTC fluorescence only increases in responses to $[Ca^{2+}]$ in

excess of 0.75 mM, far above previously reported fungal $[Ca^{2+}]_c$ concentrations (Levina *et al.*, 2006).

1.4.2 $[Ca^{2+}]_c$ measurement with recombinant aequorin

Aequorin is a luminescent Ca^{2+} reporter protein isolated from *Aequoria victoria* where it is encoded for by the *aeqA* and *aeqD* genes (Inouye *et al.*, 1985; Prasher *et al.*, 1985). Active aequorin capable of binding Ca^{2+} forms when apoaequorin binds O_2 and coelenterazine. Binding of Ca^{2+} to active aequorin then returns aequorin to the inactive apoaequorin. Coelenteramide, CO_2 are released as biproducts of this reaction along with energy released in the form of luminescence (λ = 470 nm). Aequorin luminescence is dependent on $[Ca^{2+}]_c$ allowing it to be calibrated and provide a readout of $[Ca^{2+}]_c$. Further advantages of aequorin include: large dynamic range over which $[Ca^{2+}]_c$ can be measured, lack of Ca^{2+} buffering, high selectivity for free Ca^{2+}, and its retention within the cellular compartment it has been targeted to.

Recombinant aequorin has been used to measure $[Ca^{2+}]_c$ in a wide range of different fungi (Nakajima-Shimada *et al.*, 1991; Shaw and Hoch, 2000; Greene *et al.*, 2002; Nelson *et al.*, 2004). The initial attempts to express native aequorin in filamentous fungi encountered problems with low levels of protein production (Shaw *et al.*, 2000; Nelson *et al.*, 2004). However, codon optimization of the *aeqD* gene led to substantially increased aequorin production in several filamentous fungal species, including *N. crassa* (Nelson *et al.*, 2004; Zelter, 2004).

Aequorin luminescence can be rapidly converted $[Ca^{2+}]_c$ values using the following empirically derived equation (Fricker *et al.*, 1999; Zelter, 2004).

$$pCa = 0.332588(-\log k) + 5.5593$$

where

$$k = \frac{\text{Relative Light Units (RLU).s}^{-1}}{\text{total RLU available}}$$

This equation allows determination of $[Ca^{2+}]_c$ by comparison of the luminescence at any one timepoint with the total available aequorin luminescence, and has been incorporated into automated software for aequorin based $[Ca^{2+}]_c$ measurements in *N. crassa* (Zelter, 2004).

The speed, simplicity and accuracy of $[Ca^{2+}]_c$ measurement by expression of recombinant aequorin provide a versatile, accurate and non perturbing method for determining $[Ca^{2+}]_c$ within filamentous fungal cells.

1.5 Involvement of Ca^{2+} signalling in touch sensing and osmotic stress

1.5.1 Touch sensing and Ca^{2+} signalling

The involvement of calcium signalling in plant touch sensing is well established (Braam and Davis, 1990; Knight *et al.*, 1991; Knight *et al.*, 1992; Knight *et al.*, 1993; Legue *et al.*, 1997; Bibikova *et al.*, 1997). In *Arabidopsis*, a protein that may mediate mechanically stimulated Ca^{2+} influx, and can partially complement the yeast *mid1* mutant, has recently been identified (Nakagawa *et al.*, 2007). In mammalian cells the involvement of Ca^{2+} signaling in mechanotransduction is typically via activation of phospholipase C by integrin mechano-receptors (Iqbal and Zaidi, 2005). In addition to the release of Ca^{2+}

from intracellular stores in mammalian mechano sensing, there is also evidence for influx of Ca^{2+} through the plasma membrane of osteocytes (Mikuni-Takagaki, 1999) and in the cell to cell contact sensing of He-La cells (Hashido *et al.*, 2006).

Conidia of many plant pathogenic fungi sense physical signals from the plant surface as part of the trigger for germination and initiation of appressorium formation (Hoch *et al.*, 1987; Read *et al.*, 1997; Collins and Read, 1997; Kim *et al.*, 1998; Shaw *et al.*, 2000). Ca^{2+} is required for germination and appressorium formation in *Phyllosticita ampelicida* (Shaw *et al.*, 2000) and for appressorium formation in *Zoophthora radicans* (Magalhaes *et al.*, 1991). In *Colletotrichum gloeosporioides* external Ca^{2+}, CaM and CAMK activity were all found to be required for appressoria formation after hard surface contact (Kim *et al.*, 1998). The nematode trapping of *Arthrobotrys dactyloides* involves inflation of a ring structure upon pressure applied when the nematode moves through the ring. Inhibitor studies of this response led to identification of a pathway in which G protein activation in response to touch activates $InsP_3$ production resulting in Ca^{2+} release, CaM activation and the influx of water required for the inflation response (Chen *et al.*, 2001).

Mechanical stimulation by injection of iso-osmotic media has been shown to induce $[Ca^{2+}]_c$ transients with highly reproducible Ca^{2+} signatures in hyphae of filamentous fungi (Nelson *et al.*, 2004; Bencina *et al.*, 2005). However, no similar $[Ca^{2+}]_c$ response has been reported for cells of *S. cerevisiae* (Batiza *et al.*, 1996). The $[Ca^{2+}]_c$ response to mechanical perturbation of *Aspergillus niger* involves regulation of Ca^{2+} homeostasis by PKA dependent phosporylation (Bencina *et al.*, 2005). This demonstrated that $[Ca^{2+}]_c$ signalling mechanisms of filamentous fungi are capable of interaction with other signalling pathways (Bencina *et al.*, 2005). The abrogation of growth inhibition by the fungal killer toxin KP4 by cAMP further supports the idea that cAMP and Ca^{2+} signalling are linked in filamentous fungi (Gage *et al.*, 2001). Inhibitors of stretch activated and L-type Ca^{2+} channel activity significantly inhibit contact sensing of substratum topography by hyphae of the fungal pathogen *C. albicans* (Watts *et al.*, 1998). This inhibition was believed to be mediated by a stretch-activated channel in yeast cell protoplasts of *C. albicans* (Watts *et al.*, 1998). Orthologs of the *S. cerevisiae* Cch1p and Mid1p CPCs were

found to be required for high affinity Ca^{2+} uptake in *C. albicans* similar to that in the budding yeast. Deletion of *CaCch1* and *CaMid1* caused significant inhibition of contact sensing by *C. albicans* hyphae (Brand *et al.*, 2007). These proteins are the likely target of Ca^{2+} channel inhibition and demonstrate a clear example of touch mediated Ca^{2+} influx acting in the process of fungal touch sensing.

1.5.2 The role of Ca^{2+} in osmotic stress responses

Hypo-osmotic stress may be sensed via Ca^{2+} signalling mediated processes in a range of fungal and plant cells (Taylor *et al.*, 1996; Takahashi *et al.*, 1997; Pauly *et al.*, 2001; Nelson *et al.*, 2004). In plants, these $[Ca^{2+}]_c$ responses vary between cell types with specific localization and biphasic responses in different species (Taylor *et al.*, 1996; Takahashi *et al.*, 1997). Both the nuclear and cytosolic responses of BY-2 cells generate specific and distinct responses to graded levels of osmotic stress (Pauly *et al.*, 2001). Transfer of algal rhizoid cells into hypo-osmotic media caused swelling in the cells shortly before the onset of a $[Ca^{2+}]_c$ response (Taylor *et al.*, 1996). The swelling activated Ca^{2+} influx by increasing membrane tension which activated stretch activated CPC activity (Taylor *et al.*, 1996). Membrane tension activation of stretch activated CPCs is the primary mechanism by which osmotic stress may induce a $[Ca^{2+}]_c$ response in these cells.

S. cerevisiae produces a $[Ca^{2+}]_c$ transient in response to hypo-osmotic shock believed to result from membrane tension (Batiza *et al.*, 1996; Loukin *et al.*, 2007). The amplitude of this $[Ca^{2+}]_c$ response is increased by mutations which perturb the lipid content of the plasma membrane. Altered membrane lipid content may increase membrane tension under hypo-osmotic shock leading to greater activation of the stretch activated channels (Loukin *et al.*, 2007). This hypothesis was further supported by the *S. cerevisiae* $[Ca^{2+}]_c$ response to hyper-osmotic stress (Zhou *et al.*, 2003). Application of hyper-osmotic stress to isolated vacuoles increased membrane tension resulting in activation of the stretch activated Yvc1p Ca^{2+} channel (Zhou *et al.*, 2003). $[Ca^{2+}]_c$ responses to hypo-osmotic

shock have also been reported in filamentous fungi including *Aspergillus awamori* and *N. crassa* (Nelson *et al.*, 2004; Zelter, 2004). In these experiments the hypo-osmotic shock stimulus was administered by injection of diluted growth into microwell plates. Despite administration by the method used to generate the mechanical perturbation stimulus (section 1.5.1) the $[Ca^{2+}]_c$ responses to the two stimuli were found to be distinct in both fungi (Nelson *et al.*, 2004; Zelter, 2004).

1.6 Aims of the work described in the thesis

There is now significant evidence implicating the role of Ca^{2+} signalling in fungal touch sensing. In the last 5 years there have been huge advances in both the understanding of fungal genomes and in the resources available to researchers. This project aimed to take advantage of these resources for *N. crassa* to provide direct evidence for a role for Ca^{2+} signalling in response to mechanical perturbation in this species. The aims of this research were to:

- Identify and characterise the responses to mechanical perturbation in different cell types (conidia, germ tubes and vegetative hyphae).

- Discover a physiological response to mechanical perturbation that can be quantified and determine whether the response is Ca^{2+}- mediated.

- Identify and investigate the role of $[Ca^{2+}]_c$ modulating proteins involved in the mechanical perturbation response by expressing the aequorin gene in deletion mutants in which genes encoding different components of the Ca^{2+} signalling machinery have been deleted.

- Investigate the influence of defensin antifungal proteins (MsDef1, RsAFP2, MtDef2, MtDef4) on Ca^{2+} signalling.

- Develop a high throughput aequorin-based $[Ca^{2+}]_c$ assay for antifungal compounds which target Ca^{2+} signalling and homeostasis.

Chapter 2

Materials and Methods

2.1 Chemicals

Unless otherwise stated all chemicals used in this study were purchased from Sigma-Aldrich (Sigma-Aldrich Company Ltd., Poole, Dorset, UK).

2.2 Media

All media and salt solutions were made using distilled water (dH_2O) and sterilized before use by autoclaving at 121 °C , 15 psi for 20 min. Heat-sensitive components were filter

sterilized (using Sartorius Minisart 0.2 μm filters, Goettingen, Germany) and added to the main solution after the latter was autoclaved and allowed to cool to 50 °C.

2.3 Organisms and strains

Genetically modified *Neurospora crassa* and *Escherichia coli* are containment level 1 organisms and the relevant procedures for their handling and disposal (Published by the Genetic Manipulation and Biological Safety Committee, University of Edinburgh) were followed at all times. Established sterile technique was used when appropriate.

A total of 13 *N. crassa* strains were used and or produced in this study. The genotype, source and Fungal Genetics Stock Centre (FGSC) number of all strains is shown in Table 2.1. All deletion mutants used in this study were created by the *Neurospora* Genome project and supplied by the Fungal Genetics Stock Centre by the methods described in (Colot *et al.*, 2006) (FGSC, School of Biological Sciences, University of Missouri, Kansas City, USA).

Table 2.1 *N. crassa* strains used and generated in this study. *hygR* encodes for the hygromycin resistance gene. *bar* encodes for ignite (also known as phosphinothricin or basta) resistance. *aeqS* encodes codon optimized aequorin (Nelson *et al.*, 2004).

Strain	FGSC number	Mating type	Genotype	Source
74-OR231A	987	A	wt	FGSC
22A3AWTAZ6	-	A	*hygR ,aeq S*	Alex Zelter
	11708	A	*Δmid-1, hygR*	FGSC
	11253	A	*Δyvc-1, hygR*	FGSC
	11256	A	*Δph-7, hygR*	FGSC
	11237	A	*Δena-1, hygR*	FGSC
	11249	A	*Δcax, hygR*	FGSC
wt74Ap37b	-	A	*bar, aeqS, hygR*	Chapter 5

Strain	FGSC number	Mating type	Genotype	Source
11708p8	-	A	Δ*mid-1, aeqS, bar, hygR*	Chapter 5
11253p10f1b1	-	A	Δ*yvc-1, aeqS, bar, hygR*	Chapter 5
11256p16b1a3	-	A	Δ*ph-7, aeqS, bar, hygR*	Chapter 5
11237p64b	-	A	Δ*ena-1, aeqS, bar, hygR*	Chapter 5
11249p15a2a	-	A	Δ*cax, aeqS, bar, hygR*	Chapter 5

2.4 Plasmids

The plasmids used in this study are listed in Table 2.2.

Table 2.2 Plasmids used in this study.

Plasmid	Description	Source
pAZ6	*cpc 1* protomor *aeqS* expression vector, *hygR* selection	Alex Zelter
pBARGRG1	*bar* containing expression vector	(Pall and Brunelli, 1994)
pAB19	*cpc 1* protomor *aeqS* expression vector, *bar* selection	Chapter 5

Plasmid maps can be found in Appendix B.

2.5 Culture Media and Growth Conditions

2.5.1 Culturing *E. coli*

2.5.1.1 Culture media

E. coli was grown on solid or in liquid Luria-Bertani (LB) medium (Appendix A). Glycerol stocks, made as Sambrook and Russell (Sambrook and Russell, 2001), were used for long term storage of *E. coli.*

2.5.1.2 Inoculation procedure

Liquid medium was inoculated with a sterile pipette tip used to capture individual colonies growing on solid media. Solid LB plates were inoculated with 50-200 µl of LB-bacterial cell suspension. A sterile bent glass rod was used to disperse the inoculum.

2.5.1.3 Antibiotics and other selective media

For selection of strains transformed with plasmids containing ampicillin or chloramphenicol resistance genes, 100 $\mu g ml^{-1}$ ampicillin or 170 $\mu g ml^{-1}$ chloramphenicol, respectively, were added to the media after autoclaving and once media had cooled to 50 °C.

2.5.1.4 Types of culture and growth conditions

Solid LB plates contained 15 to 20 ml LB per 8.5 cm plastic Petri dish. Media were made, autoclaved and allowed to cool to 50 °C before addition of the appropriate

antibiotics. Plates were poured before media solidification, allowed to solidify, inoculated and incubated upside down at 37 °C.

Liquid LB cultures consisted of 100 ml liquid LB in a sterile 250 ml conical flask sealed with a foam bung and covered with foil. Where appropriate, antibiotics were added before inoculation. Cultures were incubated upright in a shaking incubator at 37 °C and 200 rpm.

2.5.2 Culturing *N. crassa*

2.5.2.1 Culture Media

N. crassa was grown on solid or in liquid Vogel's media (VgS) (Vougel, 1956) using sucrose (20 g/l) as the carbon source (Appendix A). For solid media 2% Oxoid agar was added before autoclaving. All media and salt solutions were made using distilled water (dH_2O) and sterilized before use by autoclaving at 121 °C, 15 psi for 20 min.

For VgS media to be used with ignite selection, NH_4NO_3 was omitted from VgS × 50 stock solution. To replace the nitrogen source, 0.5 % (w:v) proline was used as an alternative nitrogen source as this had been found to increase the potency of ignite selection (Hays and Selker, 2000).

For Ca^{2+} the free VgS media the $CaCl_2$ was replaced with KCl to give an equivalent amount of chloride ions in the stock solution.

2.5.2.2 Culture Types

Solid VgS plates contained 20 ml solid VgS per 8.5 cm Petri dish. Plates were poured before medium solidification, inoculated, and incubated at the required temperature.

Solid VgS flasks contained 100 ml solid VgS in a 250 ml conical flask with a sponge bung and foil cover. Flasks were inoculated and grown for 7 to 10 days at 24 °C by which time maximal conidiation had occurred.

Slants consisted of 1 ml solid VgS in a sterile 75 × 12 mm glass tube sealed with a cotton wool bung. Tubes were tilted before medium solidification. After inoculation, slants were incubated at 24 °C for 7 days until maximum conidiation had occurred.

2.5.2.3 Antibiotics and other selective media

For selection of strains containing the bacterial hygromycin phosphotransferase (*hph*) gene, which confers resistance to hygromycin B (hyg), 150 μgml^{-1} hygromycin B was added to the plating media after autoclaving once media had cooled to 50 °C.

For selection using the ignite/basta resistance (*bar*) gene, which confers resistance to ignite (also known as phosphinothricin), ignite was extracted from the "Harvest" herbicide, generously donated by Marris Foston Ltd. (Bayer Crop Science Ltd., Monheim, Germany). Extraction was performed using the methods described in the protocol of Hays and Selker, (2000). The effective concentration of ignite was titrated against *Neurospora* wt 74A for each extraction (typical effective concentration was 400 μgml^{-1} ignite). All media for use with ignite selection was made from 50 × VgS salts in which the NH_4NO_3 was removed and 0.5% proline was added to the media before autoclaving.

2.5.3 Inoculation Procedures

2.5.3.1 Stock Cultures

Stock cultures of *N. crassa* were grown in VgS slants (section 2.5.2.2). Hygromycin B or

ignite was added where appropriate. Liquid VgS (2 ml) was added to mature slants and the tube vortexed (5-10 s) to produce a conidial suspension. 15 µl aliquots of conidial suspension were transferred to the top of solid VgS slants which were then incubated at 24 °C under intermittent illumination for 10 days until maximum conidiation was achieved. Stock cultures were stored at -20 °C until required or for up to 6 months.

2.5.3.2 Microwell Plates set up for 0 h, 6 h and 18 h assays

Conidia of hygromycin resistant strains used to prepare microwell plates were grown in VgS slants with no selection and incubated for 7 days at 24 °C under constant illumination. In section 3.2.1, repeated culturing of 22A3AWTAZ6 in the absence of hygromycin B was found to have no effect on discharge luminescence over 30 generations. This method of culturing ensured that conidia used in $[Ca^{2+}]_c$ assays had normal morphology and were unaffected by growth in the presence of hygromycin. As this experiment was not performed with ignite resistant strains, conidia of ignite resistant strains for use in microwell plates were grown in ignite containing VgS slants for 7 days.

Microwell plates (flat bottomed 96 well opaque white 12.8 cm × 8.8 cm plates, Thermo Fisher Scientific, Loughborough, UK) were inoculated with 100 µl of liquid VgS containing 2.5 µM or 10 µM native coelenterazine (Lux Biotechnology, Edinburgh, UK) and 1×10^6 conidia ml^{-1}. Coelenterazine was added by dissolving 15 nmol aliquots in 15 µl pre-cooled methanol in the dark before addition to the cell suspension. The final methanol concentration was not more than 0.5% which is known not to affect spore germination or hyphal growth (Kozlova-Zwinderman, 2002). After inoculation microwell plates were covered with a microplate lid (Greiner Bio One, Gloucestershire, UK), individually wrapped in tin foil and incubated in the dark at the appropriate temperature. A set of three Glowell™ were added to all plates at the point of inoculation to determine any variations in luminometer sensitivity (96 microwell plate blue light standard. Lux Biotechnology, Edinburgh, UK).

2.5.3.3 Microwell plates set up for aequorin high throughput screen

Ninety three wells of flat bottomed microwell plates (flat bottomed 96 well opaque white 12.8 cm × 8.8 cm plates (Thermo Fisher Scientific, Loughborough, UK) were inoculated with 50 µl liquid VgS containing 20 µM native coelenterazine (Lux Biotechnology, Edinburgh, UK) and 2×10^6 conidia ml^{-1}. Plates were then incubated in the dark for 6 h at 24 °C. A set of three Glowells were added to all plates at the time of inoculation (96 microwell plate blue light standard, Lux Biotechnology, Edinburgh, UK).

2. 6 Characterization of *N. crassa* growth

2.6.1 Germination rate determination

Germination rates of *N. crassa* strains were determined by inoculating an 8 well microwell culture chamber with 200 µl aliquots of conidial suspension (1×10^6 cells ml^{-1}, liquid VgS). The slide was then incubated at 24 °C in the dark for 6 h. Germination was measured every hour (including 0 h) by recording 5-10 images of the cell suspension using the ×20/0.5 NA plan fluor DIC M dry objective lens of a Nikon T2000-E Microscope. Images were recorded by a Nikon DXM1200F camera and the Nikon ACT-1 image capture program (Nikon, Kingston-upon-Thames, UK). The images were then used to count 4 sets of 100 cells to measure the germination percentage. Germination was defined as a cellular emergence from a conidium that was equal to the length of the conidium.

2.6.2 Measurement of germ tube swelling

Six rows of flat bottomed, clear plastic, 96 well microwell plates (Sterilin, Middlesex, UK) were inoculated with 100 µl aliquots of *N. crassa* conidial suspension (0.5×10^6 cells/ml, liquid VgS). The plate was then wrapped in foil and incubated at 24 °C for 6 h. A Nikon T2000-E microscope was used to image cultures using the ×20/0.5 NA plan fluor DIC M dry objective lens with a 1.5 × intermediate lens inserted. Six h after inoculation the plate was transferred to the Microlumat LB96P luminometer (Berthold Technologies, Bad Wilbad, Germany) and run on a repeated measurement protocol for 2 cycles (6 wells, cycle time 11.51 s) with no injection for control experiments and an injection of 100 µl liquid VgS on the second cycle for mechanical perturbation experiments. Immediately after the second cycle, the plate was transferred to a Nikon T2000-E microscope. A Nikon DXM 1200F digital camera and the Nikon ACT-1 image capture programme (Nikon, Kingston-upon-Thames, UK) was then used to record 10 images of control hyphae or 10 images of mechanically perturbed hyphae. Once all images were recorded the occurrence of swelling was determined. For a germ tube to be counted the following rules had to be satisfied;

1. The germ tube had to be greater than or equal to three times the length of the conidium.
2. Any swelling immediately after emergence of the germ tube from the conidium could not be counted.
3. The whole cell had to be visible in the recorded image.
4. There had to be no other cells near the tip of the germ tubes.
5. Any swelling to be counted had to be adjacent to the tip.

Images were quantified using Simple PCI (Compix Inc., Imaging Systems, USA) and annotation files were used to identify all germ tubes counted in swelling assays. Where these rules were satisfied a germ tube was counted as being swollen when the cell wall curved outwards on both sides. Cells in all the recorded images were analyzed and the percentage occurrence of hyphal swelling was determined for control and perturbed wells.

2.7 In vivo $[Ca^{2+}]_c$ measurement by luminometry

Luminometry was done using two different luminometers. Routine work was performed using an LB96P Microlumat luminometer (Berthold Technologies Bad Wilbad, Germany) controlled by a dedicated PC running the Microsoft Windows based Berthold WinGlow™ software. The luminometer allowed a maximum of two 100 µl injections into each well through built in injectors. Such injections were used to stimulate samples, or discharge aequorin from samples, when required. The luminometer was calibrated to the optimal working voltage of 1496 volts.

For experiments investigating the effects of variations in the force of the mechanical perturbation stimulus or the high throughput $[Ca^{2+}]_c$ assay, the Mithras LB 940 Luminometer (Berthold Technolgies, Bad Wilbad, Germany) was used. The Mithras luminometer was controlled by a dedicated PC running the Microsoft Windows based Mikrowin 2000™ (Berthold Technolgies, Bad Wilbad, Germany). The Mithras Luminometer has three injectors each of which can deliver a single injection of 1-100 µl liquid at three different speeds in a repeated luminometry protocol.

Flat bottomed 96 well opaque white 12.8 cm × 8.8 cm microtitre plates (Thermo Fisher Scientific, Loughborough, UK) were used in all experiments involving microwell plate luminometry. Each well has a capacity of 350 µl.

In this study repeated measurement protocols were used. The repeated protocol measures light emitted from a number of samples over the course of one experiment. To achieve this, the detector of the luminometer must move from one sample to next. The time it takes to measure every sample in the experiment and return to the starting sample is called the cycle time. The time that each sample is measured for per cycle is called the measurement time. The standard measurement time was 1 s and the standard cycle time was 11.51 s for all luminometry.

2.7.1 Standard luminometry for 0 h, 6 h and 18 h $[Ca^{2+}]_c$ assays

Microwell plates containing *N. crassa* colonies (inoculated and grown as described in section 2.5.3.2) were placed in the temperature-controlled luminometer 10 min prior to measurement. Luminescence was then measured for 11 min with one of three stimuli being provided after 57 sec. Stimuli consisted of one 100 µl injection of liquid VgS medium (mechanical perturbation), VgS medium diluted in dH_2O [1:20 v/v] (hypo-osmotic shock) or 10 mM $CaCl_2$ (high external Ca^{2+}) (Zelter, 2004). A repeated measurement protocol was used to measure luminescence, for 1 sec intervals, of six sample wells every 11.51 sec for a total of 11 min 8 sec. Six extra wells in each plate were inoculated to determine the total amount of aequorin available to bind $[Ca^{2+}]_c$. This was measured using a repeated measurement protocol lasting 11 min with one 100 µl injection of 3 M $CaCl_2$, 20% ethanol after 57 sec and one 100 µl injection of 100 mM $CaCl_2$ after 5 min 57 sec for vegetative hyphae (Nelson *et al.*, 2004). For experiments using germ tubes the injection of 3 M $CaCl_2$, 20% ethanol was sufficient. This protocol was known as a discharge protocol. Average background luminescence levels were measured by a repeated measurement protocol which took 5 readings from 96 wells (cycle time 176.2 s, measurement time 1 s). The average background luminescence for a well was subtracted from the experimental luminescence during calibration of $[Ca^{2+}]_c$.

2.7.2 Luminometry with chemical treatments

To investigate the effects of $[Ca^{2+}]_c$ modulators chemicals were added to microwells in 100 µl aliquots 12 min prior to luminometry. Chemicals were dissolved in liquid VgS to minimise any osmotic stress. In cases where this was not possible, appropriate solvent controls were included. All chemical concentrations given refer to the final concentration in a microwell after addition of the chemical and any stimulus injection into the well.

The $[Ca^{2+}]_c$ modulators used in this study included chemicals and defensin plant proteins. The defensins used in this study were MsDef1, RsAFP2, MtDef4 and KP4 initially dissolved in 10 mM or 20 mM Tris HCl pH 7.6 and were generously supplied by Dr. Dilip Shah, Rob Spellbrink and Anita Snyder (Donald Danforth Plant Science Centre, St. Louis, USA).

2.7.3 Luminometry for high throughput $[Ca^{2+}]_c$ assay

Ten min or 1 h before luminometry 50 µl aliquots of test compounds (40 µl VgS + 10 µl chemical solution) were added to 93 wells of microwell plates containing *N. crassa* colonies (inoculated and grown as described in section 2.5.3.3). Microwell plates were then transferred to the Mithras Luminometer set to 24 °C and ran on a repeated luminometry protocol, designated HTS 5. This protocol recorded luminescence of 93 wells for 10 cycles with a measurement time of 0.5 s and a cycle time of 83 s without injection or 168 s when an injection was administered in a cycle. After 4 cycles to establish resting $[Ca^{2+}]_c$, an injection of 50 µl liquid VgS was administered as the mechanical perturbation stimulus in cycle 5. One hundered µl 3M $CaCl_2$ (25% ethanol) was injected in cycle 9 to allow calibration of $[Ca^{2+}]_c$. The ethanol concentration in this protocol was higher than in the standard protocol to give the same final ethanol concentration of 10%.

2.7.4 Calibration and analysis of luminometer data

2.7.4.1 Conversion of luminescence to $[Ca^{2+}]_c$

Measurements of Relative Luminescence Units (RLU) obtained by the LB96P Microlumat luminometer were converted to values of $[Ca^{2+}]_c$ by the term bert program developed by Alex Zelter (Zelter, 2004). Term bert was written in perl

(http://www.perl.com) and used the perl data language [PDL] (http://pdl.perl.org) for complex multidimensional data manipulation. Three files were read into the program for each experiment: (1) background data, from measurement of wells containing media only; (2) sample data, from the actual experimental sample; and (3) discharge data, from samples assigned for discharge. Error type could be set to variance, standard deviation or standard error.

Measurements of RLUs obtained by the Mithras LB 940 Luminometer were recorded in different file types to those generated by the LB96P Microlumat Luminometer. These files were not compatible with the Term Bert programme. In order to determine values of $[Ca^{2+}]_c$ a formatted Microsoft Excel spreadsheet was used (created by Prof. Marc Knight, University of Durham). This spreadsheet used data from the same three files as term bert to determine $[Ca^{2+}]_c$ values for each time point where luminescence was measured. From this data average $[Ca^{2+}]_c$ values along with standard deviation were determined using Microsoft Excel.

For calibration of $[Ca^{2+}]_c$ values for data produced by the high through put $[Ca^{2+}]_c$ assay a new Excel spread sheet was produced. This file used the same calculations as the original worksheet created by Mark Knight but adapted them for use with the different format and methods used in the high through put assay.

2.7.4.2 Determining characteristics of the Ca^{2+} response

In order to compare individual $[Ca^{2+}]_c$ responses, several characteristics of the response were calculated (Fig. 2.1): (1) average resting $[Ca^{2+}]_c$ before stimulus application; (2) amplitude of the $[Ca^{2+}]_c$ transient; and (3) the full width half maximum (FWHM) (the width of the $[Ca^{2+}]_c$ transient at half maximum amplitude). Average resting $[Ca^{2+}]_c$ before stimulus application was calculated as the average $[Ca^{2+}]_c$ for the 5 time points at the start of an experiment or the average of the 4 time points prior to mechanical perturbation for high through put assays (see section 2.7.3). The amplitude of the $[Ca^{2+}]_c$ transient was

determined as the increase in $[Ca^{2+}]_c$ from the time point immediately before stimulus application to the highest value of $[Ca^{2+}]_c$ reached after stimulus application. To calculate the values of FWHM linear interpolation was used.

The points described in Fig. 2.1 refer to the calculation of the FWHM by the following equation:

$$FWHM = (0.5*(x_{max}-x_{pre})+(x_{int}-x_{max})+(x_{(int+1)}-x_{int})*((y_{int}-y)/(y_{int}-y_{(int+1)}))$$

This equation uses linear interpolation to determine the x value between x_{int} and y. This is done by the assumption that the ratio of distance between y_{int} & $y_{(int+1)}$: x_{int} & $x_{(int+1)}$ is the same as the ratio of distance between y_{int} & y : x_{int} & y.

This equation was setup in Microsoft Excel and was used for the routine determination of average values of FWHM for experimental data

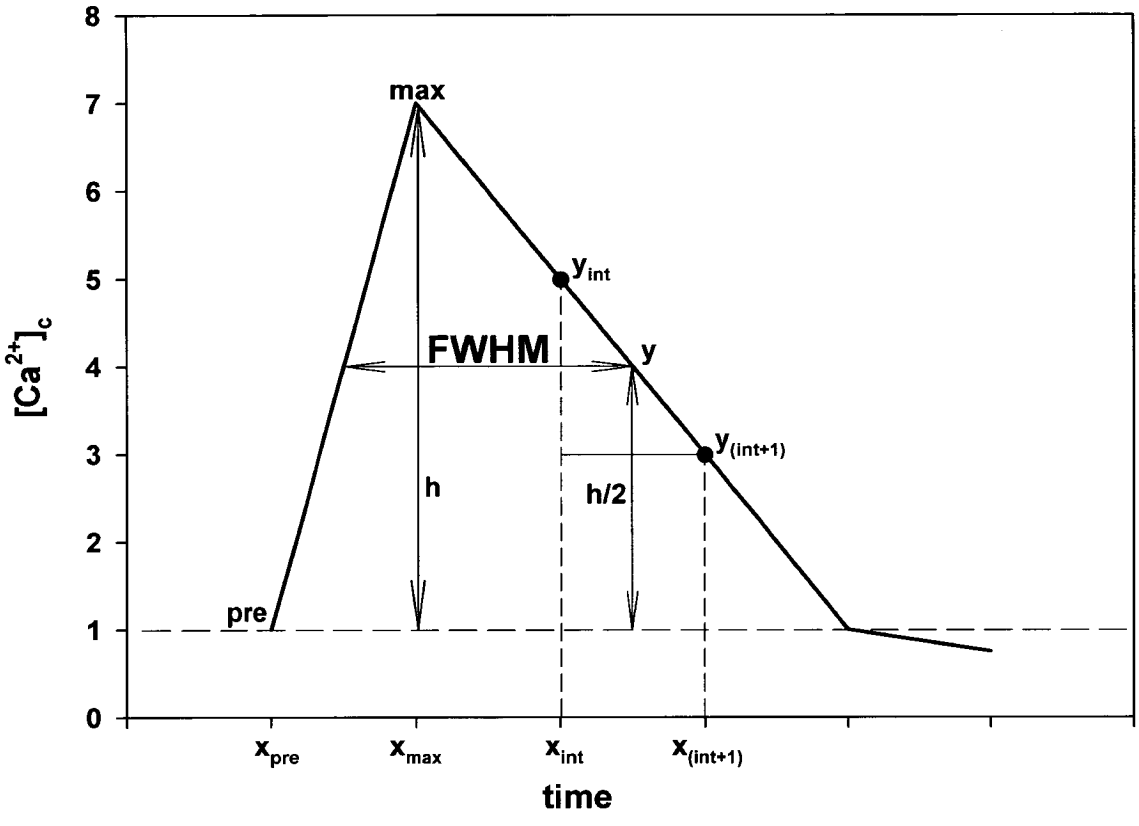

Fig 2.1. Determination of FWHM values by linear interpolation. x_{pre} = time point before stimulus application (s). x_{max} = time point at max $[Ca^{2+}]_c$ in response to stimulus (s). x_{int} = time point before y < h/2 (s). x_{int+1} = time point after y < h/2 (s). y_{int} = $[Ca^{2+}]_c$ before y < h/2 ($[Ca^{2+}]_c$). y_{int+1} = $[Ca^{2+}]_c$ after y < h/2 ($[Ca^{2+}]_c$). y = half maximum $[Ca^{2+}]_c$ ($[Ca^{2+}]_c$). h = maximum $[Ca^{2+}]_c$ in response to stimulus ($[Ca^{2+}]_c$).

2.8 Transformation and homokaryon purification of *N. crassa*

2.8.1 Preparation of conidia for electroporation

Two hundered and fifty ml conical flasks containing 100 ml solid VgS media were inoculated with conidial suspension and incubated at 24 °C for 7 days or until maximum

conidiation. The conidial suspension for inoculation was made by suspending conidia from a stock culture (see section 2.5.2.2) in 2 ml VgS media with 10 s vortexing. Three hundered µl aliquots of the resulting conidial suspension were then used for inoculation of each flask. Conidia were harvested by addition of 75 ml 1 M sorbitol (cooled to 4 °C) to the flask which was then mixed for 60 s. The suspension was then filtered through 3 layers of sterile compressor pad material (8 cm^2, 17 threads/cm^2) into a sterile 50 ml falcon tube. The filtrate was then centrifuged for 8 min at 4°C and 4000 rpm, supernatant was discarded and the pellet was resuspended in 50 ml 1 M sorbitol. This was then repeated 3 more times and after the last centrifugation the pellet was resuspended in the sorbitol remaining after decanting. Conidial concentration was then determined using a haemocytometer and the suspension was adjusted to 2.5×10^9 conidia/ ml.

2.8.2 Electroporation of *N. crassa*

In a sterile 40 µl of the conidial suspension from section 2.8.1 was mixed with 2 µl DNA (1-5 µg) and incubated on ice for 5 min. The solution was then transferred to a 0.2 ml electro-poration cuvette and electroporated (resistance: 600 Ohms, voltage: 1.5 $kVcm^{-1}$, capacitance 25 oF, BioRad Gene Pulser™, BioRad Laboratories Ltd., Herts, UK). When a beep was heard 1 ml 1 M sorbitol was added to the electroporation cuvette and mixed gently by Pasteur pipetting. Electroporated conidia were then added to 10 ml top agar at 50 °C and poured onto a 20 ml bottom agar plate (Appendix A). After the agar had set, plates were inverted and incubated at 24 °C until colonies appeared (after 2-3 days). Once individual colonies were visible they were picked and transferred to VgS slants containing appropriate selection and incubated for 7 days at 24 °C.

2.8.3 Transformant screening and homokaryon purification

Once transformants picked in section 2.8.2 had grown for 7 days they were screened for aequorin expression. A loop of conidia was suspended in 0.25 ml liquid VgS and 80 µl aliquots of the resulting cell suspension were then transferred to 2 wells of a 96 well plate. Once all transformants had been added to the plate, a 15 nmol aliquot of coelenterazine dissolved in 15 µl methanol was added to 1.2 ml liquid VgS. Twenty µl aliquots of this solution were added to each inoculated well in the microplate. The plate was then wrapped in foil and incubated for 24 h at 24 °C. After incubation the plate was transferred to the Microlumat Luminometer set to 24 °C and groups of six wells were ran under a 1.5 min discharge protocol with an injection of 3 M $CaCl_2$, 20% ethanol, at 57 s (repeated measurement, cycle time; 11.51 s, measurement time; 1 s). The luminescence emitted by each well at discharge injection was examined to identify any wells expressing aequorin.

Any transformants shown to be expressing aequorin were then entered into homokaryon purification. Loops of spores from a transformant were suspended in 0.5 ml liquid VgS and the concentration of this suspension was determined by a haemocytometer. The cell suspension was then diluted to 1000 cells/ml in liquid VgS and a 150 µl aliquot of the diluted suspension was spread on a drug amended VgS plate (section 2.5.2.2). The plate was then sealed with parafilm and incubated overnight at 24 °C. The following morning 2 colonies were excised from the plate and transferred into separate drug amended VgS slants. These slants were incubated at 24 °C for 7-10 days until maximum conidiation was achieved. The plating was then repeated until each initial transformant had been plated at least three times.

To identify any transformants that had lost aequorin expression, 80 µl aliquots of the initial, more concentrated, cell suspension were inoculated into 2 wells of a 96 well microplate. Once all transformants had been added to the plate a 15 nmol aliquot of coelenterazine dissolved in 15 µl methanol was added to 1.2 ml liquid VgS. 20 µl aliquots of this solution were added to each inoculated well in the microplate to give final

coelenterazine concentration of 2.5 μM in all wells. The plate was then wrapped in foil and incubated for 24 h at 24 °C. After incubation the plate was transferred to the Microlumat luminometer set to 24 °C and groups of six wells were ran under a 1.5 min discharge protocol with an injection of 3 M $CaCl_2$, 20% ethanol, at 57 s (repeated measurement, cycle time; 11.51 s, measurement time; 1 s). No colonies were picked from any transformant strain that did not express aequorin.

2.8.4 Modification of pAZ6 for expression of codon optimized aequorin with ignite selection

The wild type aequorin expressing strain used in chapters 3, 4 and 6 used aequorin hygromycin selection. Knock out strains created by the *Neurospora* genome project http://dartmouth.edu/~neurosporagenome acquire hygromycin resistance during gene deletion (Section 1.3.2). Therefore, an alternative selection marker was required to express aequorin in deletion mutant strains.

Hygromycin resistance is the most effective and best established antibiotic resistance marker for *N. crassa*. Phleomycin and bleomycin resistance were reported as potential antibiotic selection markers in *N. crassa* and *Aspergillus fumigatus* (Vogt *et al.*, 2005). However I found that toxicity tests with phleomycin did not give reproducible growth inhibition of *N. crassa* (data not shown). An alternative selection marker is ignite (also known as basta, phosphinothricin or PPT) resistance conferred by expression of the *bar* gene (Pall, 1993).

*Hpa*I (NEB UK) was used to excise the hygromycin resistance gene from pAZ6 (Appendix B) and the linearized pAZ6 fragment was dephosphorylated by antarctic phosphatase (NEB UK). A fragment containing a TrpC promoter, the *bar* gene for ignite resistance, and a TrpC terminator was excised from the pBARGRG1 plasmid ((Pall and Brunelli, 1994) Appendix B) using *Pml*I (NEB, UK) and *Eco*RV (Promega, UK). From this digest the 2.3 kb fragment was isolated and ligated to the pAZ6 fragment using DNA

ligase (Promega UK) to give the pAB plasmid. pAB was extracted from multiple *E. coli* colonies and a restriction analysis using *Xba*I (Promega, UK) was performed. From plasmids showing correct orientation of the *bar* gene, the pAB13 and pAB19 plasmids were selected for sequencing. To confirm the correct orientation of the bar fragment the junction between the f1 ori of pAZ6 and the *bar* fragment of pAB13 and pAB19 was sequenced using a primer with reverse complementary sequence to bp 235 to 255 of the f1 ori - 3' TGA TTA GGG TGA TGG TTC AC 5'. The sequencing reaction identified the *Hind*III, *Cla*I, *Xho*I, *Apa*I and *Kpn*I restriction sites of the pBARGRG1 polylinker adjacent to the f1 origin of replication in both plasmids. In pAB19 the *Mlu*I and *Nsi*I sites from the pBARGRG1 TrpC terminator were clearly identified providing further confirmation that the fragment had been inserted in the correct orientation. On the basis of the sequencing reaction pAB19 was selected for future use (Fig. 5.1).

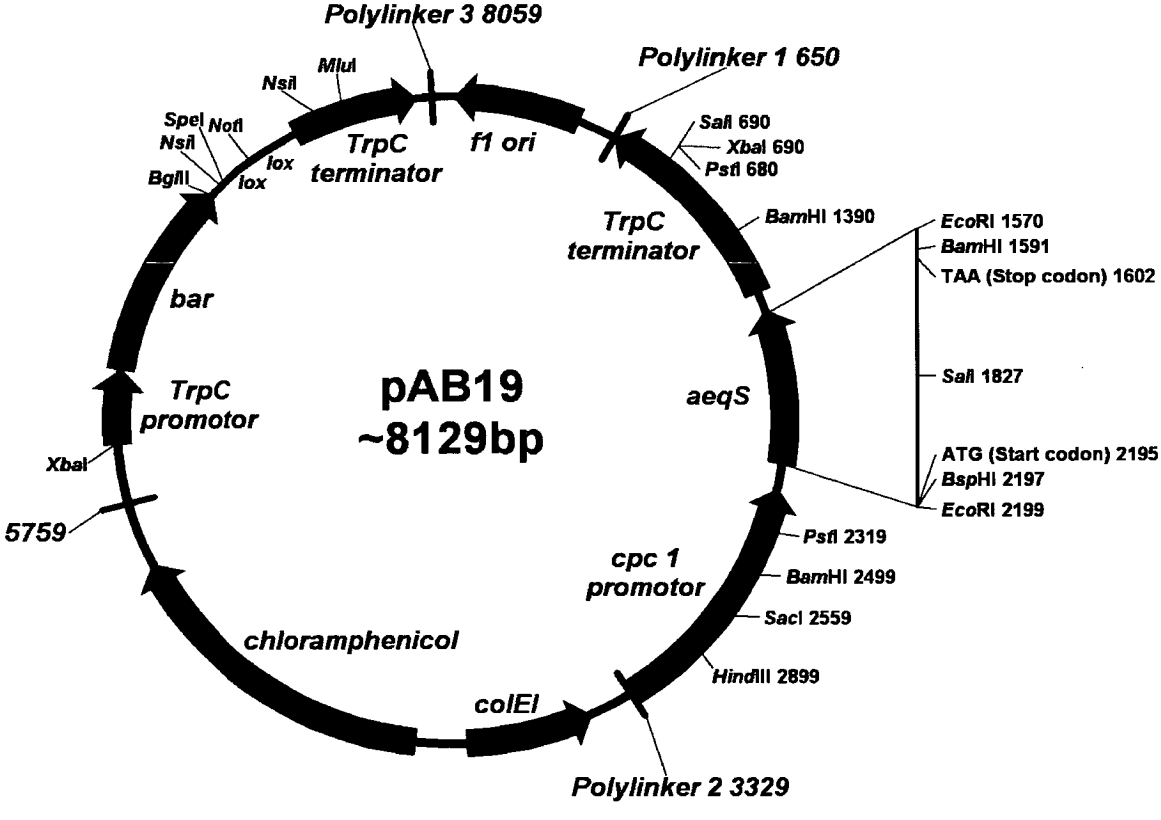

Fig. 5.1. Restriction map of the pAB19 plasmid. Polylinker 1: T7.*Kpn*I.*Apa*I.*Xho*I.*Sal*I. *Cla*I.*Hind*III; Polylinker 2: *Xba*I.*Not*I.*Sac*I.T3; Polylinker 3: *Kpn*I.*Apa*I.*Xho*I.*Cla*I. *Hind*III.

2.9 Replication, Extraction and Analysis of Plasmid DNA

2.9.1 Transforming *E. coli*

Amplification of plasmid DNA was performed by transformation of competent *E. coli* DH5α by electroporation (BioRad Gene Pulser™, BioRad Laboratories Ltd., Herts, UK) with appropriate DNA as described in (Sambrook *et al.*, 2001)

2.9.2 Extraction of plasmid DNA

Plasmid MiniPrep (GenElute, Sigma, St. Louis, USA) and Plasmid Midiprep (PureLink Hi Pure, Invitrogen, Paisley, UK) plasmid isolations were performed according to the manufacturer's instructions.

2.9.3 Determination of DNA concentration

Eight hundered µl of a 1:100 dilution of DNA:dH_2O was pipetted into a quartz cuvette placed in a spectrophotometer (BioRad Smart Spec 3000TM, BioRad Laboratories Ltd., Herts, UK). A_{260} and A_{280} were measured, with 800 µl dH_2O as a blank, and used to determine the DNA concentration (mg/ml). Sample purity was assessed by the A_{260}:A_{280} ratio in which a ratio of less than 1.8 indicates protein contamination.

2.9.4 Restriction and Analysis of DNA

Restriction digests were performed according to the manufacturer's instructions for the enzymes used. Restriction enzymes were purchased from New England Biolabs (New

England Biolabs Ltd., Hitchin, UK) or Promega (Promega Biosciences, Inc., Southampton, UK). DNA agarose gel electrophoresis was performed as described in Sambrook and Russel (Sambrook *et al.*, 2001), and a 1 kb λ DNA ladder (NEB) was used as a standard. Gels were run in BioRad MiniSubTM (BioRad Laboratories Ltd., Herts, UK) DNA cells at 5 V/cm then visualized using ethidium bromide and UV light.

2.9.5 DNA extraction and purification from agarose gels

DNA bands were excised from agarose gels, transferred to a tube and weighed. DNA was then purified with a GenElute^{TM} gel extraction kit (Sigma, Poole, UK) according to the manufacturer's instructions.

2.9.6 Ethanol Precipitation of DNA

Ten % 3M sodium acetate (pH 5.2) was added to DNA in an Eppendorf tube. Two volumes of chilled ethanol were then added and the solution was centrifuged at 13000 rpm, 4 °C for 30 min. After centrifugation the supernatant was removed and the pellet was dried in a speed vacuum. 1 vol. of 70% ethanol was then added and the pellet was centrifuged for 5 min at 13000 rpm. The supernatant was then removed and the pellet was dried again before the DNA was resuspended in the desired volume of dH_2O.

2.9.7 Preparation and ligation of DNA

DNA fragments for ligation were prepared by restriction digest, separated by agarose gel electrophoresis and extracted, as described in sections 2.9.4 and 2.9.5. Where appropriate, DNA was dephosphorylated using Antartic phosphatase (New England Biolabs Ltd., Hitchin, UK) which was then removed by ethanol precipitation as described in section

2.9.6. DNA was ligated using T4 DNA polymerase (Promega Biosciences, Inc., Southampton, UK), according to the manufacturer's instructions. After ligation the reaction mixture was transformed as described in section 2.9.1, and *E. coli* transformants were analysed by *STET* plasmid DNA extraction (section 2.9.8) and restriction digests (section 2.9.4).

2.9.8 *STET* plasmid DNA extraction from *E. coli*

An *E. coli* colony was transferred from an LB plate culture to 50 µl of STET buffer in an Eppendorf tube using a sterile glass rod. 4 µl of lysozyme was added and the solution was mixed by repeated pipetting. After 10 min incubation at room temperature the tube was placed in a heating block set to 95 °C for 50 s and centrifuged for 10 min (13000 rpm, room temperature). The resulting pellet was removed and 40 µl of isopropanol was added to the supernatant. The mixture was then centrifuged at 13000 rpm for 30 min at 4 °C after which the supernatant was removed and the pellet was washed with 70% ethanol. The pellet was then dried in a speed vacuum for 2 min and a restriction digest and analysis was performed (section 2.9.4).

2.9.9 Primer design and DNA sequencing

Primers were supplied by Sigma Genosys (Sigma-Aldrich Company Ltd., Poole, Dorset, UK). DNA sequencing was performed by the School of Biological Sciences Sequencing Service, Ashworth Laboratories, University of Edinburgh, Edinburgh.

Chapter 3

Characterisation of the $[Ca^{2+}]_c$ and Physiological Responses to Mechanical Perturbation

3.1 Introduction

Expression of recombinant aequorin is now a well established technique for measurement of $[Ca^{2+}]_c$ in filamentous fungi. Codon optimization of the *aeqD* gene facilitated great

increases in the levels of recombinant aequorin production in a range of species (Nelson *et al.*, 2004). These methods were further improved by the creation of software for fast, automated calibration of luminescence into values of $[Ca^{2+}]_c$ (Zelter, 2004). $[Ca^{2+}]_c$ responses to three external stimuli, namely mechanical perturbation, hypo-osmotic shock and high external Ca^{2+}, were identified and characterized in established colonies of *Aspergillus awamori* and *Neurospora crassa* (Nelson, 1999; Nelson *et al.*, 2004; Zelter, 2004). These $[Ca^{2+}]_c$ responses had stimulus specific characteristics but the physiological roles of the responses were not assessed (Nelson *et al.*, 2004; Zelter, 2004).

These stimuli were all administered by injection of different liquids into microwell cultures: iso-osmotic growth media for mechanical perturbation, growth media diluted 1:20 with dH_20 for hypo-osmotic shock and 100 mM $CaCl_2$ for high external Ca^{2+}. This method of application results in there being elements of mechanical perturbation in both the hypo-osmotic and high external Ca^{2+} stimuli. The $CaCl_2$ in the solution used for the high external Ca^{2+} stimulus is dissolved in dH_2O and therefore there may be an element of osmotic stress in this stimulus. As mechanical perturbation is administered by injection of iso-osmotic growth media into a microwell no other stimuli are involved. For these reasons the 'cleaner', more specific mechanical perturbation stimulus was investigated in more detail in the research described in this chapter.

The aims of the work described in this chapter were: (1) to determine the $[Ca^{2+}]_c$ response to mechanical perturbation of three different cell types (conidia, germ tubes and vegetative hyphae); (2) to develop a robust and accurate assay for the effects of Ca^{2+} modulators on $[Ca^{2+}]_c$ responses in *N. crassa*; (3) to identify a quantifiable response to mechanical perturbation.

3.2 Results

3.2.1 Refinement of $[Ca^{2+}]_c$ measurement using recombinant codon optimized aequorin

Previous studies used the presence of hygromycin B in the growth media as selective pressure to maintain expression of codon optimized aequorin (Nelson, 1999; Kozlova-Zwinderman, 2002; Nelson *et al.*, 2004; Zelter, 2004). To improve the comparison of results obtained with transformed cultures with results from wild type cultures, hygromycin B was removed from the growth medium used to prepare conidia for $[Ca^{2+}]_c$ measurement. Three *N. crassa* cultures were grown in the absence of hygromycin B for 30 sub cultures and no significant reduction in discharge luminescence was observed. For these reasons all *N. crassa* cultures to be used for luminometry were grown in the absence of hygromycin B for 7 days after which conidia were harvested and used for the measurement of $[Ca^{2+}]_c$.

3.2.2 $[Ca^{2+}]_c$ responses in vegetative hyphae

To assess whether my experimental approach for preparing and manipulating *N. crassa* produced the same results as previously obtained by Zelter (2004), vegetative hyphae in 18 h cultures were subjected to mechanical perturbation, hypo-osmotic shock and high external Ca^{2+} treatments.

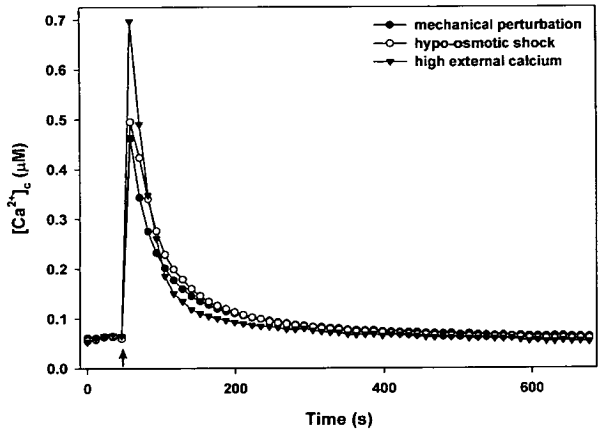

Figure 3.1. $[Ca^{2+}]_c$ responses to mechanical perturbation, hypo-osmotic shock and high external Ca^{2+}. The arrow at 57 seconds shows the point when the stimulus was applied.

The $[Ca^{2+}]_c$ response to hypo-osmotic shock was slightly more prolonged than the response to mechanical perturbation with a significantly larger FWHM value ($p = < 0.01$) (Fig. 3.1). The response to high external Ca^{2+} resulted in a greater amplitude compared with the response to mechanical perturbation. This occurred despite a more rapid removal of Ca^{2+} from the cytoplasm as the FWHM was significantly smaller than in the mechanical perturbation response ($p = < 0.05$). The features of these responses are in accordance with the results obtained by Zelter (2004) providing validation of the assay method used in this study.

3.2.2.1 Dose dependency of the mechanical perturbation response

As the mechanical perturbation stimulus is generated by the injection of iso-osmotic growth medium into a microwell, altering the speed with which media is injected into a microwell, and the volume of medium injected at a given speed, will alter the strength of the mechanical perturbation stimulus (Haley *et al.*, 1995). The Berthold Mithras Luminometer has three different speeds of injection and injection volume can be set to any value between 1 and 100 μl. These features were used to test the dose dependency of the $[Ca^{2+}]_c$ response to mechanical perturbation.

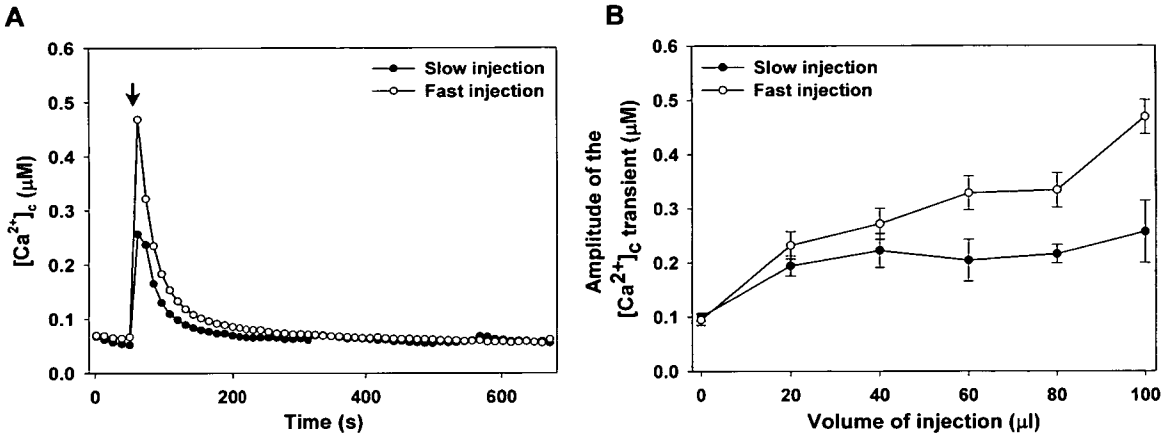

Fig 3.2. A. The $[Ca^{2+}]_c$ response of vegetative hyphae to mechanical perturbation at varying injection speeds. Arrow represents the administration of a 100 μl injection of iso-osmotic growth medium. **B.** Amplitude of the $[Ca^{2+}]_c$ response to mechanical perturbation with varying injection volume and injection speed.

Figure 3.2 demonstrates that amplitude of the $[Ca^{2+}]_c$ response to mechanical perturbation is dose dependent with respect to the strength of mechanical perturbation. The small increases with differing injection volumes suggest that further increases in the strength of mechanical perturbation may cause further increases in the amplitude of the $[Ca^{2+}]_c$ response. One potential problem with these measurements is that with the increased force hyphae may have ruptured allowing Ca^{2+} in the external media to mix with cytoplasmic aequorin. This could result in artificially high $[Ca^{2+}]_c$ response amplitudes. When luminescence values from experimental and discharge protocols were examined, the luminescence readings in the discharge protocols were vastly in excess of the experimental readings. This demonstrates that the total pool of aequorin in the hyphae did not interact with external Ca^{2+}, and therefore hyphae were not ruptured. It should be noted that this data shows the $[Ca^{2+}]_c$ response of a population of *N. crassa* to mechanical perturbation. Increased forces of mechanical perturbation may result in a greater percentage of the population within a microwell responding or an increased response in a fixed population of cells. The data presented in Fig. 3.2 cannot distinguish these two possibilities.

3.2.2.2 The role of extra-cellular Ca^{2+} in the $[Ca^{2+}]_c$ response to mechanical perturbation in vegetative hyphae

Despite a range of *in vitro* evidence, release of Ca^{2+} ions from intracellular stores of filamentous fungal cells has not been previously demonstrated satisfactorily *in vivo*. The highly selective Ca^{2+} chelator BAPTA was used to remove Ca^{2+} ions from the extracellular medium (initial $[Ca^{2+}] \sim 0.68$ mM in liquid VgS medium).

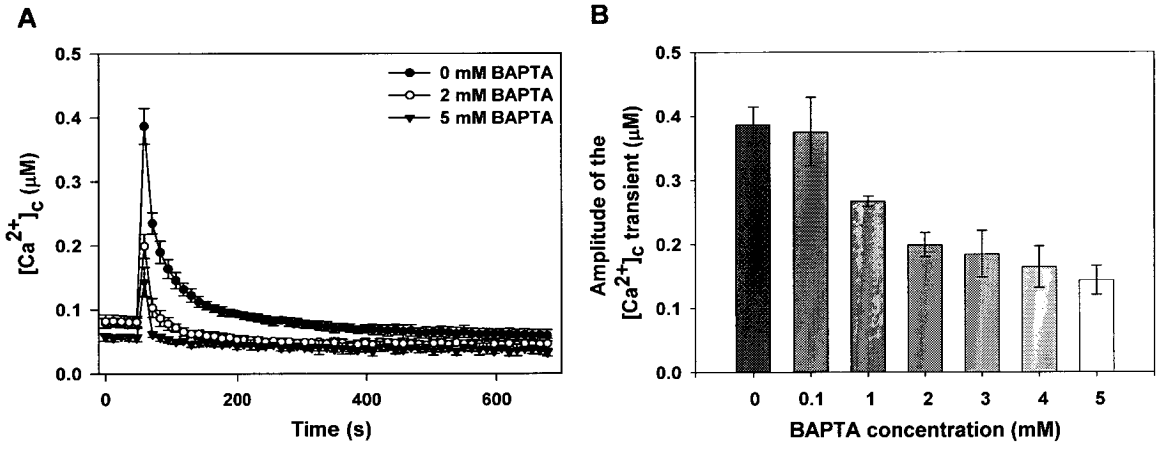

Fig. 3.3. A. $[Ca^{2+}]_c$ response of vegetative hyphae to mechanical perturbation in the presence of BAPTA. Arrow represents time of administration of mechanical perturbation stimulus. **B.** Amplitude of the $[Ca^{2+}]_c$ response in the presence of varying concentrations of BAPTA.

Figure 3.3 shows that extracellular Ca^{2+} is involved in the $[Ca^{2+}]_c$ response to mechanical perturbation. Figure 3.3B suggests the inhibition by BAPTA is dose dependent. In Fig. 3.3A there is a reduction in resting $[Ca^{2+}]_c$ caused by 5 mM BAPTA. At this concentration, Ca^{2+} chelation may be complete to the extent that the concentration gradient across the plasma membrane is reversed. If this is the case, and removal of Ca^{2+} at 5 mM BAPTA is complete, then Ca^{2+} ions released in response to mechanical perturbation must have originated from intracellular Ca^{2+} stores.

3.2.3 The effects of mechanical perturbation on germ tubes

In the vegetative hyphal cultures examined in section 3.2.2 a hyphal mat formed above the growth medium in the microwell. This growth outside of the liquid media may inhibit the even distribution of chemical agents to all of the vegetative hyphae in a $[Ca^{2+}]_c$ assay, potentially resulting in local concentrations varying significantly. The hyphal mat will encounter the mechanical perturbation stimulus before hyphae in the liquid medium below the mat which might generate an uneven stimulus distribution. A further problem is that an 18 h culture contains different types of differentiated hyphae. It is important to emphasise that when examining the $[Ca^{2+}]_c$ response in this assay we are observing the $[Ca^{2+}]_c$ response of an entire culture, not the response of individual hyphae. In order to gain more reliable information, the individual colonies in a microwell should be as homogeneous as possible. As germ tubes have not differentiated into different cell types and do not form a hyphal mat they should represent a more homogeneous culture to investigate with this $[Ca^{2+}]_c$ assay.

3.2.3.1 Sensitivity of germ tubes to mechanical perturbation

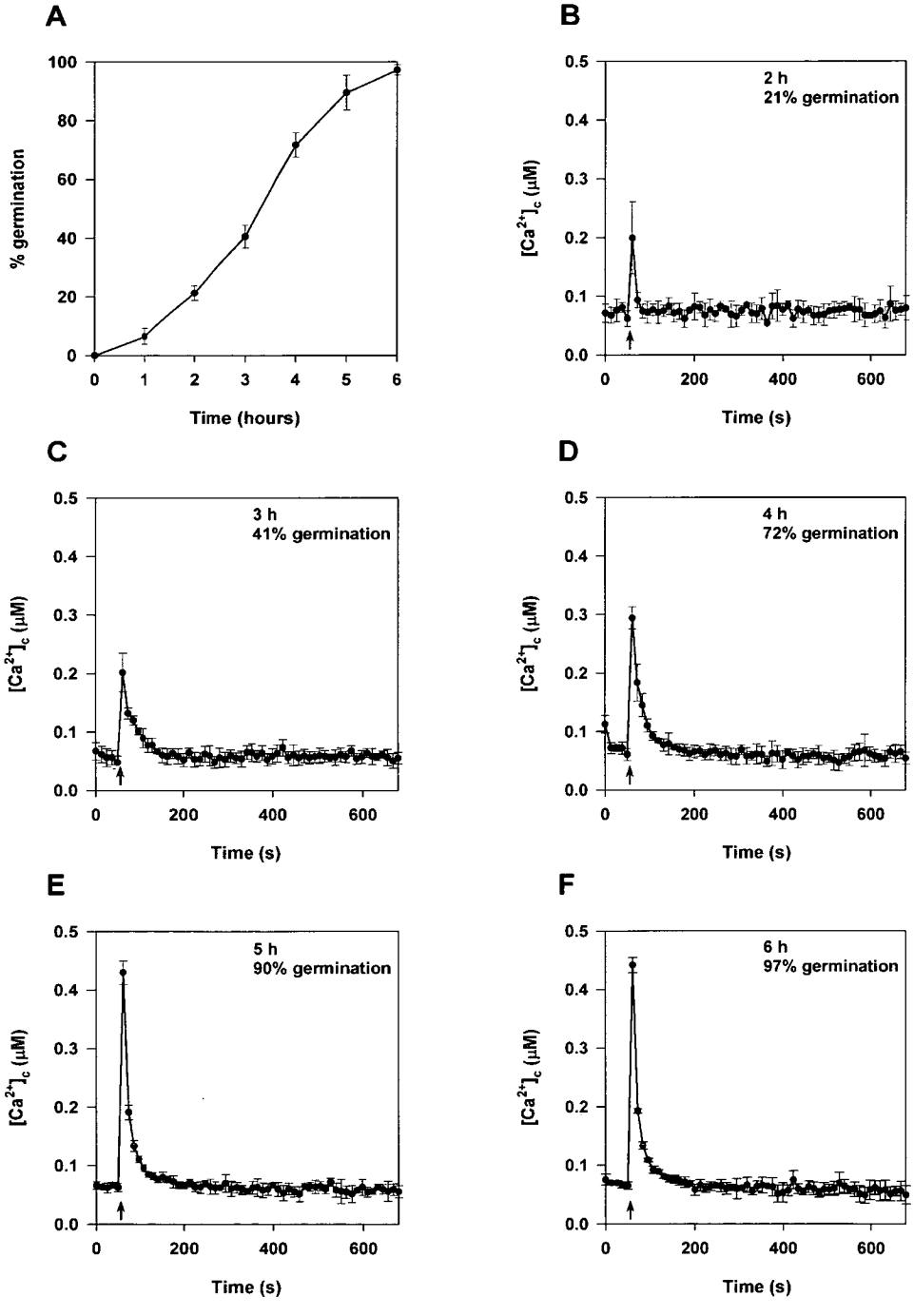

Fig. 3.4. The $[Ca^{2+}]_c$ response of germ tubes of different ages to mechanical perturbation.

A. Percentage germination of wild type *N. crassa* strain 22A3AWTAZ6 with time.

B-F. Mechanical perturbation responses of germ tubes from 2-6 h after inoculation. Arrows represent point of stimulus administration.

The rate of conidial germination was measured in 200 µl aliquots from conidial suspensions containing 1×10^6 conidia per ml. Conidial germination was initiated within 1 h of inoculation and was close to 100% after 6 h (Fig. 3.4A). From 2-5 h the amplitudes of the $[Ca^{2+}]_c$ response to mechanical perturbation successively increased. There was little difference in the amplitudes of $[Ca^{2+}]_c$ responses at 5 and 6 h.

The rate of germination correlated well with the increase in total aequorin present (Fig. 3.5). The amount of aequorin present in conidia and conidial germ tubes at the 0 and 1 h timepoints were too low to obtain reliable $[Ca^{2+}]_c$ measurements (see section 3.2.3.2).

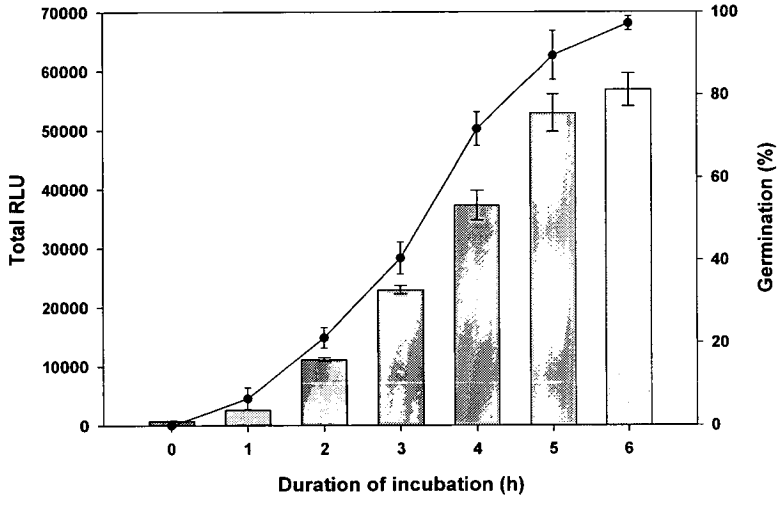

Fig. 3.5. Correlation of rate of conidial germination with amount of aequorin in conidial germlings. Bars = total discharge luminescence. Solid line = percentage germination.

When the experiment was repeated, $[Ca^{2+}]_c$ responses, aequorin accumulation and germination rates were all very similar. This demonstrates that germ tube cultures are physiologically homogeneous, produce sufficient cytoplasmic aequorin for reliable assaying of $[Ca^{2+}]_c$, and produce a robust $[Ca^{2+}]_c$ response to mechanical perturbation. After 6 h growth, germination was found to be repeatedly above 95% with sufficient levels of aequorin production. The results of Fig. 3.4 and Fig. 3.5 demonstrate that assaying *N. crassa* at 6 h post inoculation provides a uniform cell population producing sufficient aequorin for accurate measurement of $[Ca^{2+}]_c$. Six h cultures of germlings were selected for future experiments because they had reached > 95% germination and they

had accumulated sufficient aequorin to generate highly reproducible Ca^{2+} signatures in response to mechanical perturbation.

3.2.3.2 Measurement of $[Ca^{2+}]_c$ responses at low levels of aequorin expression

In the last section I concluded that when aequorin expression is too low, measurements of $[Ca^{2+}]_c$ are invalid. This is because the calibration used to convert aequorin luminescence to $[Ca^{2+}]_c$ produces artificially elevated values for resting $[Ca^{2+}]_c$. This is shown by plotting resting $[Ca^{2+}]_c$ as the *y* axis, and the total RLU emitted in the discharge protocol as the *x* axis (Fig. 3.6).

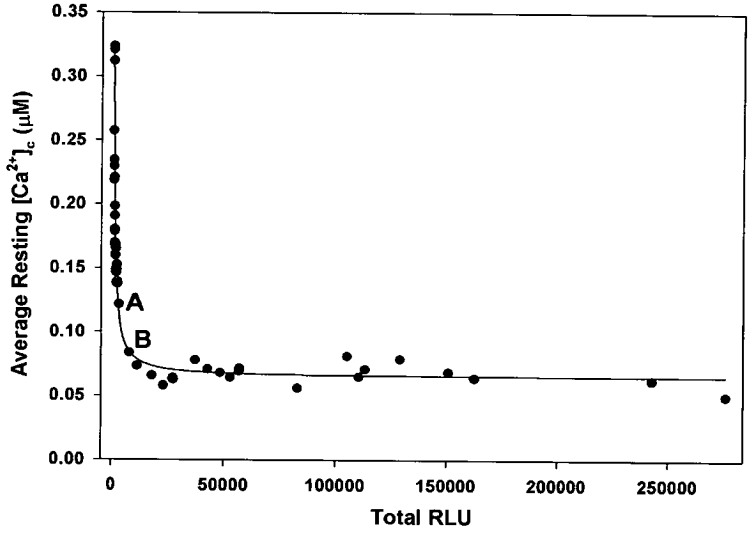

Fig. 3.6. Graph demonstrating effect of the level of available aequorin on resting $[Ca^{2+}]_c$. The two data points labelled on the graph have values as follows: A, total RLU = 3364, Resting $[Ca^{2+}]_c$ = 0.122 µM; B, total RLU = 7805, Resting $[Ca^{2+}]_c$ = 0.0837 µM.

The data presented in Fig. 3.6 was compiled from $[Ca^{2+}]_c$ assays performed by the standard method described in section 2.7.1. The length of culture incubation varied (0-30 h) as did the temperature of incubation prior to luminometry (4 °C or 24 °C). However all cultures were transferred to the luminometer (set at 24 °C) 10 min prior to measurement to allow the measurement temperature to reach 24 °C.

Figure 3.6 shows that for quantitative measurement of $[Ca^{2+}]_c$ a threshold level of cellular aequorin, determined from discharge data, is required. From the information presented in Fig. 3.6 this level should be ~ 7800 RLU (point B, Fig. 3.6).

3.2.3.3 $[Ca^{2+}]_c$ responses of germ tubes to mechanical perturbation, hypo-osmotic shock and high external Ca^{2+}

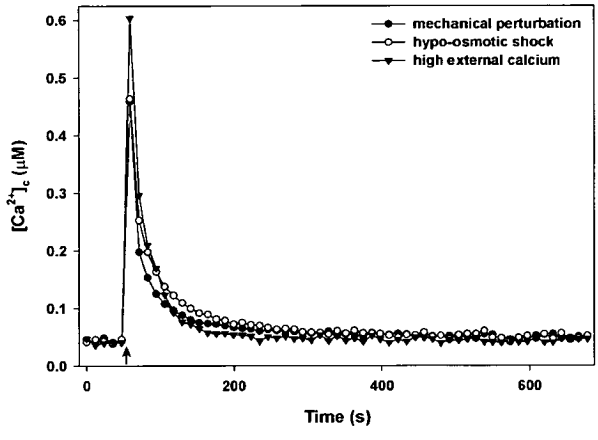

Fig. 3.7. The $[Ca^{2+}]_c$ responses of 6 h cultures to various stimuli. The arrow at 57 seconds shows the point of stimulus application.

Figure 3.7 shows the $[Ca^{2+}]_c$ responses of germ tubes to mechanical perturbation, hypo-osmotic shock and high external Ca^{2+}. The responses of germ tubes were similar to those obtained by vegetative hyphae (section 3.2.2). The $[Ca^{2+}]_c$ response to hypo-osmotic shock again exhibited a significantly greater FWHM value than the response to mechanical perturbation ($p = < 0.01$). An interesting difference in the data between the two cell types was that the FWHM values were much more variable in vegetative hyphae than in germ tubes. This was demonstrated by the standard deviations for the FWHM values in vegetative hyphae being typically 10 times greater than in germ tubes. This provides further evidence that germ tubes provide a more consistent and reliable cell population in which to analyse $[Ca^{2+}]_c$ responses to various stimuli.

3.2.3.4 Dose-dependency of the $[Ca^{2+}]_c$ response to mechanical perturbation in germ tubes

In vegetative hyphae the amplitude of the $[Ca^{2+}]_c$ response to mechanical perturbation was found to be dose-dependent with respect to the strength of mechanical perturbation (see section 3.2.2.1). This showed that either the amplitude of $[Ca^{2+}]_c$ responses increases in all cells that respond or that the number of cells that respond to the mechanical perturbation stimulus is increasing.

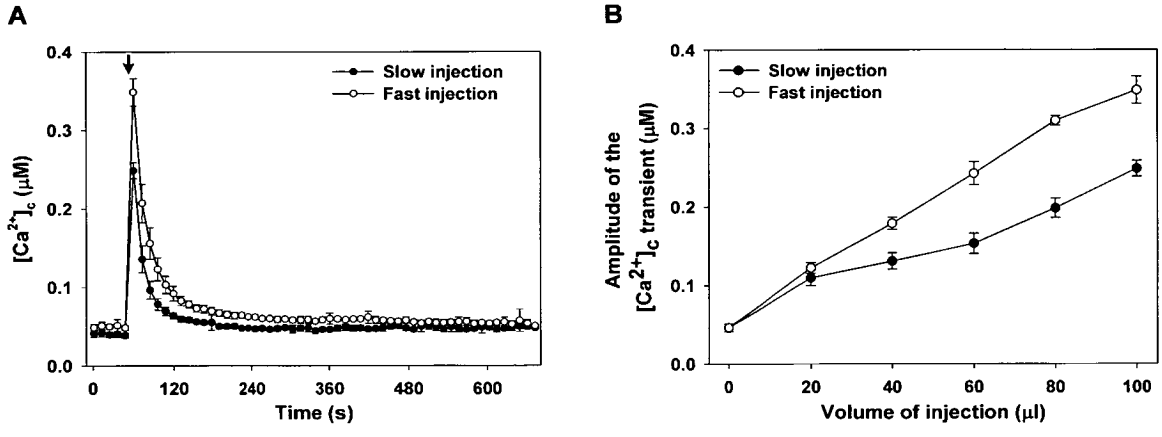

Fig 3.8. Dose-dependency of $[Ca^{2+}]_c$ response to mechanical perturbation in germ tubes. **A.** $[Ca^{2+}]_c$ responses to injection of 100 µl VgS media at different injection rates. Arrow represents point of medium injection. **B.** Amplitudes of $[Ca^{2+}]_c$ responses to a range of different injection volumes at different rates of injection.

Figure 3.8 shows that the amplitude of the $[Ca^{2+}]_c$ response to mechanical perturbation in germ tubes is also dose-dependent with respect to the strength of the mechanical perturbation. Figure 3.8A clearly shows a significant increase in the amplitude of the $[Ca^{2+}]_c$ response when injection speed, and therefore strength of mechanical perturbation, was increased ($p = < 0.01$). Figure 3.8B shows that successive increases in injection volume caused a progressive increase in the amplitude of $[Ca^{2+}]_c$ responses. This was observed at both injection speeds but was more pronounced and more consistent at the fast injection speed.

The gradual increase in $[Ca^{2+}]_c$ amplitudes at fast injection speed was greater and more consistent than the increase observed in vegetative hyphae (see section 3.2.2.1). The results presented in Figure 3.2 and Figure 3.8 shows that $[Ca^{2+}]_c$ responses to mechanical perturbation of germ tubes are more reproducible than vegetative hyphae.

3.2.3.5 Effects of extracellular pH on the $[Ca^{2+}]_c$ response to mechanical perturbation

$[Ca^{2+}]_c$ modulating agents may modify the pH of media in which they are dissolved. Any alteration of external pH may effect the movement of ions across the plasma membrane and increased alkalinity inhibits Ca^{2+} removal after high external Ca^{2+} treatment in *S. cerevisiae* (Forster and Kane, 2000). In previous work chemicals were administered in the medium used to generate the mechanical perturbation stimulus. An alternative approach is to add aliquots of the chemical dissolved in VgS media before the stimulus is applied. This method gives chemicals the chance to spread throughout a cell suspension and to interact with any potential targets in the cells. To examine the effects of these different approaches aliquots of VgS media were adjusted to a range of pH values using hydrochloric acid or sodium hydroxide.

Table 3.1 Effects of injection and pre-treatment of pH adjusted VgS media. Effects on amplitude were tested using students t-test and all effects were found to be significant at the 0.01 level.

pH of VgS medium	Effect on amplitude of $[Ca^{2+}]_c$ response when injected	Effect on amplitude of $[Ca^{2+}]_c$ response when pre-treated
4.1	Decrease	Decrease
7.6	Increase	No significant effect
8.0	Increase	No significant effect
9.6	Increase	No significant effect

Table 3.1 summarizes the results of the pH effects on $[Ca^{2+}]_c$ responses to mechanical perturbation. In all experiments, increasing the alkalinity of the VgS media added increased the resting $[Ca^{2+}]_c$ (data not shown). This effect became progressively more pronounced with increasing alkalinity. In the two different methods used to alter pH, pre-treatment displayed far less effect on the $[Ca^{2+}]_c$ transient. Adding solutions prior to stimulation allows the solutions time to mix with the cell suspension, potentially giving better distribution of a possible $[Ca^{2+}]_c$ modulator. Better distribution will reduce localized variations in concentration and provide a more reliable and accurate assessment of a $[Ca^{2+}]_c$ modulator. For these reasons it was decided that in all future $[Ca^{2+}]_c$ assays pre-treatment should be the method of addition for all potential $[Ca^{2+}]_c$ modulators.

3.2.3.6 Involvement of extracellular Ca^{2+} in the $[Ca^{2+}]_c$ response to mechanical perturbation

Saccharomyces cervisiae produces a $[Ca^{2+}]_c$ response to hypo-osmotic shock but not mechanical perturbation (Batiza *et al.*, 1996). The $[Ca^{2+}]_c$ response to hypo-osmotic shock involves influx of both external Ca^{2+} and Ca^{2+} from internal stores (Batiza *et al.*, 1996). In section 3.2.2.2, evidence was presented that showed the $[Ca^{2+}]_c$ response to mechanical perturbation in vegetative hyphae may involve intracellular Ca^{2+} release.

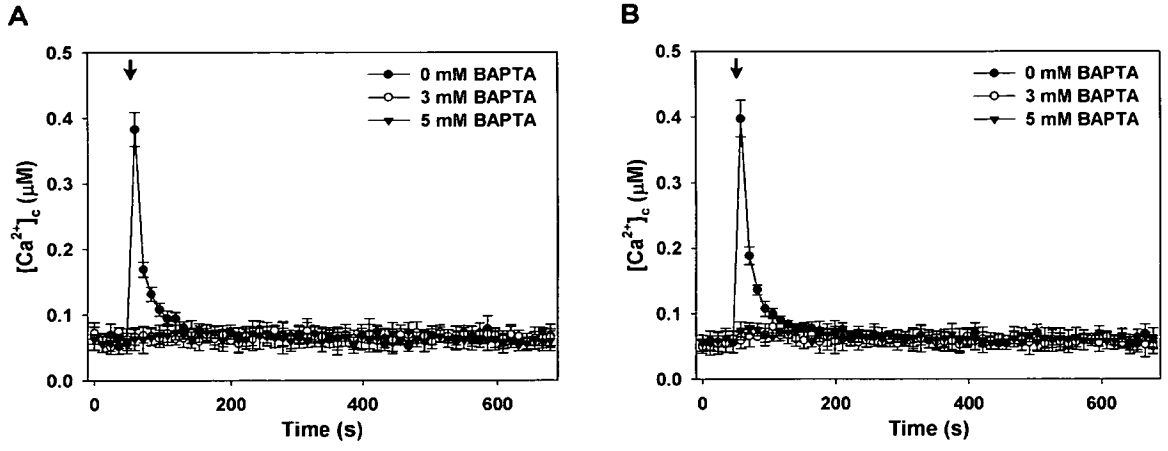

Fig. 3.9. A. The effect of 3 mM and 5 mM BAPTA on the $[Ca^{2+}]_c$ response to mechanical perturbation. **B.** The effect of 3 mM and 5 mM BAPTA on the $[Ca^{2+}]_c$ response to hypo-osmotic shock. Arrows represent time of stimulus administration.

In the initial test 3 mM and 5 mM BAPTA were found to completely abolish the $[Ca^{2+}]_c$ responses to both mechanical perturbation and hypo-osmotic shock (Fig. 3.9). This suggests that Ca^{2+} chelation was complete and that the $[Ca^{2+}]_c$ responses to both mechanical perturbation and hypo-osmotic shock were completely dependent upon influx of external Ca^{2+}.

To confirm the results of Ca^{2+} chelation, the responses to mechanical perturbation and hypo-osmotic shock were analysed in media in which all Ca^{2+} ions had been omitted (Fig. 3.10). To ensure normal morphology and viability of the conidia used in this experiment, the conidia were harvested from cultures grown on normal Ca^{2+} containing media. For the Ca^{2+}- free experiments 5 ml Ca^{2+} free liquid VgS medium was added to a slant which was then vortexed and the resulting cell suspension was removed as quickly as possible. Removing Ca^{2+} ions from around conidia by this method completely abolished the $[Ca^{2+}]_c$ response to mechanical perturbation (Fig. 3.10A). In contrast, the response to hypo-osmotic shock in the Ca^{2+}-free medium resulted in a much reduced $[Ca^{2+}]_c$ amplitude (Fig. 3.10B).

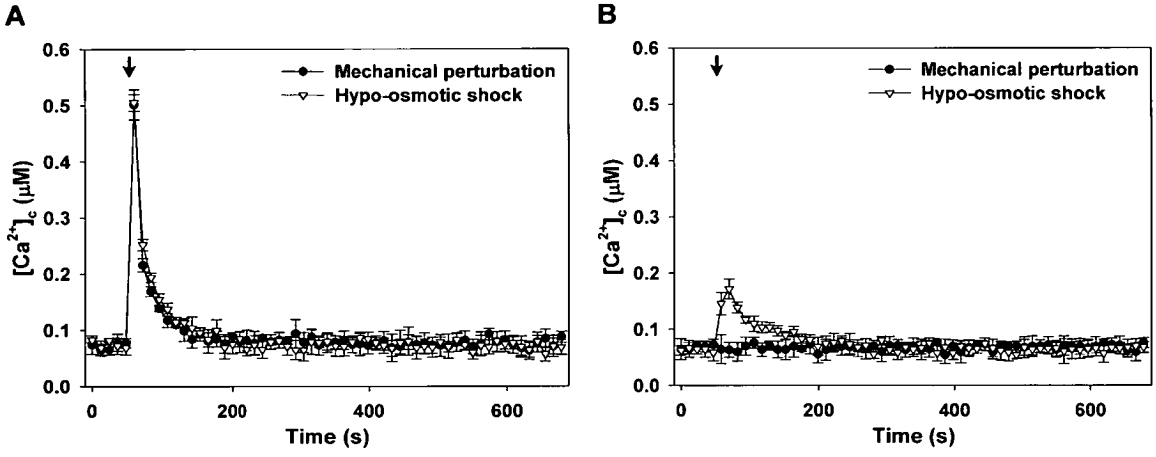

Fig. 3.10. A. $[Ca^{2+}]_c$ responses to mechanical perturbation and hypo-osmotic shock in standard, Ca^{2+}-containing VgS media. **B.** $[Ca^{2+}]_c$ responses to mechanical perturbation and hypo-osmotic shock where Ca^{2+} ions were omitted from all media used in the experiment. Arrows represent time of stimulus administration.

To further assess whether the $[Ca^{2+}]_c$ response to hypo-osmotic shock involves a small element of intracellular Ca^{2+} release, the effects of lower concentrations of BAPTA were investigated (Fig. 3.11).

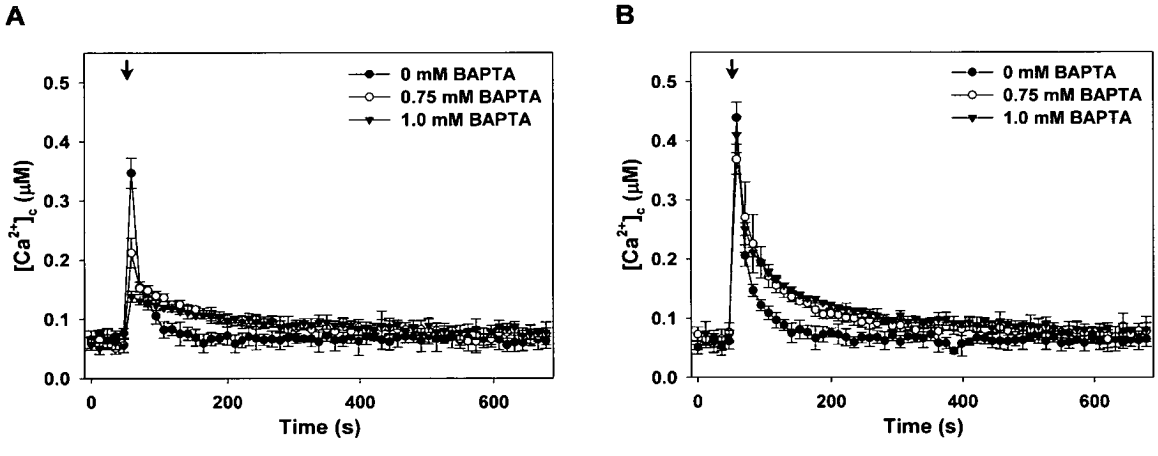

Fig. 3.11. $[Ca^{2+}]_c$ responses to mechanical perturbation and hypo-osmotic shock in the presence of low BAPTA concentrations **A.** $[Ca^{2+}]_c$ response to mechanical perturbation. **B.** The $[Ca^{2+}]_c$ response to hypo-osmotic shock. Arrows represent time of stimulus administration.

At 1 mM and 0.75 mM BAPTA there was a stimulus-specific effect on the Ca^{2+} responses to mechanical perturbation and hypo-osmotic shock (Fig. 3.11). At concentrations of > 1.5 mM the $[Ca^{2+}]_c$ responses to both stimuli were abolished (data not shown). The difference in the sensitivity of both responses to external $[Ca^{2+}]$ suggests that there may be variations in the mechanisms by which the $[Ca^{2+}]_c$ responses are generated.

3.2.3.7 Physiological response of germ tubes to mechanical perturbation – the hyphal swelling assay

The next stage of this work was to determine if germ tubes exhibited a physiological response to mechanical perturbation, and if the $[Ca^{2+}]_c$ and the physiological responses were part of the same signalling process. Germ tubes grown and subjected to mechanical stimulation were imaged with a 20 × dry objective in a clear plastic microwell plate.

When 6 h cultures of *N. crassa* were subjected to mechanical perturbation by injection of iso-osmotic growth media, swelling at the germ tube tip was observed in a large proportion of the cells (Fig. 3.12). Figure 3.12A shows an image of an unperturbed germ tube (control) recorded before administration of mechanical perturbation. Figure 3.12B shows a germ tube ~ 20 min after having been subjected to mechanical perturbation in which the tip of the germ tube has swollen. The emergence of a new hypha is also visible in this image and recovery of polarized growth typically began 20 min or more after mechanical perturbation.

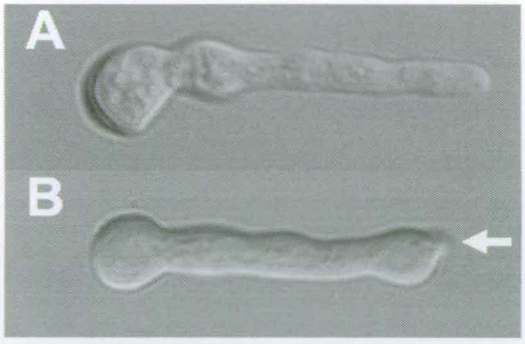

Fig. 3.12. Germ tube swelling caused by mechanical perturbation. **A.** Unperturbed germ tube with no hyphal swelling. **B.** Germ tube after mechanical perturbation. Note the emergence of a new germ tube from the swelling.

Mechanical perturbation appeared to temporarily disrupt polarized growth and cause a transient non-polar growth of germ tube tips. The extent of swelling varied between different germ tubes and due to the nature of the mechanical perturbation stimulus it was not possible to image a specific individual germ tube before and after the stimulus was administered.

Because of this variation, the swelling response was measured in populations of 6 h old germ tubes subjected to mechanical stimulation (Fig. 3.13). To assess the physiological response in more detail the method of microplate preparation used in the $[Ca^{2+}]_c$ assay was optimized for microscopy (section 2.6.3).

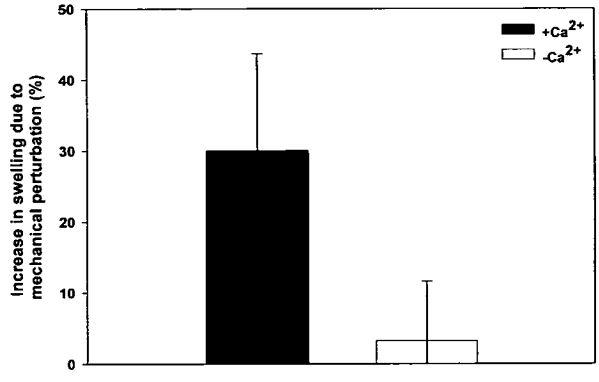

Fig. 3.13 Requirement of external Ca^{2+} for the germ tube swelling in response to mechanical perturbation. The y-axis represents the percentage increase in occurrence of swelling in germ tubes compared with the unperturbed control germ tubes.

The occurrence of swelling in response to mechanical perturbation was significantly higher than in unperturbed germ tubes (n = 6, $p < 0.05$) (Fig. 3.13). The mechanical perturbation stimulus responsible for the increase in apical swelling was identical to that used in $[Ca^{2+}]_c$ assays. To determine the involvement of the $[Ca^{2+}]_c$ response to mechanical perturbation in the swelling response, Ca^{2+}-free VgS medium was used. In Fig. 3.10, removal of external Ca^{2+} abolished the $[Ca^{2+}]_c$ response to mechanical perturbation and Fig. 3.13 shows it caused a clear and significant inhibition of apical swelling (n = 6, $p = < 0.01$). Despite the large inhibition of apical swelling, the failure of Ca^{2+} removal to completely abolish apical swelling provides evidence that other factors may be involved in this swelling response.

3.2.5 Conidial response to mechanical perturbation

In section 3.2.3.1, it was shown that insufficient aequorin was available for accurate measurement of $[Ca^{2+}]_c$ in the 0 h and 1 h cultures. In this section experiments are described in which possible changes in $[Ca^{2+}]_c$ were analysed in ungerminated conidia producing very low levels of aequorin.

At low levels of aequorin, the amount of luminescence detected during the response to mechanical perturbation may be very close to that of background luminescence. It was therefore possible that conidia do produce a $[Ca^{2+}]_c$ response to mechanical perturbation but because of the low levels of aequorin this response may not normally be detected.

In an attempt to increase the level of aequorin in a conidial suspension, inoculated clear plastic microwell plates were incubated in the dark at 4 °C for 0, 1, 2, 3, 4, 5, 6 and 24 h prior to luminometry. Percentage conidial germination and the $[Ca^{2+}]_c$ responses of the samples were analysed in plates prepared in parallel. Incubation at 4 °C had previously been found to increase aequorin production without affecting the $[Ca^{2+}]_c$ response to hypo-osmotic shock in *S. cerevisiae* (Batiza et al., 1996). For luminometry, microwell plates were transferred to the Microlumat luminometer (set to 24 °C) 10 min prior to experimentation to reach normal measurement temperature.

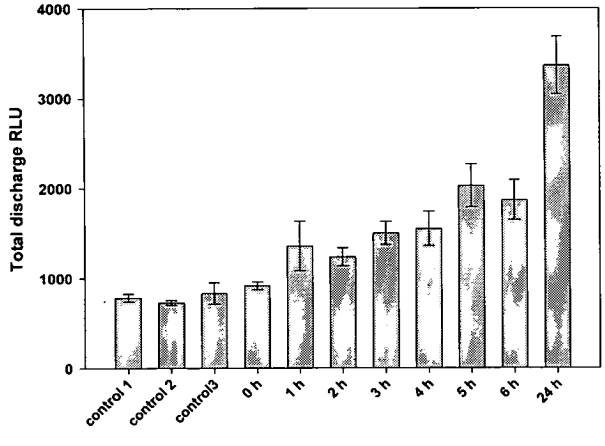

Fig. 3.14. Average total RLU in control RLU profiles and conidial suspenions subjected to standard discharge protocols. Control 1- injection of liquid VgS medium into liquid VgS medium; Control 2 – injection of liquid VgS medium into wild type *N. crassa* conidial suspension containing 2.5 μM coelenterazine; Control 3 – injection of liquid VgS into aequorin expressing *N. crassa* conidial suspensions in the absence of coelenterazine. n values for controls were all n = 30 and for all other experiments n = 6.

Discharging the total aequorin in conidial suspensions incubated for different periods at 4 °C showed that the amount of aequorin present increased with time (Fig. 3.14) despite there being no increase in germination (Fig. 3.15). Even after 24 h incubation at 4 °C, however, conidial suspensions did not produce enough luminescence (>7800 RLU) required for accurate calibration of $[Ca^{2+}]_c$ (see section 3.2.3.2). Nevertheless, mechanical perturbation of these conidial suspensions suggested that there might be a very small increase in luminescence at the time of mechanostimulation (Fig. 3.15).

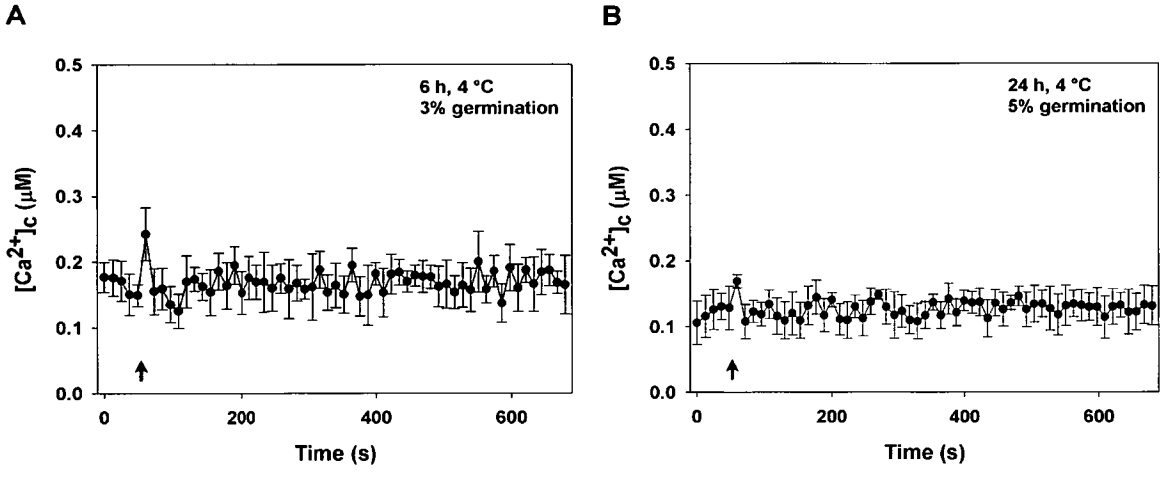

Fig. 3.15. $[Ca^{2+}]_c$ responses of conidia to mechanical perturbation. **A.** Response to mechanical perturbation after 6 h incubation at 4 °C. **B.** Response to mechanical perturbation after 24 h incubation at 4 °C. Arrows represent the application of the mechanical perturbation stimulus.

To investigate the possibility that the luminescence increase might have been caused by the injection of the mechanical perturbation stimulus, three controls were analysed: (1) injection of liquid VgS medium into a microwell plate containing liquid VgS medium on its own; (2) injection of liquid VgS medium into a microwell containing untransformed wild type *N. crassa* and 2.5 μM coelenterazine; and (3) injection of liquid VgS medium into a microwell containing liquid VgS medium with an aequorin-expressing *N. crassa* strain in the absence of coelenterazine.

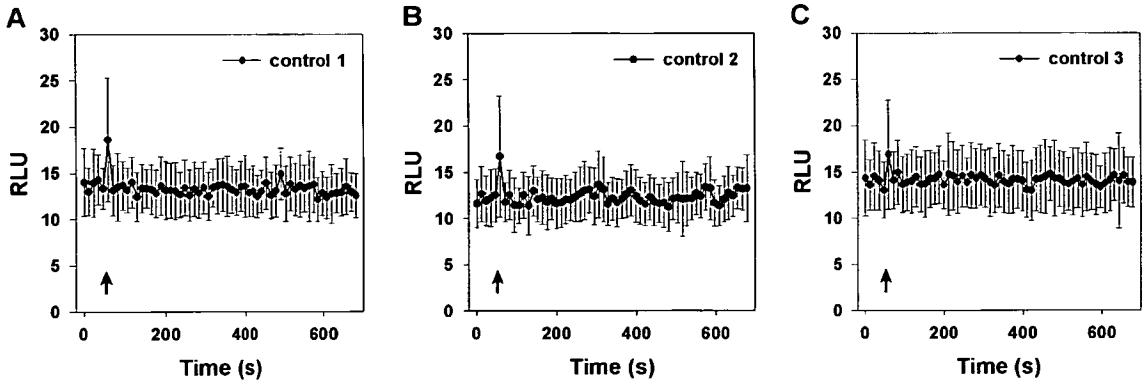

Fig. 3.16 RLU profiles of injection controls. Arrows represent time of injection. Individual controls are as follows:

A. injection of liquid VgS into Vogel's media

B. injection of liquid VgS into wild type *N. crassa* solution and 2.5 μM coelenterazine

C. injection of liquid VgS into aequorin expressing *N. crassa* strain 22A3AWTAZ6 in the absence of coelenterazine.

In each case the microwell plates were incubated in the dark at 24 °C for 6 h prior to luminometry. The mean RLU profiles are shown in Fig. 3.16. Despite the generation of aequorin luminescence being impossible for each treatment, injection of VgS media still caused a significant increase in luminescence in every control ($p = < 0.01$). Thus the very small increase in luminescence observed in Fig. 3.15 is an artefact due to the forceful addition of VgS liquid medium through the injectors into the microwell.

The results from these experiments demonstrate that conidia, in contrast to germ tubes or vegetative hyphae, do not produce a $[Ca^{2+}]_c$ response to mechanical perturbation.

3.3 Discussion

3.3.1 Germ tubes provide a sensitive and reliable population for $[Ca^{2+}]_c$ assays

Previous analyses of the $[Ca^{2+}]_c$ responses in filamentous fungi using the aequorin $[Ca^{2+}]_c$ assay have used established mature hyphal colonies. The results obtained here demonstrate that 6 h old cultures containing germ tubes produce more reproducible results and are thus more suitable for the aequorin assay. After a 6 h incubation germ tubes contained sufficient aequorin for accurate and reliable $[Ca^{2+}]_c$ measurement. When aequorin consumption in an experiment represents a large proportion of the available aequorin present, the linear relationship between aequorin luminescence and Ca^{2+} binding may be adversely affected (Zelter, 2004). For this purpose the previously developed term-bert software for $[Ca^{2+}]_c$ calibration (section 2.7.4) flags any experiment in which aequorin consumption exceeds 50% of total available aequorin. Results obtained here indicated that when the total aequorin produced < 7800 RLU then the resting $[Ca^{2+}]_c$ calculated was artificially increased.

3.3.2 $[Ca^{2+}]_c$ responses to mechanical perturbation and hypo-osmotic shock

Previous work has examined the $[Ca^{2+}]_c$ responses to three stimuli administered by automated injection. Of these stimuli, mechanical perturbation was the only stimulus that did not contain an element of the other stimuli. For this reason it was selected for more thorough examination. Removing Ca^{2+} from the external medium was found to inhibit both the $[Ca^{2+}]_c$ responses to mechanical perturbation and hypo-osmotic shock although inhibition of the latter was only partial.

Although the difference in FWHM between hypo-osmotic shock and mechanical perturbation was small, it was consistent and significant. These findings suggest that the kinetics, and the Ca^{2+} signalling proteins involved in each, of the two $[Ca^{2+}]_c$ responses may differ. Hypo-osmotic stress has been previously used to apply membrane tension to *N. crassa* hyphae (Silverman-Gavrila and Lew, 2003). Increased membrane tension may alter the activation of stretch activated CPCs which may be involved in Ca^{2+} influx. Although the differences between the $[Ca^{2+}]_c$ responses were small, the different results obtained with BAPTA suggest that chemical $[Ca^{2+}]_c$ modulators may assist in distinguishing the different components of the Ca^{2+} signalling machinery that are responsible for the generation of the different Ca^{2+} signatures.

3.3.3 Germ tubes respond to mechanical perturbation by Ca^{2+} dependent apical swelling

Mechanical perturbation resulted in a reproducible increase in apical germ tube swelling. The connection between the physiological and $[Ca^{2+}]_c$ response was established by removal of Ca^{2+} from the media. Previous studies on the effects of mechanical perturbation have focussed solely on the $[Ca^{2+}]_c$ response. Mechano-stimulation of germ tube tips by using optical tweezers to trap a bead in the path of a growing germ tube tip was found to cause transient cessation of apical extension and swelling at the tip (Wright *et al.*, 2007). These effects show striking similarity to those caused by the injection of iso-osmotic media into a microwell culture. A relationship between Ca^{2+} influx and hyphal swelling is further supported by A23187 treatment which was found to cause apical swelling in *N. crassa* (Reissig and Kinney, 1983).

The apical $[Ca^{2+}]_c$ gradient identified in *N. crassa* (Levina *et al.*, 1995; Silverman-Gavrila and Lew, 2000; Silverman-Gavrila *et al.*, 2003) may represent a potential mechanism by which the swelling and $[Ca^{2+}]_c$ responses to mechanical perturbation are connected. The $[Ca^{2+}]_c$ transient initiated by mechanical perturbation may temporarily disrupt this

gradient leading to the cessation of growth and apical swelling. A potential sensor for the mechanical perturbation stimulus may be the predicted stretch activated CPCs identified in *N. crassa* hyphae (Levina *et al.*, 1995).

Despite the large inhibition of swelling due to the removal of Ca^{2+}, the swelling response was not completely abolished. This suggests there may be additional components involved in the swelling response to mechanical perturbation. A possible candidate may be the actin cytoskeleton which has previously been connected to Ca^{2+} signalling in *N. crassa* (Silverman-Gavrila and Lew, 2001). A further potential candidate may be integrin proteins which are involved in the thigmotropic induction of appressoria formation in *Uromyces appendiculatus* (Corrêa *et al.*, 1996).

3.3.4 Summary of results

- Germ tubes and vegetative hyphae produce distinct $[Ca^{2+}]_c$ responses to mechanical perturbation, hypo-osmotic shock and high external Ca^{2+}.

- Conidia do not respond to mechanical perturbation with a $[Ca^{2+}]_c$ transient.

- Germ tubes from 6 h old cultures provide more reproducible and reliable measurements of $[Ca^{2+}]_c$ for the aequorin $[Ca^{2+}]_c$ assay than older vegetative hyphae.

- Germ tubes respond to mechanical perturbation by Ca^{2+} dependent apical swelling.

Chapter 4

Effects of anti-fungal proteins on the $[Ca^{2+}]_c$ responses to mechanical perturbation and hypo-osmotic shock

4.1 Introduction

The production of small, antimicrobial peptides by animals, plants and fungi is a widespread mechanism for defence against microorganisms (Broekaert *et al.*, 1995).

Defensins are an important class of these antimicrobial peptides and have been found in mammals, insects and plants (Broekaert *et al.*, 1995). Plant defensins are cysteine rich, typically between 45 to 54 amino acids long, and influence fungal morphogenesis in different ways suggesting different mechanisms of antifungal action (Gu *et al.*, 1995; Osborn *et al.*, 1995; Broekaert *et al.*, 1995). Plant defensins were divided into several classes based upon the nature of their antifungal effects. 'Morphogenic defensins' inhibit hyphal elongation with a concomitant increase in hyphal branching whilst the 'non-morphogenic defensins' only inhibit hyphal elongation (Osborn *et al.*, 1995; Thevissen *et al.*, 1996).

A role for Ca^{2+} in the antifungal mode of action of plant defensins was first suggested because the addition of Ca^{2+} inhibited the antifungal activity of several defensins. Inhibition varied between species and defensins providing further support for different modes of action (Osborn *et al.*, 1995). Two plant defensins, the morphogenic RsAFP2 from *Raphanus sativus* and the nonmorphogenic DmAMP1 from *Dahlia merckii*, were found to increase Ca^{2+} accumulation in both *N. crassa* and *Fusarium colmorum* (Thevissen *et al.*, 1996). Both defensins also caused a small but significant alkalinisation of the external medium and K^+ efflux from the treated fungal cells. Significantly, the Ca^{2+} uptake by *F. culmorum* was shown to be required for RsAFP2 antifungal activity (De Samblanx *et al.*, 1997). A modified form of RsAFP2 was found to have both increased antifungal activity and cause increased Ca^{2+} uptake by the fungal cells (De Samblanx *et al.*, 1997). The increased Ca^{2+} uptake in these experiments was measured using the $^{45}Ca^{2+}$ technique (Thevissen *et al.*, 1996; De Samblanx *et al.*, 1997). Increased Ca^{2+} uptake has been proposed to inhibit hyphal growth by disruption of the apical $[Ca^{2+}]_c$ gradient in growing hyphae of *N. crassa* (Levina *et al.*, 1995; Thevissen *et al.*, 1996). Despite the findings of increased Ca^{2+} uptake, no direct measurements of $[Ca^{2+}]_c$ in living fungal cells have been previously made.

This evidence, and the inability of RsAFP2 and DmAMP1 to form pores in artificial membranes, led to the proposal of a mechanism for the mode of action of RsAFP2 (Thevissen *et al.*, 1996; Thevissen *et al.*, 2003a). This mechanism involves RsAFP2

interacting with a receptor in the fungal plasma membrane. It was proposed that the receptor may mediate antifungal activity by transduction of a signal or facilitate insertion of RsAFP2 into the membrane resulting in ion channel formation. A single defensin binding receptor may mediate the effects of many defensins in *N. crassa*, and defensins may bind the receptor with different affinities or at different subsites of this receptor (Thevissen *et al.*, 1997). There is growing evidence that membrane lipids may act as a defensin binding receptor (Thevissen *et al.*, 2000; Thevissen *et al.*, 2003b; Thevissen *et al.*, 2004). RsAFP2 specifically interacts with glucosyl ceramide in *Pichia pastoris* membranes (Thevissen *et al.*, 2004). This interaction is required for growth arrest and membrane permeabilization in the antifungal action of this defensin (Thevissen *et al.*, 2004). The glucosyl ceramide content of membranes had no effect on DmAMP1 antifungal activity and the interaction of DmAMP1 with sphingolipids in *S. cerevisiae* membranes was not required for this antifungal activity (Thevissen *et al.*, 2000; Thevissen *et al.*, 2003a).

Other antifungal plant defensins reported to alter $[Ca^{2+}]_c$ homeostasis include the morphogenic MsDef1 isolated from *Medicago sativa* (Spelbrink *et al.*, 2004). MsDef1 was found to inhibit mammalian L-type Ca^{2+} channel activity in a similar fashion to the structurally unrelated antifungal protein KP4 (Spelbrink *et al.*, 2004). KP4 is a virally encoded antifungal toxin produced by infected strains of *Ustilago maydis* which inhibits voltage gated, L-type Ca^{2+} channel activity in mammalian cells (Gu *et al.*, 1995). The involvement of Ca^{2+} signalling in the KP4 mechanism of action is supported by the abolition of its antifungal activity by the addition of exogenous Ca^{2+} (Gu *et al.*, 1995; Gage *et al.*, 2001). KP4 inhibits growth by reversible binding to *U. maydis* which is believed to inhibit Ca^{2+} uptake via Ca^{2+} channel inhibition (Gage *et al.*, 2001).

In chapter 3 of this study $[Ca^{2+}]_c$ responses to mechanical perturbation and hypo-osmotic shock were identified and characterized in germ tubes. Evidence from experiments in which Ca^{2+} was removed from the external medium suggested that the two responses may be generated by different mechanisms. The aims of this chapter were: (1) to determine the effects of antifungal proteins on $[Ca^{2+}]_c$ homeostasis in *N. crassa*; and (2) to identify

differences in the effects of these antifungal proteins on Ca^{2+} signatures to mechanical perturbation and hypo-osmotic shock.

4.2 Results

To characterise the effects of four plant defensins and KP4, $[Ca^{2+}]_c$ responses to mechanical perturbation and hypo-osmotic shock were assayed at two protein concentrations. It has been reported that defensin concentrations > 10 μM typically cause a large, cation sensitive, membrane permeabilization whilst permeabilization at lower defensin concentrations is more resistant to increased cation strength (Thomma *et al.*, 2003). Permeabilization of fungal membranes with defensins at concentrations above 10 μM is believed to be independent of the interaction of defensins with receptors in the plasma membrane (Thevissen *et al.*, 1999). Therefore, in order to provide a reliable and accurate assessment of the defensin effects on the Ca^{2+} signalling machinery and homeostasis in *N. crassa*, all antifungal proteins were assayed at 1 μM and 4 μM.

4.2.1 Effects of MsDef1 on the $[Ca^{2+}]_c$ responses to mechanical perturbation and hypo-osmotic shock

MsDef1, isolated from *M. sativa*, is a morphogenic plant defensin that inhibited growth of *F. graminearum* by inducing hyphal hyper branching (Spelbrink *et al.*, 2004).

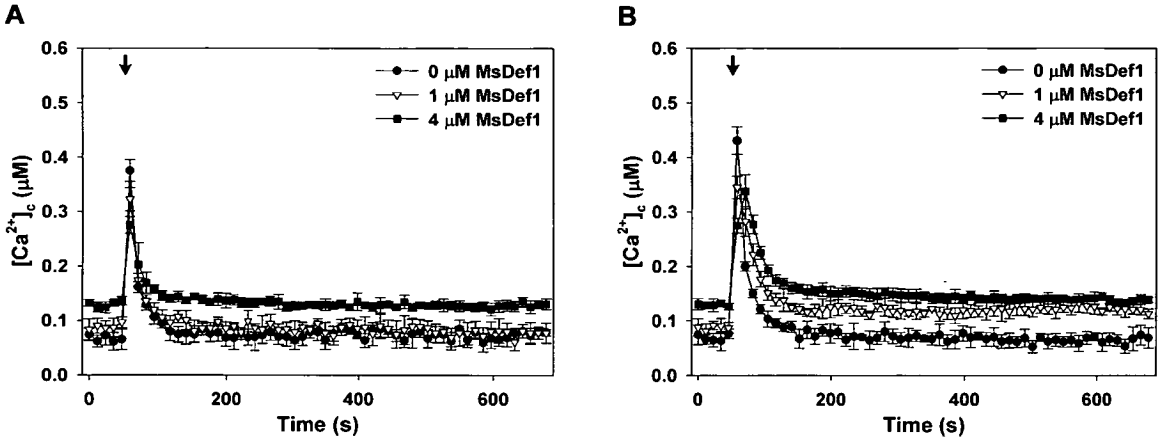

Fig. 4.1. A. Effects of MsDef1 on the $[Ca^{2+}]_c$ response to mechanical perturbation. **B.** Effects of MsDef1 on the $[Ca^{2+}]_c$ response to hypo-osmotic shock. Arrows at 57 s represent time of stimulus administration.

MsDef1 caused significant inhibition ($p = < 0.01$) of the amplitude of the $[Ca^{2+}]_c$ responses to mechanical perturbation and hypo-osmotic shock (Fig. 4.1). MsDef1 also caused a concentration dependent increase in resting $[Ca^{2+}]_c$ (Fig. 4.1). The $[Ca^{2+}]_c$ response to hypo-osmotic shock was more prolonged in the presence of MsDef1 and, in the presence of 4 µM MsDef1 the time to reach the maximum amplitude was delayed by 11.51 s (Fig. 4.1B). At both concentrations of MsDef1 the return to the elevated resting $[Ca^{2+}]_c$ was completed 10 min after mechanical perturbation, but not after hypo-osmotic shock was applied.

4.2.2 Effects of MtDef2 on the $[Ca^{2+}]_c$ responses to mechanical perturbation and hypo-osmotic shock

MtDef2 isolated from *Medicago truncatula* had previously been found to little antifungal activity against *N. crassa* despite exhibiting significant similarity in its molecular structure to MsDef1 (Spelbrink *et al.*, 2004).

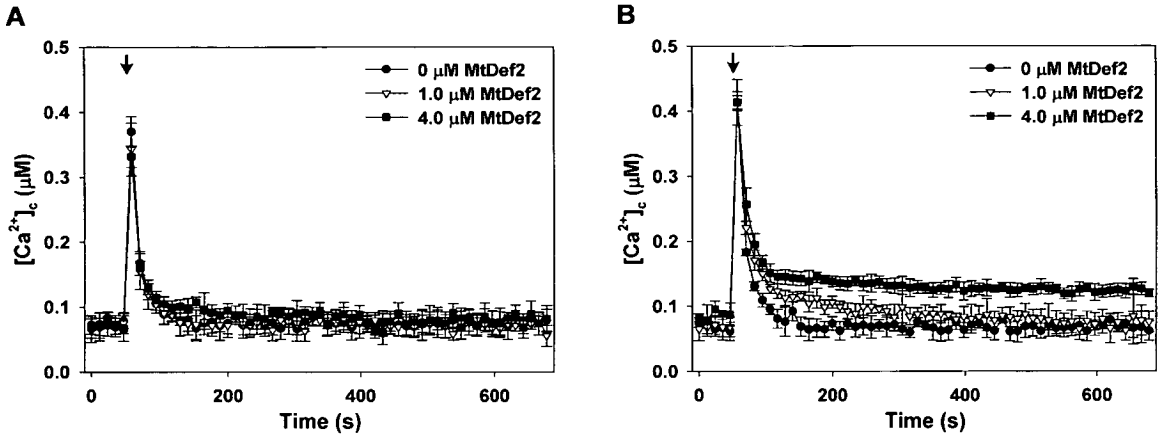

Fig. 4.2. A. Effects of MtDef2 on the $[Ca^{2+}]_c$ response to mechanical perturbation. **B.** Effects of MtDef2 on the $[Ca^{2+}]_c$ response to hypo-osmotic shock. Arrows at 57 s represent time of stimulus administration.

MtDef2 had no significant effect on the $[Ca^{2+}]_c$ amplitudes in response to both mechanical perturbation and hypo-osmotic shock (Fig. 4.2). Resting $[Ca^{2+}]_c$ was only increased after hypo-osmotic shock when 4 μM MtDef2 was applied (Fig. 4.2B).

4.2.3 Effects of MtDef4 on the $[Ca^{2+}]_c$ responses to mechanical perturbation and hypo-osmotic shock

MtDef4, isolated from *M. truncatula* is a non-morphogenic defensin that caused potent inhibition of conidial germination in *Fusarium graminearum* germination but did not induce hyphal hyper branching (Ramamoorthy *et al.*, 2007).

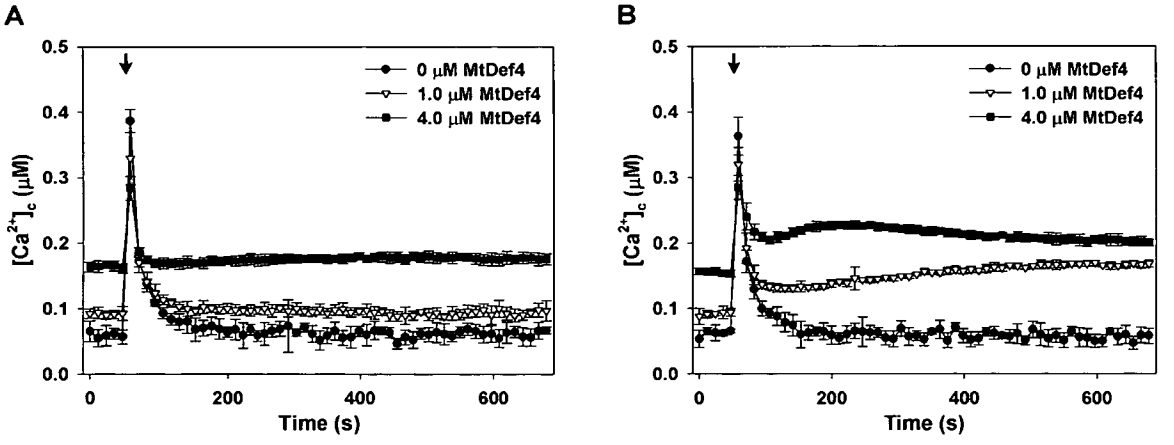

Fig. 4.3. A. Effects of MtDef4 on the $[Ca^{2+}]_c$ response to mechanical perturbation. **B.** Effects of MtDef4 on the $[Ca^{2+}]_c$ response to hypo-osmotic shock. Arrows at 57 s represent time of stimulus administration.

MtDef4 caused significant inhibition ($p = < 0.01$) of the amplitude of the $[Ca^{2+}]_c$ responses to mechanical perturbation and hypo-osmotic shock when applied at both 1 µM and 4 µM concentrations (Fig. 4.3). There was consistently a small increase in resting $[Ca^{2+}]_c$ with 1 µM MtDef4 and a much larger increase when 4 µM was applied (Fig. 4.3). This increase in resting $[Ca^{2+}]_c$ was larger than that caused by MsDef1. In contrast to MsDef1, the maximum $[Ca^{2+}]_c$ in response to hypo-osmotic shock was not delayed by 4 µM MtDef4. However after an initial reduction in the $[Ca^{2+}]_c$, a small but extended secondary $[Ca^{2+}]_c$ transient was observed (Fig. 4.3B). At both concentrations of MtDef4 the return to resting $[Ca^{2+}]_c$ was complete 10 min after mechanical perturbation but not hypo-osmotic shock.

4.2.4 Effects of RsAFP2 on the $[Ca^{2+}]_c$ responses to mechanical perturbation and hypo-osmotic shock

RsAFP2, isolated from *R. sativus*, is a morphogenic plant defensin that inhibited growth of *F. graminearum* by inducing hyphal hyper branching (Spelbrink *et al.*, 2004).

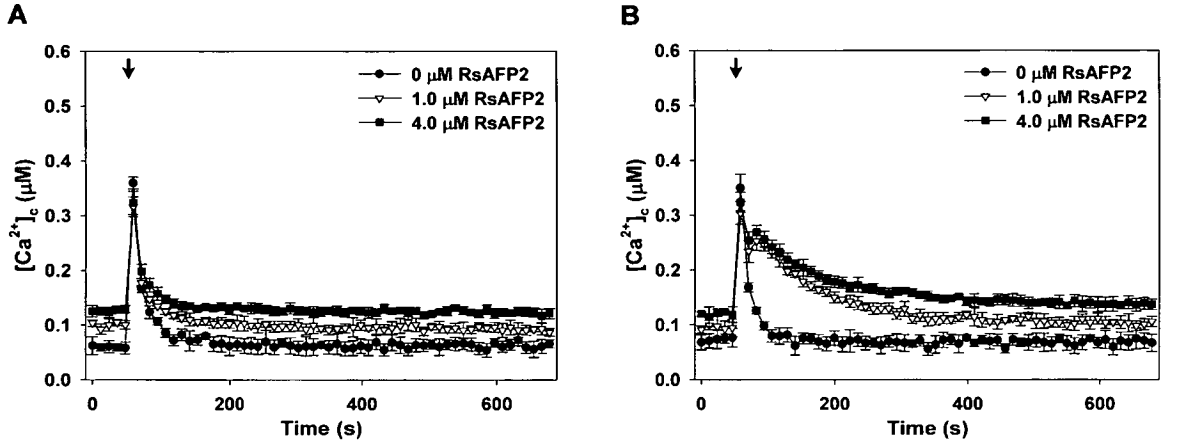

Fig. 4.4. A. Effects of RsAFP2 on the $[Ca^{2+}]_c$ response to mechanical perturbation. **B.** Effects of RsAFP2 on the $[Ca^{2+}]_c$ response to hypo-osmotic shock. Arrows at 57 s represent time of stimulus administration.

One µM and 4 µM RsAFP2 significantly inhibited ($p = < 0.01$) the amplitudes of the $[Ca^{2+}]_c$ responses to mechanical perturbation and hypo-osmotic shock (Fig. 4.4). RsAFP2 increased the resting $[Ca^{2+}]_c$ and this was concentration dependent (Fig. 4.4). As with MsDef1, MtDef2 and MtDef4 (Figs. 4.1-4.3), the elevated $[Ca^{2+}]_c$ recovered within 10 min after the application of mechanical perturbation but not after hypo-osmotic shock. The $[Ca^{2+}]_c$ response to hypo-osmotic shock was biphasic in the presence of RsAFP2 with a small $[Ca^{2+}]_c$ peak following an initial larger $[Ca^{2+}]_c$ peak (Fig. 4.4B).

4.2.5 Effects of KP4 on the $[Ca^{2+}]_c$ responses to mechanical perturbation and hypo-osmotic shock

The antifungal protein, KP4, produced by *U. maydis*, inhibits voltage gated, L-type Ca^{2+} channel activity in mammalian cells (Gu *et al.*, 1995) and inhibits growth by dose dependent hyper branching of *F. graminearum* hyphae (Spelbrink *et al.*, 2004).

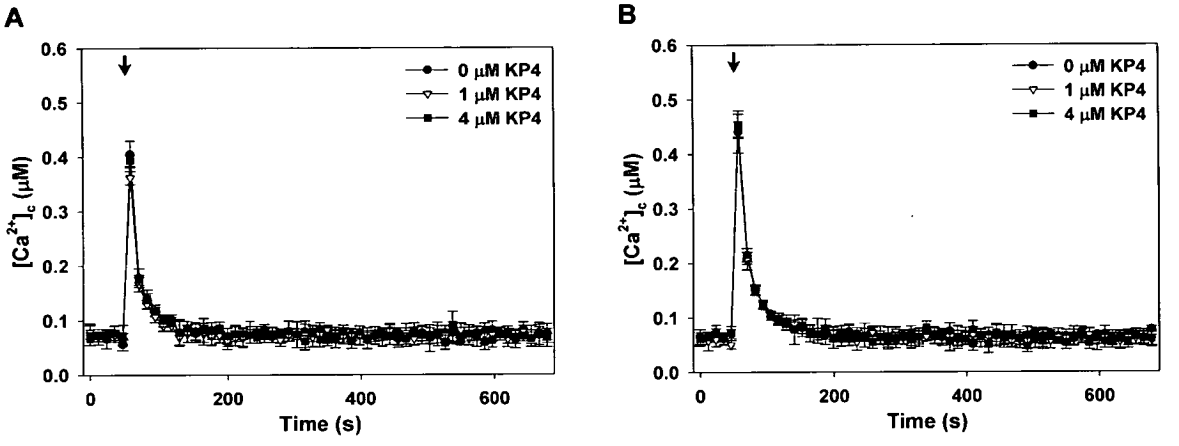

Fig. 4.5. A. Effects of KP4 on the $[Ca^{2+}]_c$ response to mechanical perturbation. **B.** Effects of KP4 on the $[Ca^{2+}]_c$ response to hypo-osmotic shock. Arrows at 57 s represent time of stimulus administration.

KP4 caused no significant or reproducible effect on the $[Ca^{2+}]_c$ responses to mechanical perturbation or hypo-osmotic shock and resting $[Ca^{2+}]_c$ (Fig. 4.5).

4.2.6 Comparison of defensin effects on the $[Ca^{2+}]_c$ responses to mechanical perturbation and hypo-osmotic shock

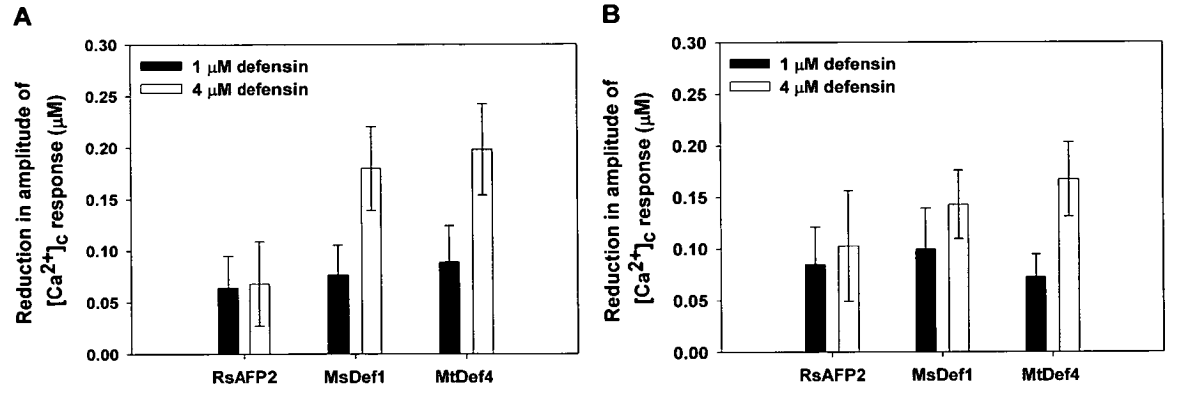

Fig. 4.6. Effects of 1 μM and 4 μM RsAFP2, MsDef1 and MtDef4 on the amplitudes of the $[Ca^{2+}]_c$ responses to mechanical perturbation and hypo-osmotic shock. Data from each well from all $[Ca^{2+}]_c$ assays with the different defensins were compiled, and means

and standard deviations were plotted (n = 18). **A.** Reduction in amplitude of the $[Ca^{2+}]_c$ response to mechanical perturbation. **B.** Reduction in amplitude of the $[Ca^{2+}]_c$ response to hypo-osmotic shock.

MsDef1 and MtDef4 caused large, dose dependent reduction in the amplitudes of the $[Ca^{2+}]_c$ responses to mechanical perturbation and hypo-osmotic shock (Fig. 4.6). The inhibition of the $[Ca^{2+}]_c$ amplitude caused by RsAFP2 was less affected by defensin concentration, especially in the $[Ca^{2+}]_c$ response to mechanical perturbation (Fig. 4.6).

4.3 Discussion

4.3.1 The effects of antifungal proteins on Ca^{2+} signalling in *N. crassa*

The increased resting $[Ca^{2+}]_c$ and inhibition of the amplitude of the $[Ca^{2+}]_c$ response to mechanical perturbation after treatment with MsDef1 support the findings of Spelbrink *et al.* (2004) who demonstrated that MsDef1 inhibited L-type Ca^{2+} channel activity in mammalian cells and increased the accumulation of $^{45}Ca^{2+}$ by hyphae of *N. crassa.* Spellbrink *et al.* (2004). Increased Ca^{2+} uptake was also observed after treatment with four known Ca^{2+} channel blockers, including KP4, leading to the proposal that the increased Ca^{2+} uptake was an artefact of the methodology. My data showed that the $[Ca^{2+}]_c$ resting level was increased (Fig. 4.1) suggesting that MsDef1 either permeabilizes *N. crassa* germlings allowing Ca^{2+} entry or inhibited the active efflux of Ca^{2+} from the cytoplasm (Fig. 4.1). Although there was not complete inhibition of amplitude with 4 μM MsDef1 treatment, 10 μM MsDef1 was previously shown to be required to block 90% of Ca^{2+} current through the $Ca_v1.2$ L-type Ca^{2+} channels in mammalian cells (Spelbrink *et al.*, 2004). Despite increasing $^{45}Ca^{2+}$ accumulation in *F. graminearum* (Spelbrink et al., 2004) and inhibiting the $[Ca^{2+}]_c$ response to hypo-osmotic shock in *Aspergillus awamori* (Nelson et al., 2004) KP4 had no effect on the $[Ca^{2+}]_c$ responses or resting $[Ca^{2+}]_c$ in this study.

RsAFP2, MtDef4 and MsDef1 were all found to inhibit the amplitude of the $[Ca^{2+}]_c$ responses to mechanical perturbation and hypo-osmotic shock. Of these defensins, only MsDef1 has previously been found to inhibit Ca^{2+} channel activity (Spelbrink *et al.*, 2004). As these defensins increased resting $[Ca^{2+}]_c$, the inhibition of Ca^{2+} influx may be due to permeabilization of the plasma membrane or perturbation of the $[Ca^{2+}]_c$ homeostatic mechanism (e.g. by inhibition of a Ca^{2+} pump or Ca^{2+} antiporter). Increased growth inhibition may be linked to either of these processes occurring and there is a clear correlation between the dose response curves for growth inhibition and Ca^{2+} uptake for RsAFP2 (Thevissen *et al.*, 1996). Proteins with potent antifungal activity against both *N. crassa* and *F. graminearum* (Spelbrink et al., 2004; Dilip Shah, personal communication), namely MsDef1, MtDef4 and RsAFP2, had severe effects on the $[Ca^{2+}]_c$ responses to mechanical perturbation and hypo-osmotic shock and resting $[Ca^{2+}]_c$ in this study. MtDef2 and KP4 were less potent in inhibiting fungal growth (Spelbrink *et al.*, 2004) and had little, if any, effects on Ca^{2+} signalling in *N. crassa*. The findings of this work and of previous investigations provide strong evidence of correlation between antifungal activity and perturbation of Ca^{2+} signalling and Ca^{2+} homeostasis.

4.3.2 Mechanical perturbation and hypo-osmotic shock

The more pronounced effects of defensins on the $[Ca^{2+}]_c$ response to hypo-osmotic shock may be due to osmotic stress increasing plasma membrane permeabilization. Application of various plant defensins to *N. crassa* resulted in more rapid permeabilization to SYTOX green in water than in growth media (Thevissen *et al.*, 1999). Resting $[Ca^{2+}]_c$ after application of hypo-osmotic shock was increased by MsDef1, MtDef2, MtDef4 and RsAFP2, suggesting that following this treatment the germ tubes were more impaired in their $[Ca^{2+}]_c$ homeostatic mechanisms, perhaps because of increased permeability of their plasma membrane.

Hypo-osmotic stress applied to germlings may cause influx of water into the fungal cells potentially resulting in cell swelling and increased tension of the plasma membrane. If

defensins form pores in the plasma membrane as previously suggested (Thevissen *et al.*, 2003a), increased tension may result in a greater opening of these pores and therefore a greater influx of Ca^{2+} into the cytoplasm. This membrane tension may also increase the flux through CPCs activated by the application of hypo-osmotic shock, resulting in the increased FWHM for the $[Ca^{2+}]_c$ responses to hypo-osmotic shock in both vegetative hyphae and germ tubes (sections 3.2.2 and 3.2.3.3). Hypo-osmotic shock may result in the activation of different Ca^{2+} pump and transporter proteins that remove Ca^{2+} from the cytoplasm compared to those activated by mechanical perturbation. Reduced activation of these proteins in response to hypo-osmotic shock could explain both the increased FWHM in the absence of defensins and the increased resting $[Ca^{2+}]_c$ after hypo-osmotic shock in the presence of MsDef1, RsAFP2, MtDef2 or MtDef4.

4.3.3 Mechanism of antifungal protein action

The increased resting $[Ca^{2+}]_c$ that resulted from the addition of each of the defensins used here suggest that they may be inserted into the plasma membrane as had been previously suggested for DmAMP1 (Thevissen *et al.*, 2000). The increase in resting $[Ca^{2+}]_c$ was similar in both MsDef1 and RsAFP2 treatment and both treatments caused an increased duration in the $[Ca^{2+}]_c$ response to hypo-osmotic shock. Alkalinization of the external medium by RsAFP2 treatment (Thevissen *et al.*, 1996) could not have caused the increased resting $[Ca^{2+}]_c$ in Fig. 4.4 as the previously reported alkalinization was at pH levels far below those found to increase resting $[Ca^{2+}]_c$ in section 3.2.3.5. MtDef4 caused a greater increase in resting $[Ca^{2+}]_c$ than the other defensins although the effect on the $[Ca^{2+}]_c$ response to hypo-osmotic shock was notably different to both RsAFP2 and MsDef1. Despite its low antifungal activity against *N. crassa*, MtDef2 still increased resting $[Ca^{2+}]_c$ although only after hypo-osmotic shock. The differential effects of the four defensins on the $[Ca^{2+}]_c$ responses to mechanical perturbation and hypo-osmotic shock suggest they may target different proteins in *N. crassa*. The common increase in resting $[Ca^{2+}]_c$ observed after defensin treatment suggests a shared basic mechanism of interaction with the plasma membrane although this interaction may occur at different

sites or involve different lipids or receptors. If the defensins bind to different sites on the plasma membrane they may come into contact with different proteins (e.g. MtDef4 and MsDef1 may directly or indirectly interact with CPCs because both defensins inhibited the amplitudes of the $[Ca^{2+}]_c$ responses in this study).

Despite significantly increasing the resting $[Ca^{2+}]_c$, MtDef4 did not induce hyphal hyper branching in *F. graminearum* (Ramamoorthy *et al.*, 2007) suggesting that increased $[Ca^{2+}]_c$ does not provide a signal for hyphal branching. This finding is consistent with recent results obtained by Zelter (2004) who found that hyphal hyper branching in the *spray*, *frost* and *cot-1* mutants was not accompanied by increases in resting $[Ca^{2+}]_c$. The hyper branching response of *N. crassa* to MtDef4 and MsDef1 may be regulated by MAP kinase signalling. Disruption of MAP kinase signalling in *F. graminearum* resulted in increased sensitivity to these defensins (Ramamoorthy *et al.*, 2007). Recent evidence has revealed that the *Pisum sativum* defensin 1 (Psd1) inhibits cell cycle progression via interaction with a cyclin F protein (Lobo *et al.*, 2007). If permeabilization of the plasma membrane is required for the internalization of defensins, perturbation of $[Ca^{2+}]_c$ homoeostasis may be a bi-product of defensin action and not the cause of antifungal activity.

4.4 Summary

The main findings of this chapter were:

- Defensin antifungal plant proteins increased resting $[Ca^{2+}]_c$ in *N. crassa.*
- Perturbation of $[Ca^{2+}]_c$ homeostasis by antifungal proteins correlates with potency of fungal growth inhibition.
- Defensins have differential effects on the $[Ca^{2+}]_c$ responses to mechanical perturbation and hypo-osmotic shock suggesting that different components of the Ca^{2+} signalling machinery contribute to their Ca^{2+} signatures
- Both morphogenic and nonmorphogenic defensins are capable of increasing $[Ca^{2+}]_c$ yet only the morphogenic defensins increase hyphal branching.

Chapter 5

Investigation of the Ca^{2+} signalling machinery involved in the responses to mechanical perturbation and hypo-osmotic shock

5.1 Introduction

Mechanical stimulation and hypo-osmotic shock by media injection have been shown to induce $[Ca^{2+}]_c$ transients with highly reproducible Ca^{2+} signatures in hyphae of filamentous fungi (Nelson *et al.*, 2004; Zelter, 2004; Bencina *et al.*, 2005). In both germ tubes and vegetative hyphae of *N. crassa* the $[Ca^{2+}]_c$ response to hypo-osmotic shock had a greater FWHM than the response to mechanical perturbation (Chapter 3; Zelter, 2004). Removal of external Ca^{2+} (section 3.2.3.6, Fig. 3.10) and treatment with four defensin plant proteins (Chapter 4) had stimulus specific effects on the $[Ca^{2+}]_c$ responses to the two stimuli. This suggested the $[Ca^{2+}]_c$ responses may be generated by different mechanisms and potentially involve different components of the Ca^{2+} signalling machinery. *Neurospora crassa* possesses many predicted Ca^{2+} signalling proteins that may influence $[Ca^{2+}]_c$ (Zelter *et al.*, 2004), and the activity of these proteins may differ in the $[Ca^{2+}]_c$ responses to mechanical perturbation and hypo-osmotic shock.

The aims of the research described in this chapter were: (1) to express codon optimized aequorin and measure $[Ca^{2+}]_c$ in deletion mutants in which genes encoding different components of the Ca^{2+} signalling machinery had been deleted; (2) by using these deletion mutants, to identify proteins responsible for generating the $[Ca^{2+}]_c$ responses of germ tubes to mechanical perturbation and hypo-osmotic shock; (3) to determine if responses to these stimuli involve different components of the Ca^{2+} signalling machinery; (4) to determine which proteins were involved in both the $[Ca^{2+}]_c$ and germ tube swelling responses to mechanical perturbation.

5.2 Results

5.2.1 Transformation of *Neurospora* wt 74A and deletion mutants with pAB19

To identify proteins involved in the $[Ca^{2+}]_c$ response to mechanical perturbation a range of deletion mutants were transformed with the pAB19 plasmid (as described in section 2.8). Transformants were screened for aequorin expression and homokaryons were purified from 8-12 of these heterokaryotic aequorin expressing strains (section 2.8.3). The purified homokaryotic transformants were then analysed for aequorin expression and conidial germination (section 2.8.3). For a strain to be suitable for analysis of $[Ca^{2+}]_c$ responses, a germination rate that was > 90% and total discharge of aequorin that generated luminescence > 8000 RLUs in germ tubes 6 h after inoculation, was required.

Knock out strains encoding the following predicted proteins were selected: MID-1 (a CPC), YVC-1 (a CPC), ENA-1 (a cation ATPase), PH-7 (a cation ATPase) and CAX (a Ca^{2+}/H^+ exchanger). Two knockout strains that would have been desirable to transform with the aequorin gene (Δ*cch1* that lacked the CPC, CCH-1, and Δ*nca-1* that lacked the Ca^{2+}-ATPase, NCA-1) were ascospore lethal and only available as heterokaryons in the Δ*mus* genetic background (see section 1.3.2). Ascospore lethal heterokaryons could not be transformed with the plasmids used in this study as they carried both ignite and hygromycin resistance markers. To overcome these problems, the roles of CCH-1 and NCA-1 were analysed by disrupting their activity with pharmacological inhibitors.

5.2.3 Use of elevated coelenterazine concentrations in deletion mutants transformed with aequorin

Despite homokaryon purification and optimization of the $[Ca^{2+}]_c$ assay, it was not

possible to achieve sufficient aequorin luminescence in all strains using 2.5 μM coelenterazine that had been previously optimized for the aequorin assay in *Aspergillus awamori* (Nelson, 1999).

To determine if an increased coelenterazine concentration could be used to increase the aequorin luminescence in *N. crassa*, the amount of aequorin luminescence obtained after total aequorin discharge was compared after the conidial germlings were incubated with 2.5 μM or 10 μM coelenterazine. Increasing the coelenterazine concentration to 10 μM caused no significant increase in background luminescence but increased the total discharge luminescence by an average factor of 5.6 in 3 aequorin transformed strains (wild type, wt74Ap37b; Δ*cax*, 11249p15a2a; and Δ*ph-7*, 11256p16b1a3).

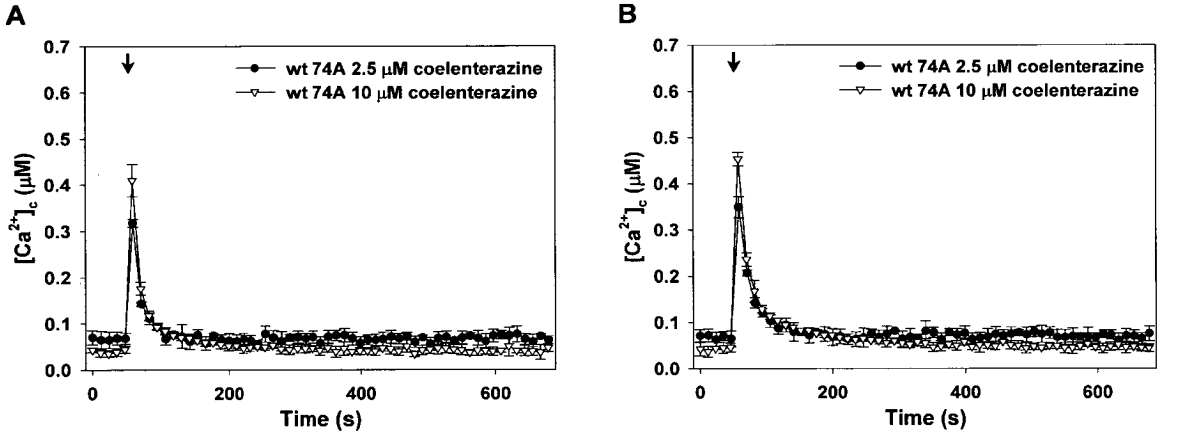

Fig. 5.2. $[Ca^{2+}]_c$ responses of aequorin expression wild type *N. crassa* to mechanical perturbation and hypo-osmotic shock at 2.5 μM and 10 μM coelenterazine. **A.** $[Ca^{2+}]_c$ response to mechanical perturbation. **B.** $[Ca^{2+}]_c$ response to hypo-osmotic shock. Arrows represent points of stimulus administration.

In all experiments 10 μM coelenterazine decreased resting $[Ca^{2+}]_c$ (Fig. 5.2). This finding correlates with results presented in section 3.2.3.2 in which increased levels of luminescence resulting from complete aequorin discharge decreased the resting $[Ca^{2+}]_c$. 10 μM coelenterazine increased the amplitude of all $[Ca^{2+}]_c$ responses to both mechanical perturbation and hypo-osmotic shock in all strains tested (Fig. 5.2).

These results show that 10 μM coelenterazine provides reliable measurement of $[Ca^{2+}]_c$ in strains producing low levels of aequorin. Whenever 10 μM coelenterazine was required, all associated controls were assayed at this concentration.

5.2.4 Involvement of CPCs in the $[Ca^{2+}]_c$ responses to mechanical perturbation and hypo-osmotic shock

5.2.4.1 Δ*yvc* caused an increased $[Ca^{2+}]_c$ amplitude in response to mechanical perturbation and hypo-osmotic shock

In *S. cerevisiae* the *yvc1* gene encodes a stretch activated, vacuolar CPC (Palmer *et al.*, 2001; Zhou *et al.*, 2003) involved in Ca^{2+} influx in response to hyper-osmotic shock (Denis and Cyert, 2002). *Saccharomyces cerevisiae* responds to hypo-osmotic shock, but not mechanical perturbation, with a transient $[Ca^{2+}]_c$ increase involving Ca^{2+} influx from internal Ca^{2+} stores and the extracellular media (Batiza *et al.*, 1996).

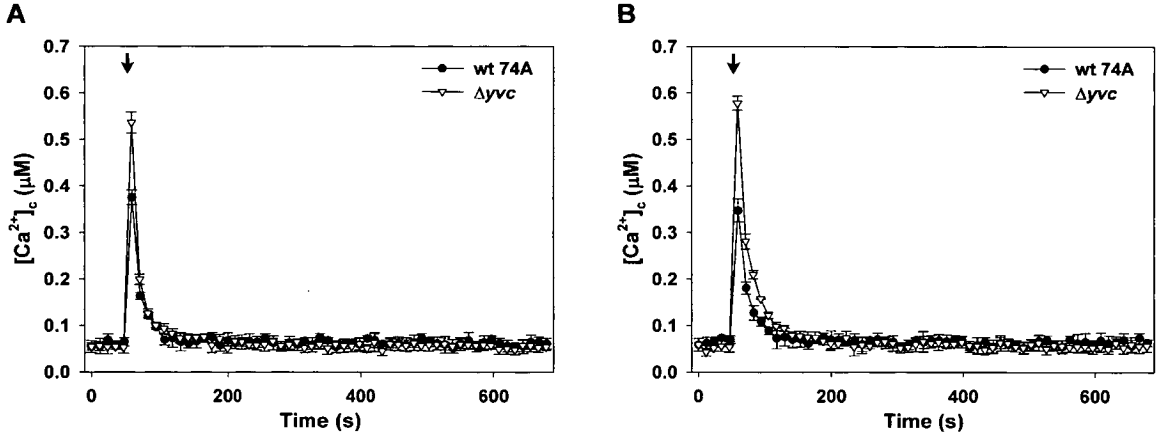

Fig. 5.3. Effects of *yvc* deletion on the $[Ca^{2+}]_c$ responses to mechanical perturbation and hypo-osmotic shock in *N. crassa*. **A.** $[Ca^{2+}]_c$ response to mechanical perturbation in wt74Ap37b (wild type) and 11253p10f1b1 (Δ*yvc*) strains. **B.** $[Ca^{2+}]_c$ response to hypo-osmotic shock in wt74Ap37b and 11253p10f1b1 strains. Arrows represent points of stimulus administration. Coelenterazine concentration = 2.5 μM.

Deletion of the *yvc* gene caused a significant increase in the amplitude of the $[Ca^{2+}]_c$ responses to mechanical perturbation and hypo-osmotic shock (both stimuli $p = < 0.01$)(Fig. 5.3). Δ*yvc* had no effect on the resting $[Ca^{2+}]_c$ or on the FWHM of the $[Ca^{2+}]_c$ response to both stimuli.

5.2.4.2 MID-1 is involved in the $[Ca^{2+}]_c$ responses to mechanical perturbation and hypo-osmotic shock

Yeast *mid1* was first identified due to its involvement in the Ca^{2+} accumulation that was found to occur in response to α factor treatment (Iida *et al.*, 1994). Mid1p is believed to act in the same pathway as the Cch1p protein, or potentially as a component of a CPC along with Cch1p (Fischer *et al.*, 1997; Paidhungat and Garrett, 1997). Mid1p expressed in mammalian cells has stretch activated Ca^{2+} permeable channel activity (Kanzaki *et al.*, 1999). The $[Ca^{2+}]_c$ responses of *S. cerevisiae* to a range of stimuli including glucose readdition to glucose starved cells (Tokes-Fuzesi *et al.*, 2002), alkaline stress (Viladevall *et al.*, 2004) and amiodarone treatment (Courchesne and Ozturk, 2003), were all inhibited by deletion of the *mid1* gene.

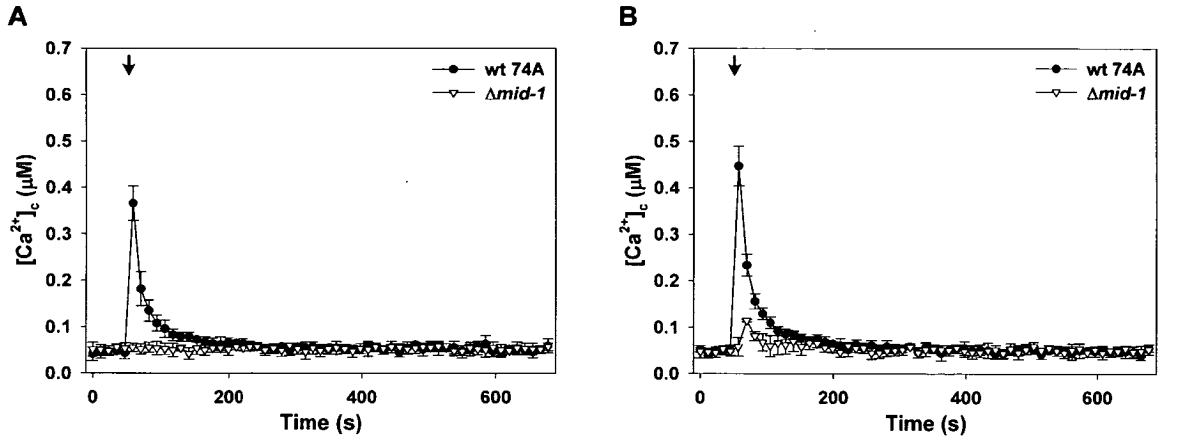

Fig. 5.4. Effects of the *mid-1* deletion on the $[Ca^{2+}]_c$ responses to mechanical perturbation and hypo-osmotic shock. **A.** $[Ca^{2+}]_c$ response to mechanical perturbation in wt74Ap37b (wild type) and 11708p8g (Δ*mid-1*) strains. **B.** $[Ca^{2+}]_c$ response to hypo-osmotic shock in wt74Ap37b and 11708p8g strains. Arrows represent points of stimulus administration. Coelenterazine concentration = 10 μM.

Deletion of *mid-1* abolished the $[Ca^{2+}]_c$ response to mechanical perturbation (Fig. 5.4A). The $[Ca^{2+}]_c$ response to hypo-osmotic shock was not totally abolished with a small, slightly delayed increase in $[Ca^{2+}]_c$ (Fig. 5.4B). To confirm that the aequorin expressing *mid-1* deletion mutant was capable of measuring changes in $[Ca^{2+}]_c$, H_2O_2 was used to permeabilize the plasma membrane (Fig. 5.5).

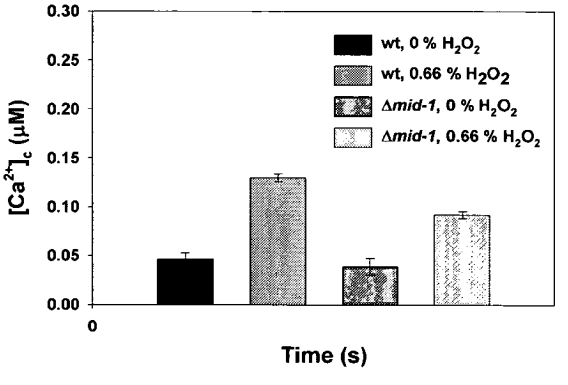

Fig. 5.5. Effects of H_2O_2 on resting $[Ca^{2+}]_c$ in germ tubes of the wt74Ap37b and 11708p8g strains. Coelenterazine concentration = 10 μM.

Twelve min pre-treatment with 0.66% H_2O_2 causes increased $[Ca^{2+}]_c$ without completely permeabilizing the plasma membrane (section 6.2.2.1). 0.66% H_2O_2 caused a large increase in resting $[Ca^{2+}]_c$ in both the wild type and Δ*mid-1* strain (Fig. 5.5). This demonstrated that it was possible to readily detect changes in $[Ca^{2+}]_c$ in the aequorin expressing Δ*mid-1* strain.

5.2.4.2 The MID-1 protein is involved in the germ tube swelling response to mechanical perturbation

Ca^{2+} dependent apical swelling occurs when germ tubes are subjected to mechanical perturbation (section 3.2.3.7). Abolition of the $[Ca^{2+}]_c$ response to mechanical perturbation by *mid-1* deletion suggested MID-1 may be involved in the germ tube swelling response to mechanical perturbation.

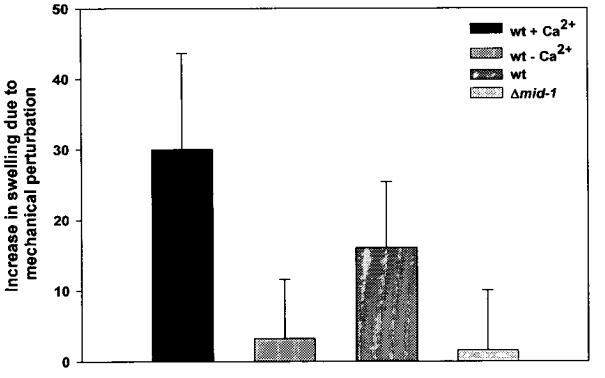

Fig. 5.6. The effect of Δ*mid-1* on the increase in apical swelling due to mechanical perturbation. The data for the ± Ca^{2+} experiments shown here is the same as that shown in Fig. 3.13. Strains used in the experiment to assess the influence of the *mid-1* experiments were wt74Ap37b (wild type) and 11708p8g (Δ*mid-1*).

In all 6 experiments performed the increase in apical swelling due to mechanical perturbation was significantly lower in the Δ*mid-1* ($p = < 0.05$) than in wild type germlings (Fig. 5.6). As with the effects of Ca^{2+} removal from the wild type, deletion of the *mid-1* gene did not completely abolish the apical swelling response of germ tubes

suggesting other mechanisms may be additionally involved in the swelling response to mechanical perturbation in *N. crassa.*

5.2.4.3 L-type Ca^{2+} channel activity may be involved in the $[Ca^{2+}]_c$ responses to mechanical perturbation and hypo-osmotic shock

The *N. crassa* CCH-1 protein has significant similarity to the yeast Cch1p and mammalian L-type Ca^{2+} channels (Zelter *et al.*, 2004). The effects of two L-type Ca^{2+} channel inhibitors (verapamil and diltiazem), were tested. Verapamil and diltiazem inhibited the Ca^{2+} dependent thigotropism and galvanotropism of *C. albicans* at concentrations of 0.25 mM and 0.5 mM respectively (Watts *et al.*, 1998; Brand *et al.*, 2007).

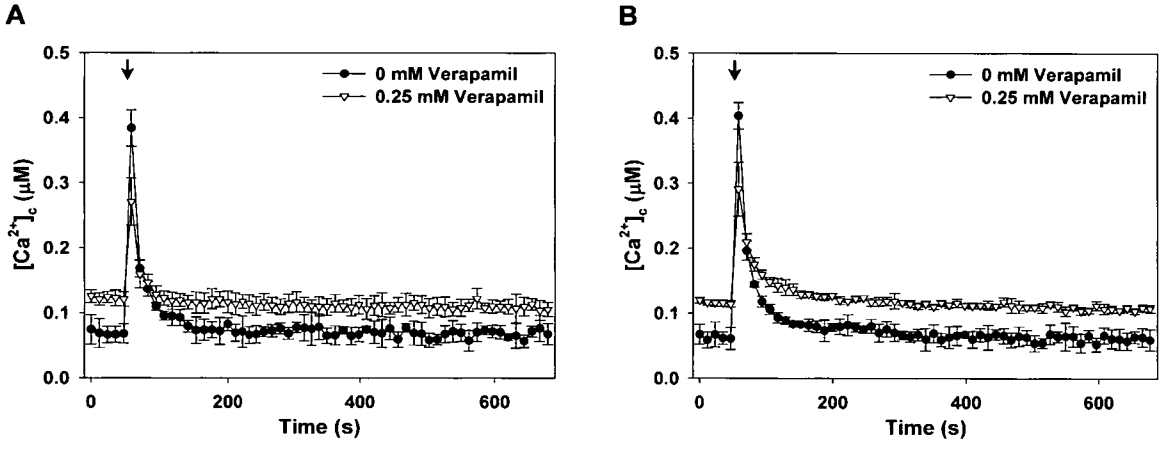

Fig. 5.7. Effects of verapamil on the $[Ca^{2+}]_c$ responses to mechanical perturbation and hypo-osmotic shock. **A.** Effect of 0.25 mM verapamil on the $[Ca^{2+}]_c$ response to mechanical perturbation. **B.** Effect of 0.25 mM verapamil on the $[Ca^{2+}]_c$ response to hypo-osmotic shock. Arrows represent points of stimulus administration. The strain used was wild type 22A3AWTAZ6.

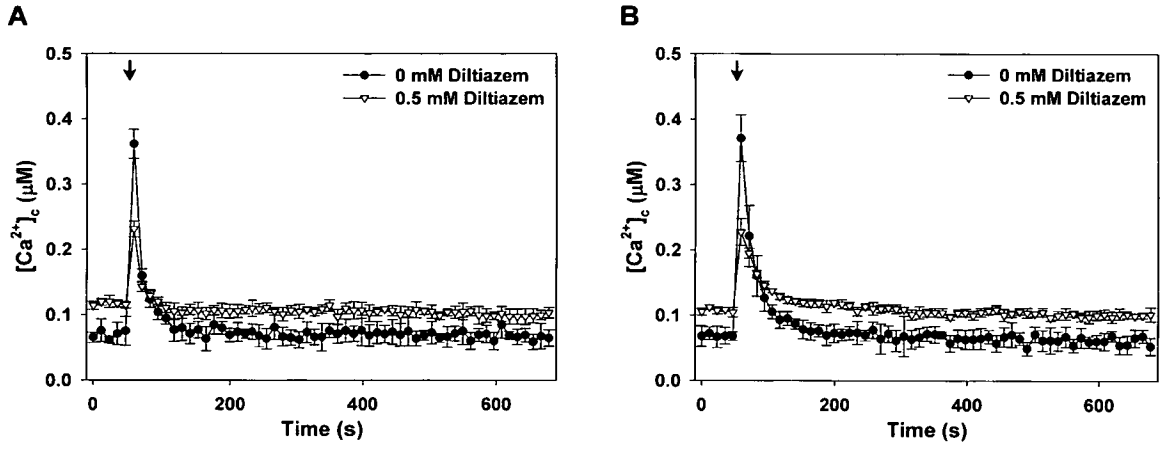

Fig. 5.8. Effects of diltiazem on the $[Ca^{2+}]_c$ responses to mechanical perturbation and hypo-osmotic shock. **A.** Effect of 0.5 mM diltiazem on the $[Ca^{2+}]_c$ response to mechanical perturbation. **B.** Effect of 0.5 mM diltiazem on the $[Ca^{2+}]_c$ response to hypo-osmotic shock. Arrows represent points of stimulus administration. The strain used was wild type 22A3AWTAZ6.

Both inhibitors significantly (both $p = < 0.01$) reduced the amplitudes of the $[Ca^{2+}]_c$ responses to mechanical perturbation and hypo-osmotic shock (Fig. 5.7 and 5.8). Both verapamil and diltiazem also increased the resting $[Ca^{2+}]_c$. The effects of verapamil and diltiazem on the amplitude of the $[Ca^{2+}]_c$ response to mechanical perturbation and resting $[Ca^{2+}]_c$ were concentration dependent (data not shown).

5.2.5 Involvement of cation ATPases in the $[Ca^{2+}]_c$ responses to mechanical perturbation and hypo-osmotic shock

5.2.5.3 SERCA type Ca^{2+} ATPase activity is involved in the $[Ca^{2+}]_c$ responses to mechanical perturbation and hypo-osmotic shock

The *nca-1* gene is predicted to encode a protein similar to mammalian SERCA-type ATPases (Benito *et al.*, 2000; Zelter *et al.*, 2004). As the Δ*nca-1* strain was ascospore lethal, it was not transformed with the aequorin gene in this study (see section 5.2.2).

Cyclopiazonic acid (CPA) is a highly selective inhibitor of SERCA ATPases (Seidler *et al.*, 1989) and was used to inhibit NCA-1 activity instead.

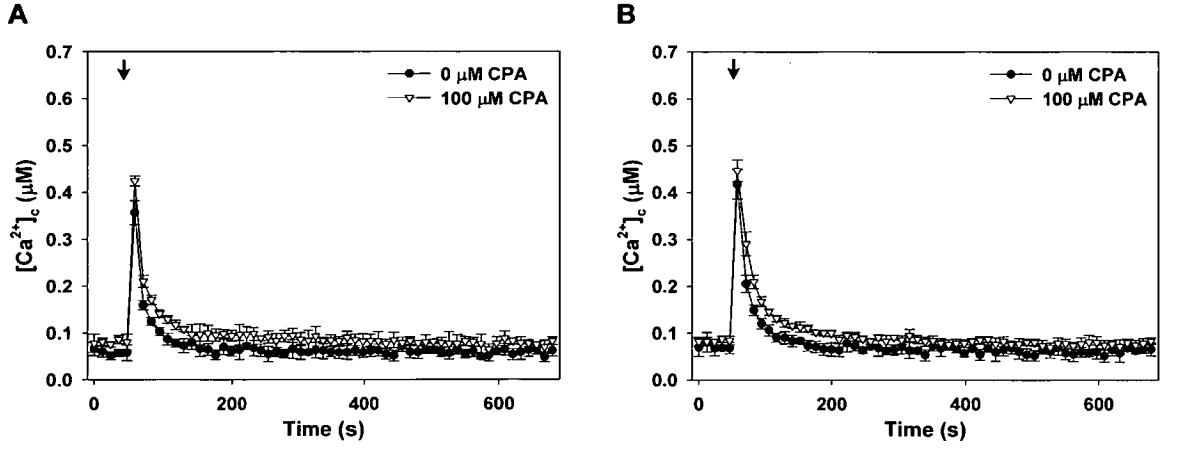

Fig. 5.9. Effects of CPA on the $[Ca^{2+}]_c$ responses to mechanical perturbation and hypo-osmotic shock. **A.** Effect of 100 μM CPA on the $[Ca^{2+}]_c$ response to mechanical perturbation. **B.** Effect of 100 μM CPA on the $[Ca^{2+}]_c$ response to hypo-osmotic shock. Arrows represent times of stimulus administration. Coelenterazine concentration = 2.5 μM. Wild type strain used was 22A3AWTAZ6.

Inhibition of SERCA activity by 100 μM CPA significantly increased the amplitude of the $[Ca^{2+}]_c$ response to mechanical perturbation ($p = < 0.01$ for two of three experiments, $p = < 0.05$ for a third) (Fig. 5.9). In contrast, 100 μM CPA had no significant effect on the amplitude of the $[Ca^{2+}]_c$ response to hypo-osmotic shock (Fig. 5.9B). 100 μM CPA caused a significant increase in the resting $[Ca^{2+}]_c$ ($p = < 0.01$)(Fig. 5.9). 100 μM CPA caused an average increase of 5.35 s in FHWM in response to hypo-osmotic shock whilst the average increase in FWHM in response to mechanical perturbation was 0.49 s, and an increase was only observed in two out of three experiments.

5.2.5.1 PH-7 and ENA-1 are involved in the $[Ca^{2+}]_c$ responses to mechanical perturbation and hypo-osmotic shock

ph-7 was predicted to encode a Ca^{2+} ATPase based upon genetic and functional evidence (Benito *et al.*, 2000). In contrast to *ph-7*, *ena-1* was predicted to encode a Na^+-ATPase and expression of ENA-1 complemented a Na^+-sensitive mutant of *S. cerevisiae* (Benito *et al.*, 2000).

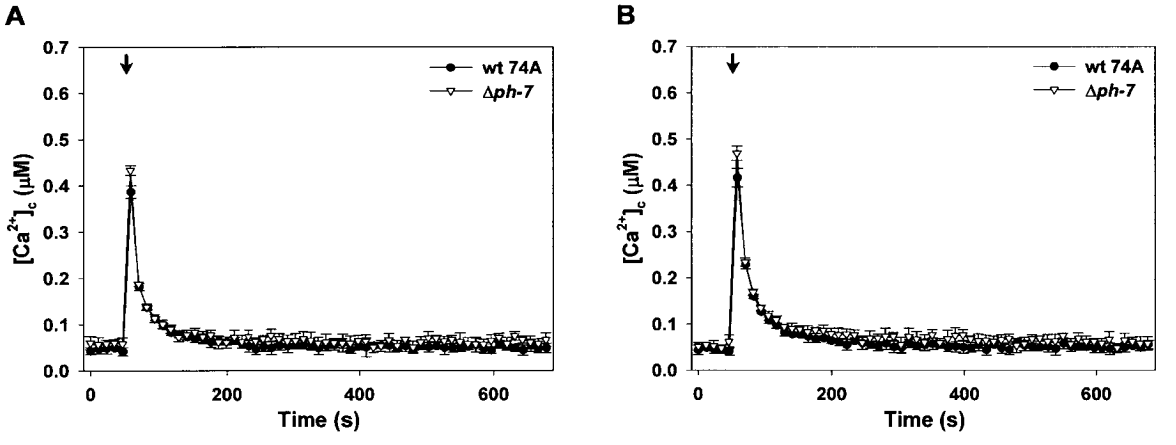

Fig. 5.10. Effects of the *ph-7* deletion on the $[Ca^{2+}]_c$ responses to mechanical perturbation and hypo-osmotic shock. **A.** $[Ca^{2+}]_c$ response to mechanical perturbation in wt74Ap37b (wild type) and 11256p16b1a3 (Δ*ph-7*) strains. **B.** $[Ca^{2+}]_c$ response to hypo-osmotic shock in wt74Ap37b and 11256p16b1a3 strains. Arrows represent points of stimulus administration. Coelenterazine concentration = 10 μM.

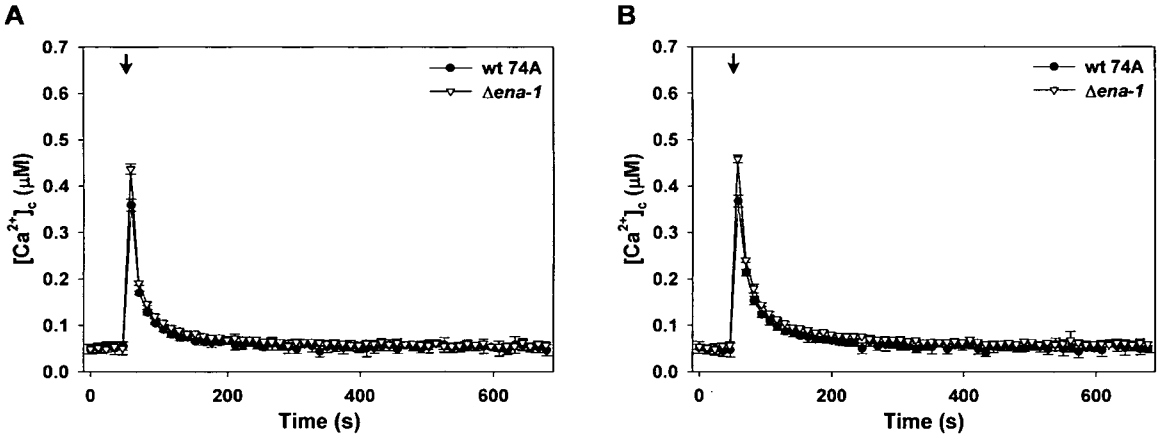

Fig. 5.11. Effects of the *ena-1* deletion on the $[Ca^{2+}]_c$ responses to mechanical perturbation and hypo-osmotic shock. **A.** $[Ca^{2+}]_c$ response to mechanical perturbation in wt74Ap37b (wild type) and 11237p64b (Δ*ena-1*) strains. **B.** $[Ca^{2+}]_c$ response to hypo-osmotic shock in wt74Ap37b and 11237p64b strains. Arrows represent points of stimulus administration. Coelenterazine concentration = 2.5 μM.

Deletion of the *ph-7* gene significantly increased the amplitudes of the $[Ca^{2+}]_c$ responses to mechanical perturbation ($p = < 0.01$) and hypo-osmotic shock ($p = < 0.05$)(Fig. 5.10). Similarly, deletion of *ena-1* caused significantly increased the amplitude of the $[Ca^{2+}]_c$ responses to mechanical perturbation ($p = < 0.01$) and hypo-osmotic shock ($p = < 0.01$)(Fig. 5.11). Deletion of neither gene had any effect on resting $[Ca^{2+}]_c$.

5.2.6 Role of CAX in the $[Ca^{2+}]_c$ responses to mechanical perturbation and hypo-osmotic shock

CAX is a vacuolar Ca^{2+}/H^+ exchanger which influences vacuolar Ca^{2+} accumulation and has homology to the vacuolar Vcx1p Ca^{2+}/H^+ exchanger of *S. cerevisiae* (Margolles-Clark *et al.*, 1999; Zelter *et al.*, 2004).

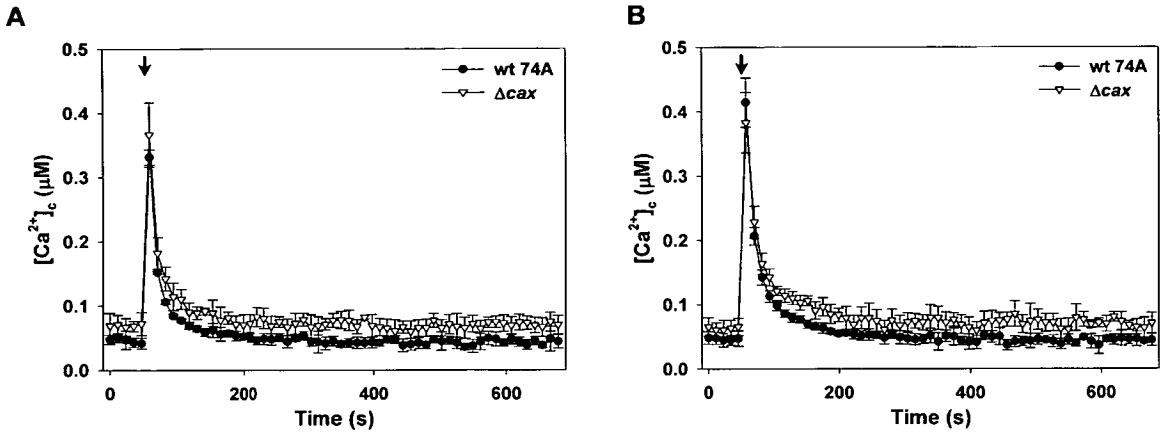

Fig. 5.12. Effects of *cax* gene deletion on the $[Ca^{2+}]_c$ responses to mechanical perturbation and hypo-osmotic shock. **A.** $[Ca^{2+}]_c$ response to mechanical perturbation in wt74Ap37b (wild type) and 11249p15a2a (Δ*cax*) strains. **B.** $[Ca^{2+}]_c$ response to hypo-osmotic shock in wt74Ap37b and 11249p15a2a. Arrows represent points of stimulus administration. Coelenterazine concentration = 10 μM.

Deletion of the *cax* gene had no reproducibly significant effect on the amplitudes of the $[Ca^{2+}]_c$ responses to mechanical perturbation or hypo-osmotic shock (Fig. 5.12). Figure 5.12 suggests CAX may be involved in the regulation of resting $[Ca^{2+}]_c$. However, there was no significant difference in resting luminescence before $[Ca^{2+}]_c$ calibration of wild type and Δ*cax* strains. The apparent increased resting $[Ca^{2+}]_c$ is an artefact in the Δ*cax* strain and is a result of the low amount of aequorin present in this strain (see section 3.2.3.2).

5.3 Conclusions

5.3.1 CPCs are involved in the $[Ca^{2+}]_c$ and swelling responses to mechanical perturbation

5.3.1.2 Roles for MID-1 and CCH-1

Since the original identification of the *mid-1* gene in the *N. crassa* genome (Borkovich et al., 2004; Zelter *et al.*, 2004), further annotation has indicated that it lacks the C terminal transmembrane domain reported in Zelter *et al.* (2004). *N. crassa* MID-1 contains a glucosylphoshpatidylinositol (GPI) attachment domain that may attach MID-1 to the cell wall or plasma membrane (de Groot *et al.*, 2003). This strongly suggests that the *N. crassa* MID-1 protein is incapable of independent CPC activity. Despite this, deletion of *mid-1* in *N. crassa* caused complete abolition of the $[Ca^{2+}]_c$ increase and inhibited the swelling response to mechanical perturbation, indicating an essential requirement for MID-1 in these responses. Inhibition of L-type Ca^{2+}-channel activity caused inhibition of Ca^{2+} mediated galvanotropism that was comparable to deletion of the CaCch1p protein in *C. albicans* (Brand *et al.*, 2007). Deletion of CaMid1p and CaCch1p caused similar inhibition of thigmotropism and double deletion of these genes in the same strain had no cumulative effect providing strong evidence that the two proteins function together as a mechano-sensing activator of Ca^{2+} influx (Brand *et al.*, 2007). Despite strong evidence for Mid1p and Cch1p in *S. cerevisiae* functioning in the same pathway, a direct interaction between the two proteins has not been shown (Yoshimura *et al.*, 2004). Although both Cch1p and Mid1p localize to the plasma membrane colocalization was not observed (Yoshimura *et al.*, 2004). The predicted structure of *N. crassa* MID-1 shows no similarity to any known mammalian or plant Ca^{2+} channels (Zelter *et al.*, 2004). This evidence, combined with the data presented in this chapter, suggest that MID-1 and CCH-1 may act in the same pathway or form a mechano-sensing Ca^{2+} CPC in *N. crassa.*

The increased resting $[Ca^{2+}]_c$ caused by the L-type Ca^{2+}-channel inhibitors verapamil and

diltiazem was a surprising result that cannot be explained by inhibition of L-type Ca^{2+} channel activity. The increase in resting $[Ca^{2+}]_c$ may have been due to an unspecific increase in plasma membrane permeability. Both verapamil and diltiazem are amphipathic compounds with properties similar to certain local anaesthetics, such as dibucaine. These properties give them the potential to disturb the plasma membrane bilayer by causing increasing membrane fluidity, as found for dibucaine in *E. coli* (Andersen *et al.*, 2006).

The effects of verapamil and diltiazem are in marked contrast to the findings of KP4 (section 4.2.5) which has been previously shown to block mammalian L-type Ca^{2+} channels (Gage *et al.*, 2002). The lack of an inhibitory effect for KP4 may be because its specific target in the mammalian L-type Ca^{2+} channel is lacking in the CCH-1 protein.

5.3.1.2 Role for YVC

The increased amplitude in response to mechanical perturbation caused by the *yvc* deletion was initially unexpected. This increase is considerably larger than any caused by impairment of ATPase activity. The *N. crassa* YVC protein has high levels of similarity to the *S. cerevisiae* Yvc1p protein (Zelter *et al.*, 2004) which has been found to mediate Ca^{2+} influx from the vacuole in response to hyper-osmotic shock (Denis and Cyert, 2002). A possible explanation for this finding may be related to the phenomenon of Ca^{2+} induced Ca^{2+} release which has been well characterized in mammalian cells (Berridge *et al.*, 2003). Mechanical perturbation may cause the uptake of Ca^{2+} via CCH-1 and MID-1 and an initially small elevation in $[Ca^{2+}]_c$ may activate YVC on the vacuolar membrane. YVC activation may cause a much larger $[Ca^{2+}]_c$ increase close to the vacuolar membrane which in turn activates Ca^{2+} pumps and or Ca^{2+} transporters located in the vacuolar membrane. If *yvc* is deleted the Ca^{2+} pumps/transporters may not be activated until sufficient Ca^{2+} has diffused from the plasma membrane to provide a suitably high $[Ca^{2+}]_c$ level at the vacuolar membrane.

5.3.2 Removal of Ca^{2+} from the cytoplasm

5.3.2.1 Role for NCA-1

SERCA Ca^{2+} ATPases in other systems have low transport rates but high affinities for Ca^{2+} ions. This feature allows them to respond to modest elevations in Ca^{2+} levels and set basal $[Ca^{2+}]_c$ (Berridge *et al.*, 2003). Inhibition of Ca^{2+} removal from the cytoplasm and the increased resting $[Ca^{2+}]_c$ shown in Fig. 5.9 correspond with these characteristics and provide evidence of SERCA ATPase activity playing an important role in *N. crassa* $[Ca^{2+}]_c$ homeostasis. NCA-1 in *Neurospora* is predicted to encode a SERCA Ca^{2+} ATPase localized to the endoplasmic reticulum (Benito *et al.*, 2000; Zelter *et al*, 2004). These results suggest that the endoplasmic reticulum may act as an intracellular Ca^{2+} store in *N. crassa* and is involved in the regulation of resting $[Ca^{2+}]_c$ and elevated $[Ca^{2+}]_c$ produced in response to different stimuli.

5.3.2.2 Roles for ENA-1 and PH-7

Deletion of either the *ph-7* or *ena-1* gene increased the amplitude of the $[Ca^{2+}]_c$ response to mechanical perturbation and hypo-osmotic shock. Previously, *ph-7* was predicted to encode a Ca^{2+} ATPase (Benito *et al.*, 2000). This result supports the theory and shows PH-7 to be involved in the removal of Ca^{2+} from the cytoplasm. In contrast to *ph-7*, *ena-1* was predicted to encode a Na^+-ATPase. The increased $[Ca^{2+}]_c$ amplitude due to *ena-1* deletion may be because ENA-1 is involved in unspecific Ca^{2+} transport, or it may be due to perturbations in Na^+ transport affecting the activity of a Ca^{2+} pump or transporter. Although disruption of no single ATPase abolished the $[Ca^{2+}]_c$ response, investigations of mammalian Ca^{2+} signalling and SERCA ATPases have found that the $[Ca^{2+}]_c$ signalling machinery may be able to compensate for reduced activity of its individual components (Berridge *et al.*, 2003). The results presented here suggest that some of the

large number of Ca^{2+} pumps and transporters may act cooperatively to remove increased Ca^{2+} from the cytosol.

5.3.3 Specificity of $[Ca^{2+}]_c$ responses to mechanical perturbation and hypo-osmotic shock

Of all the conditions examined in this chapter only Δ*mid-1* and inhibition of SERCA activity caused different effects on the $[Ca^{2+}]_c$ responses to mechanical perturbation and hypo-osmotic shock. The effect of Δ*mid-1* on the $[Ca^{2+}]_c$ response to hypo-osmotic shock was similar to the effect of Ca^{2+} removal from the media (section 3.2.3.6, Fig 3.10). The small increase in $[Ca^{2+}]_c$ may represent release of $[Ca^{2+}]_c$ from intracellular stores. However deletion of the predicted vacuolar CPC, YVC, had the same effect on $[Ca^{2+}]_c$ responses to both mechanical perturbation and hypo-osmotic shock.

Treatment with 100 μM CPA increased the amplitude of the $[Ca^{2+}]_c$ response to mechanical perturbation but not hypo-osmotic shock. This, combined with the increased effect on FWHM in response to hypo-osmotic shock, suggests SERCA ATPase activity differs in the two $[Ca^{2+}]_c$ responses. In the study by Nelson *et al.* (2004) the effect of 20 μM CPA on resting $[Ca^{2+}]_c$ was much more severe in *A. awamori* than the effect seen in Fig. 5.9. This may reflect differences in the Ca^{2+} signalling machinery between these two species and may be explained by some of the large number of Ca^{2+} transporters identified in the genome of *N. crassa* (Zelter *et al.*, 2004) acting to compensate for the inhibited activity of the CPA target.

Overall the results of this chapter provide little evidence for the $[Ca^{2+}]_c$ responses to mechanical perturbation and hypo-osmotic shock being mediated by different $[Ca^{2+}]_c$ modulating proteins. However as indicated in section 3.3.2, it should be remembered that a major component of the Ca^{2+} response to hypo-osmotic shock is the Ca^{2+} response to mechanical perturbation because of the way in which the hypo-osmotic shock is

administered by squirting diluted medium into the cultures in the individual wells of the microwell plates.

5.4 Summary

- MID-1 is required for both the $[Ca^{2+}]_c$ and germ tube swelling responses to mechanical perturbation.
- MID-1 in *N. crassa* is predicted to be attached to the cell wall or plasma membrane via a GPI domain (de Groot *et al.*, 2003) and is probably not capable of Ca^{2+} channel activity on its own.
- MID-1 may act as mechanosensor and mediate Ca^{2+} influx via regulation of the CCH-1 protein.
- Efflux of Ca^{2+} from the cytoplasm requires the activity of multiple ATPases including PH-7 and possibly ENA-1.
- SERCA ATPase activity is involved in the regulation of $[Ca^{2+}]_c$ homeostasis.

Chapter 6

Development of the aequorin $[Ca^{2+}]_c$ assay for use as a high throughput screen to discover novel antifungal agents

6.1 Introduction

Strong evidence for the involvement of Ca^{2+} signalling in the mode of action of antifungal compounds comes from work in *S. cerevisiae*. The antifungal activity of miconazole, itraconazole and terbinafine, all medically important antifungal drugs, was enhanced by treatment with a range of antagonists of Ca^{2+} signalling (Edlind *et al.*, 2002). The antifungal activity of these compounds was significantly increased by disruption of calcineurin and the Crz1p transcription factor. Increased resting $[Ca^{2+}]_c$ due to azole or terbinafine treatment would normally activate calcineurin, leading to alterations in Ca^{2+} transporter activity that result in the normal $[Ca^{2+}]_c$ resting level being restored (Edlind *et al.*, 2002). Furthermore, treatment with the antifungal agent amiodarone has recently been shown to induce a $[Ca^{2+}]_c$ transient response in *S. cerevisiae* (Courchesne and Ozturk, 2003).

The primary objective of a high throughput screening assay is to rapidly identify active compounds from large chemical libraries (Zhang *et al.*, 1999) and high throughput assays are now an essential aspect of pharmaceutical drug discovery (Inglese *et al.*, 2006). Advantageous properties for a high throughput screen include:

- Simplicity, ideally avoiding technically demanding processes (Baniecki *et al.*, 2007).
- Avoiding the involvement of components that require excessive safety and disposal precautions (Baniecki *et al.*, 2007).
- A high throughput screen (HTS) using living cells: for any compound to be effective it needs to exert its antimicrobial activity on living cells (Baniecki *et al.*, 2007).
- A high signal to noise ratio to provide clear distinction of positive results (Baniecki *et al.*, 2007).
- The identification of false positive or false negative results; this represents a significant problem with HTS assays (Inglese *et al.*, 2006).
- Sufficient sensitivity to recognize compounds with low or partial activity (Inglese *et al.*, 2006).
- Potential for adaptation to provide greater information or to examine different

types of cell culture is highly beneficial (Baniecki *et al.*, 2007).

- Above all, a HTS assay should be highly robust and reproducible (Baniecki *et al.*, 2007).

High throughput screens have been developed with the potential to identify different species of opportunistic fungal pathogens (Diaz and Fell, 2004; Leinberger *et al.*, 2005). Rapid identification of fungal pathogens is crucial for the treatment of immuno-compromised patients (Diaz *et al.*, 2004; Leinberger *et al.*, 2005). Detection of potential antifungal compounds is another key potential application of high throughput screens. A colorimetric assay for the measurement of the activity of antifungal compounds on *C. albicans* biofilm formation has been developed with the potential for application as a HTS (Ramage *et al.*, 2001). Further work developed a HTS capable of testing combinations of different potential antifungal compounds to identify additive effects on *C. albicans* growth (Borisy *et al.*, 2003). Another high throughput assay developed for *C. albicans* measured plasma membrane permeablization, a common feature of many antifungal compounds (Ziegelbauer *et al.*, 1999). The potential for plant antifungal proteins to target Ca^{2+} signalling (see Chapter 4) also generates potential benefit for screening Ca^{2+} modulating chemicals in the identification of fungicides.

The aequorin assay developed in Chapter 3 and previous studies (Nelson *et al.*, 2004; Zelter, 2004) generated a robust and reliable method for $[Ca^{2+}]_c$ measurement in *N. crassa*. Because of the rapidity of the Ca^{2+} response, it is possible to distinguish primary effects and secondary effects of agonists or inhibitors acting on Ca^{2+} signalling. This was demonstrated with antifungal proteins (Chapter 4) and pharmacological agents (Chapter 5). Despite providing detailed, reliable, and reproducible results, when using the standard protocol for $[Ca^{2+}]_c$ measurement (section 2.7.1), relatively few compounds can be analyzed in a single day. With pre-addition of compounds and measurement of luminescence and discharge data the analysis of two samples using the standard aequorin assay takes approximately 1 h. This is in addition to the period required for inoculation and incubation of the fungal samples in the 96 microwell plates prior to luminometry.

The potential role for Ca^{2+} signalling in antifungal activity, the homology between the Ca^{2+} signalling mechanisms of *N. crassa* with other fungi, including the pathogenic *Magnaporthe grisea* (Zelter *et al.*, 2004), and the robust nature of the $[Ca^{2+}]_c$ response to mechanical perturbation led to an investigation of its potential for use as a high throughput screen to discover novel antifungal compounds that target Ca^{2+} signalling and/or Ca^{2+} homeostasis. The aims of the results described in this chapter were: (1) to increase the throughput of the aequorin $[Ca^{2+}]_c$ assay; (2) to evaluate the effects of a wider range of antifungal compounds on the $[Ca^{2+}]_c$ response to mechanical perturbation in *N. crassa*; (3) to perform blind testing of compounds using an aequorin based high throughput assay and compare the results obtained with the same compounds but using the standard aequorin assay; (4) to critically evaluate the potential of antifungal screening by examining perturbations in Ca^{2+} signalling.

6.2 Results

6.2.1 Optimization of experimental procedure

6.2.1.1 Development of assay method

The primary objective was to adapt the aequorin assay for $[Ca^{2+}]_c$ measurement using the whole of a 96 microwell plate in a single experiment. The assay needed to provide detailed, reproducible $[Ca^{2+}]_c$ measurements with a greatly increased rate of throughput. For this purpose, a routine assay method for measurement of $[Ca^{2+}]_c$ in a 96 well plate was designed. In each plate, 93 wells were available for measurement of $[Ca^{2+}]_c$ responses with 3 wells being used for Glowell standards (Lux Biotechnology, Edinburgh UK).

For luminescence measurements across 93 wells, the luminometry protocol was reduced to the smallest possible number of measurements necessary. The $[Ca^{2+}]_c$ response needed to provide information on resting $[Ca^{2+}]_c$, amplitude of the $[Ca^{2+}]_c$

transient and the duration of the $[Ca^{2+}]_c$ transient. For $[Ca^{2+}]_c$ calibration a measurement of discharge luminescence was also required.

Measuring luminescence in 93 wells for 0.5 s per well (compared to measuring luminescence for 1 s per well in 6 wells in the standard assay) increased the cycle time (i.e. the time required for one measurement of luminescence in each well) from 11.51 s to 83 s. As calibration of the $[Ca^{2+}]_c$ uses the $RLU.s^{-1}$ that are measured, the reduced measurement time was taken account of by appropriately modifying the $[Ca^{2+}]_c$ calibration. Considering the key requirements of the assay and the increased cycle time, a protocol was designed. This protocol consisted of 10 cycles beginning 10 min after sample pre-treatment. Cycles 1-4 determined resting $[Ca^{2+}]_c$; in cycle 5 mechanical perturbation was applied and amplitude was recorded; cycles 6-8 measured the duration of the $[Ca^{2+}]_c$ transient; at cycle 9 an aequorin discharge injection was applied to each well; and there was a final reading of luminescence at cycle 10. A luminescence trace produced by this protocol is shown in Fig. 6.1A and the calibrated $[Ca^{2+}]_c$ response is shown in Fig. 6.1B. A greater number of solutions (i.e. cell suspension, chemical treatment, mechanical perturbation stimulus and discharge solution instead of just cell suspension, chemical treatment and mechanical perturbation stimulus) were required to be added to each well during this protocol so an alternative method of microplate inoculation was designed which involved reduced volumes of each solution (see section 2.5.3.3). The protocol for the high throughput method is described in section 2.7.3.

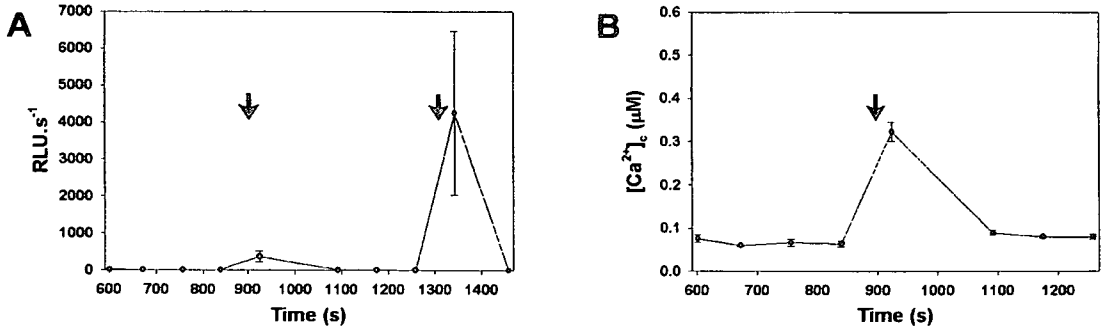

Fig. 6.1. Luminescence and $[Ca^{2+}]_c$ traces produced by the high throughput assay protocol described in section 2.7.3. **A.** Luminescence trace of the high throughput assay protocol. Mechanical perturbation was administered at 923 s (first arrow) and discharge was administered at 1342 s (second arrow). **B.** $[Ca^{2+}]_c$ response of the wild type (22A3AWTAZ6) to mechanical perturbation, administration represented by arrow. n = 3 wells for this experiment.

This method provided readings of the $[Ca^{2+}]_c$ amplitude following stimulation, resting $[Ca^{2+}]_c$, and the return to resting $[Ca^{2+}]_c$ following stimulation. The increased cycle time of the high throughput assay was further increased from 83 s to 168 s by introducing two steps: injection of iso-osmotic medium for mechanical perturbation and injection of 3 M $CaCl_2$ (25% ethanol) to fully discharge the remaining aequorin. The reduced resolution of this assay, due to the reduced number of RLU measurements, meant that FWHM values were not reliable as the measurement taken after the mechanical perturbation measurement was 168 s later.

The high throughput assay protocol is based upon a single discharge reading taken at the point of discharge injection, as discussed in the next section.

6.2.1.2 Discharge calibration for high throughput assay

In the 6 h $[Ca^{2+}]_c$ assay using germ tubes, the total aequorin available to bind Ca^{2+} per well was determined by discharging the aequorin in a separate set of wells, from those containing the experimental sample. To increase the throughput, and also to reduce

running time of the assay, the use of a single discharge injection per well was investigated.

To determine the relationship between RLU values measured immediately after the discharge injection and the total RLU values following discharge, an additional 7 cycles were added to the end of the luminometry protocol described in section 6.2.1.1. This experiment determined whether RLU values after discharge were elevated past cycle 9 (i.e. immediately after discharge). In all wells the RLU values returned to resting level in cycle 10. The total area under the trace of discharge was plotted against luminescence emitted at the discharge injection (see Fig. 6.1A), and was also plotted with a linear regression for this data (Fig. 6.2).

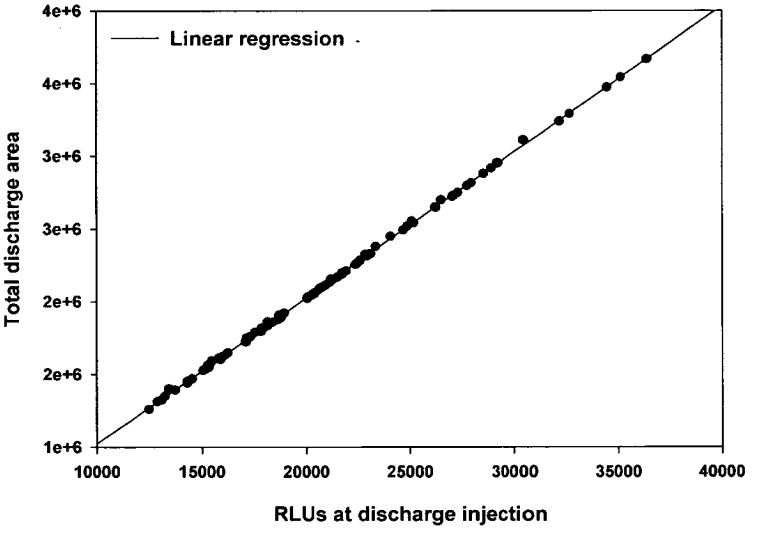

Fig. 6.2. Graph of luminescence at discharge injection against total area under the discharge trace (see Fig. 6.1A). A linear regression for this data was also plotted. Total discharge area was calculated using the equation in section 1.4.2.

Figure 6.2 shows a strong correlation between RLU values at the discharge injection and the total area under the discharge trace. The strength of the correlation was confirmed by an r^2 value of 0.9997. For $[Ca^{2+}]_c$ calibration an average value of total discharge area divided by RLU at discharge injection was determined. This value was used for $[Ca^{2+}]_c$ calibration to allow the discharge measurement to be obtained by

using a single reading instead of from a more complex, separate discharge protocol (see section 2.7.1).

When aequorin consumption exceeds 50% of the total available aequorin, the relationship between $[Ca^{2+}]_c$ and aequorin luminescence may lose the linear nature upon which the $[Ca^{2+}]_c$ calibration is based (Zelter, 2004; section 1.4.2). To prevent misinterpretation of data produced by this assay, aequorin consumption was determined for each well and incorporated into the $[Ca^{2+}]_c$ calibration (section 6.2.1.4).

6.2.1.3 The effects of reducing the number of wells per sample for the high throughput assay

In the standard $[Ca^{2+}]_c$ assay performed with germ tubes (section 2.7.1), $[Ca^{2+}]_c$ responses are measured in six wells. Use of fewer wells per sample increased the throughput of the $[Ca^{2+}]_c$ assay. Previous work used 6 wells per experiment to provide a compromise between the time taken to measure $[Ca^{2+}]_c$ in multiple samples and the accuracy of the data obtained. The effects of reducing the numbers of wells on these parameters needed to be assessed.

Table 6.1. Effects of wells per sample on the number of samples per plate.

Wells per sample	Samples per plate
3	31
4	23
5	18
6	15

Table 6.1 demonstrates the relationship between wells per sample and samples per plate. To assess the importance of the number of wells per sample, data from previous experiments on germ tubes in which the dose-dependency of the $[Ca^{2+}]_c$ response in germ tubes was measured by using the fast injection speed but varying the volume of iso-osmotic medium injected, was used (section 3.2.3.4). This data contained a range

of different $[Ca^{2+}]_c$ amplitudes at which there were varying levels of standard deviation (Figs. 3.8 and 6.3). However the use of different injection speeds in the high throughput assay was not considered. This data was only used here to assess, using the students t-test, how varying the number of wells influenced the accuracy of the data collected. The high throughput protocol only used fast injection with 50 µl of iso-osmotic medium (section 2.7.3).

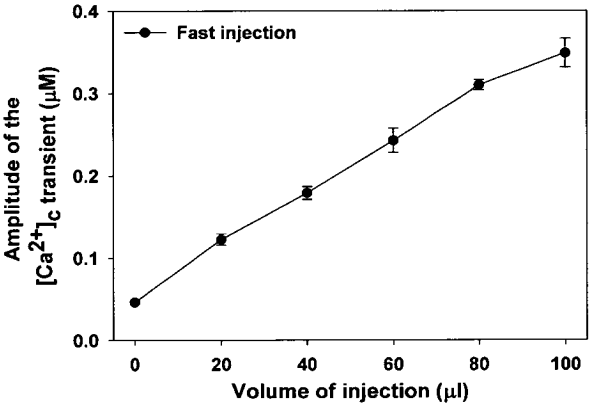

Fig. 6.3. Effects of increased injection volume on the amplitude of $[Ca^{2+}]_c$ responses to mechanical perturbation in germ tubes. This experiment is described fully in section 3.2.3.4. This Figure was previously shown as Fig. 3.8, but is also included here for convenience.

Amplitudes of the $[Ca^{2+}]_c$ responses to injecting different volumes of medium from 3, 4, 5 or 6 wells were compared by the student's t test to determine their p values. The p values provided by this analysis were then plotted (Fig. 6.4). The p value given by the students t-test is a description of the probability of a difference in two sets of results occurring at random. The p value may range from 1 to 0 and low levels of p demonstrate a small probability that the results may occur by random and therefore a high probability that the difference in results was due to a variable examined in an experiment. The two threshold levels below which a p value is considered significant are 0.05 and 0.01.

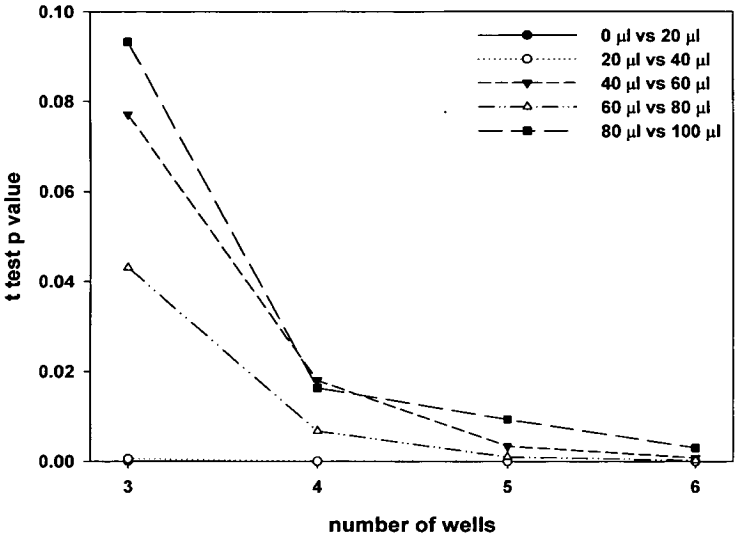

Fig. 6.4 A graph showing the influence of well number on the student's t-test p value when the amplitudes of $[Ca^{2+}]_c$ responses to mechanical perturbation by the injection of different volumes of iso-osmotic medium was compared.

Figure 6.4 shows that increasing the number of wells from 3 to 4 substantially reduced the p values in the different comparisons. For comparisons of 40 µl vs 60 µl and 80 µl vs 100 µl injection volumes, this decrease in p values was over the range at which results become significantly different. On the basis of these results, 4 wells per sample were selected for use in the high throughput assay.

6.2.1.4 Development of a Microsoft Excel™ worksheet for calibration of $[Ca^{2+}]_c$

Calibration of $[Ca^{2+}]_c$ in the standard 6 h assay used either the term bert program (section 2.7.4.1; Zelter, 2004) developed from a Microsoft Excel™ worksheet created by Professor Marc Knight (Durham University) or the Microsoft Excel™ worksheet itself. Section 6.2.1.2 demonstrated that an accurate measurement of total aequorin could be performed from a single RLU measurement immediately following a discharge injection. The change in methodology and format of the data required adaptation of Marc Knights Microsoft Excel™ worksheet for $[Ca^{2+}]_c$ calibration.

To use the adapted aequorin $[Ca^{2+}]_c$ assay in a commercial high throughput screen. The data produced by the assay should be rapidly calibrated and easy to understand.

The Microsoft Excel™ worksheet was designed with several key functions:

1. Macros and cell referencing were used to automate the data analysis as far as possible by reducing manual operation of the worksheet to a minimum.
2. Luminescence data was easy to insert and sorted automatically.
3. Statistical comparisons between sample data and control values were performed for amplitude and resting $[Ca^{2+}]_c$, warnings when low levels of aequorin were recorded, were included.
4. Data from each experiment were summarized separately from calibration.

6.2.2 The use of the high through put $[Ca^{2+}]_c$ assay

The aequorin HTS was designed to identify potential antifungal compounds that influenced the $[Ca^{2+}]_c$ response to mechanical perturbation. To provide a proof of concept for this assay, a range of compounds were screened by blind testing. All compounds included in the assay (Table 6.2) had been previously examined for their effects of the $[Ca^{2+}]_c$ response to mechanical perturbation or were examined in the next section.

6.2.2.1 Effect of $[Ca^{2+}]_c$ modulators in the standard $[Ca^{2+}]_c$ assay

To provide a baseline of data for subsequent comparison with data from a blind testing using the high throughput assay, all the compounds to be used in the blind testing were initially assessed using the standard assay. The effects of several of these compounds on the $[Ca^{2+}]_c$ response to mechanical perturbation have already been described in this thesis (Table 6.2).

Table 6.2. Compounds used in the blind testing described in section 6.2.2.2.

Compound	Concentrations used	Results
BAPTA	0.75 mM, 3.0 mM	Section 3.2.3.6, Figs. 3.9 and 3.11
RsAFP2	1 μM, 4 μM	Section 4.2.4, Fig. 4.4
MtDef2	1 μM, 4 μM	Section 4.2.2, Fig. 4.2
Verapamil	0.25 mM	Section 5.2.4.3, Fig. 5.7
Diltiazem	0.5 mM	Section 5.2.4.3, Fig. 5.8
Cyclopiazonic acid	100 μM	Section 5.2.5.3, Fig. 5.9
DMSO	1%	Section 6.2.2.1, Fig. 6.5A
10 mM Tris HCl	4.8%	Section 6.2.2.1, Fig. 6.5A
Ethanol	1%	Section 6.2.2.1, Fig. 6.5B
Methanol	1%	Section 6.2.2.1, Fig. 6.5B, D
NaCl	0.2 M	Section 6.2.2.1, Fig. 6.5C
Triton X-100	0.1%	Section 6.2.2.1, Fig. 6.5C
Ketoconazole	0.75 $\mu g.ml^{-1}$	Section 6.2.2.1, Fig. 6.5D
Amphotericin B	6 $\mu g.ml^{-1}$, 60 $\mu g.ml^{-1}$	Section 6.2.2.1, Fig. 6.5E
H_2O_2	0.66%, 6.6%	Section 6.2.2.1, Fig. 6.5F

All compounds tested were dissolved into stock solutions using dH_2O, DMSO, methanol or ethanol. Stock solutions were then added to liquid VgS media before treatment of fungal samples (final solvent concentration 1%). Defensin samples were dissolved in 10 mM Tris HCl before addition to VgS media (final concentration 4.8% Tris HCl). A control of 12.3% dH_2O (i.e. 12.3% dH_2O in VgS medium) was required to give equivalent dH_2O concentration in hydrogen peroxide (H_2O_2) experiments. The results obtained with these compounds are summarized in Table 6.3.

Table 6.3. Effects of compounds tested for the high throughput assay. - = compound had no significant effect. ↓ = compound caused a significant reduction ($p = < 0.05$) in $[Ca^{2+}]_c$ amplitude or resting $[Ca^{2+}]_c$. ↑ = compound caused a significant increase ($p = < 0.05$) in $[Ca^{2+}]_c$ amplitude or resting $[Ca^{2+}]_c$.

Compound	**Effect on $[Ca^{2+}]_c$ amplitude**	**Effect on resting $[Ca^{2+}]_c$**
BAPTA	↓	-
RsAFP2	↓	↑
MtDef2	-	-
Verapamil	↓	↑
Diltiazem	↓	↑
Cyclopiazonic acid	↑	↑
DMSO	-	-
Tris HCl	-	-
Ethanol	-	-
Methanol	-	-
NaCl	↓	↑
Triton X-100	↓	↑
Ketoconazole	-	-
Amphotericin B	↓	↑
H_2O_2	↓	↑

Of the new compounds assessed and not previously described (see Tables 6.2 and 6.3), triton X-100 exhibited effects on the $[Ca^{2+}]_c$ response to mechanical perturbation which were consistent with plasma membrane permeabilization. 0.1% Triton X-100 significantly increased resting $[Ca^{2+}]_c$ and severely inhibited, or totally abolished, the $[Ca^{2+}]_c$ response to mechanical perturbation ($p = < 0.01$ in all cases)(Fig. 6.5 C). 0.2 M NaCl significantly inhibited the amplitude of the $[Ca^{2+}]_c$ response to mechanical perturbation ($p = < 0.01$) and delayed the maximum $[Ca^{2+}]_c$ reached by 11.51 s (Fig. 6.5C). 0.2 M NaCl caused a small but significant increase in resting $[Ca^{2+}]_c$ ($p = < 0.05$)(Fig. 6.5C). The effects of NaCl are most likely due to ionic stress although effects on putative Na^+/Ca^{2+} exchangers in *N. crassa* (Zelter *et al.*, 2004) may be involved. Amphotericin B and ketoconazole are two known antifungal compounds. 0.75 μgml^{-1} ketoconazole had no effect on the $[Ca^{2+}]_c$ response to mechanical perturbation or resting $[Ca^{2+}]_c$ (Fig. 6.5D). Both 6 and 60 μgml^{-1} amphotericin B significantly increased resting $[Ca^{2+}]_c$ ($p = < 0.01$) and nearly abolished the $[Ca^{2+}]_c$ response to mechanical perturbation (Fig. 6.5E). 0.66% and 6.6% hydrogen peroxide significantly increased the resting $[Ca^{2+}]_c$ ($p = < 0.01$) and nearly abolished the $[Ca^{2+}]_c$ response to mechanical perturbation (Fig. 6.5F). The increased the resting $[Ca^{2+}]_c$ following H_2O_2 treatment is likely to be the result of plasma membrane permeabilization due to oxidative stress (Price *et al.*, 1994).

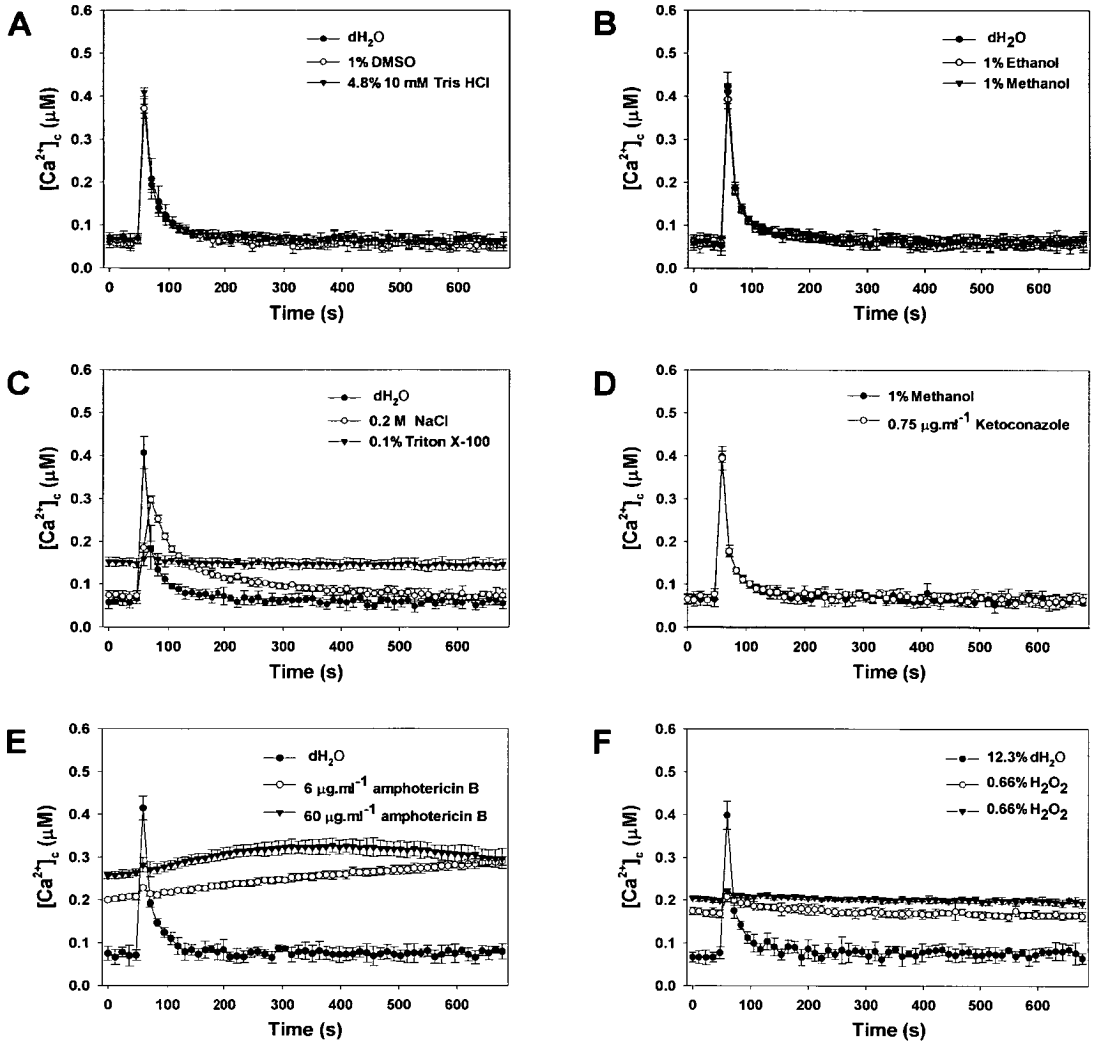

Fig. 6.5. Effects of compounds used in blind testing on the $[Ca^{2+}]_c$ response to mechanical perturbation. **A, B.** Effect of the solvents 1% DMSO, 4.8% 10 mM Tris HCl, 1% ethanol, and 1% methanol. **C.** Effects of NaCl and Triton X-100. **D.** Effect of ketoconazole. **E.** Effects of amphotericin B, dissolved in 1% DMSO. **F.** Effects of H_2O_2 against 12.3% dH_2O control.

6.2.2.2 Blind testing of unknown compounds using the high throughput assay

In the standard 6 h assay cultures were pre-treated with compounds for 12 min before luminometry to allow time for mixing. As part of the blind testing, 6 h old germ tube suspensions were pretreated in the microwell plates with the unknown compounds for

10 min and 1 h to determine which method produced the best results. This experiment was performed on two successive days to allow assessment of the variability in the high throughput assay.

The unknown compounds were initially distributed in the wells of a 96 microwell plate by Dr. Emma Perfect (Lux Biotechnology). Fifty µl samples of each of these compounds were then added to corresponding wells in a microwell plate pre-inoculated as described in section 2.5.3.3 using a multi-channel pipette. Compounds were labelled in groups based upon their solvent and each group was identified by a letter. Different samples within each group were given a number which was combined with the group letter to allow identification in a plate map e.g A1, C2 etc.. To allow comparison of experimental and control samples in blind testing assays, the control for each solvent was number 1.

The sample in each well was subjected to mechanical perturbation and $[Ca^{2+}]_c$ measurements were obtained according to the high throughput assay protocol described in section 2.7.3. The sample identities were revealed after $[Ca^{2+}]_c$ calibration and were compared with the results obtained using the standard germ tube assay (section 6.2.2.1). The findings of the high throughput assay (Fig. 6.6) were compared with those obtained by the germ tube assay and classified into three groups: (1) correct; (2) missed positive; and (3) false positive (Table 6.4).

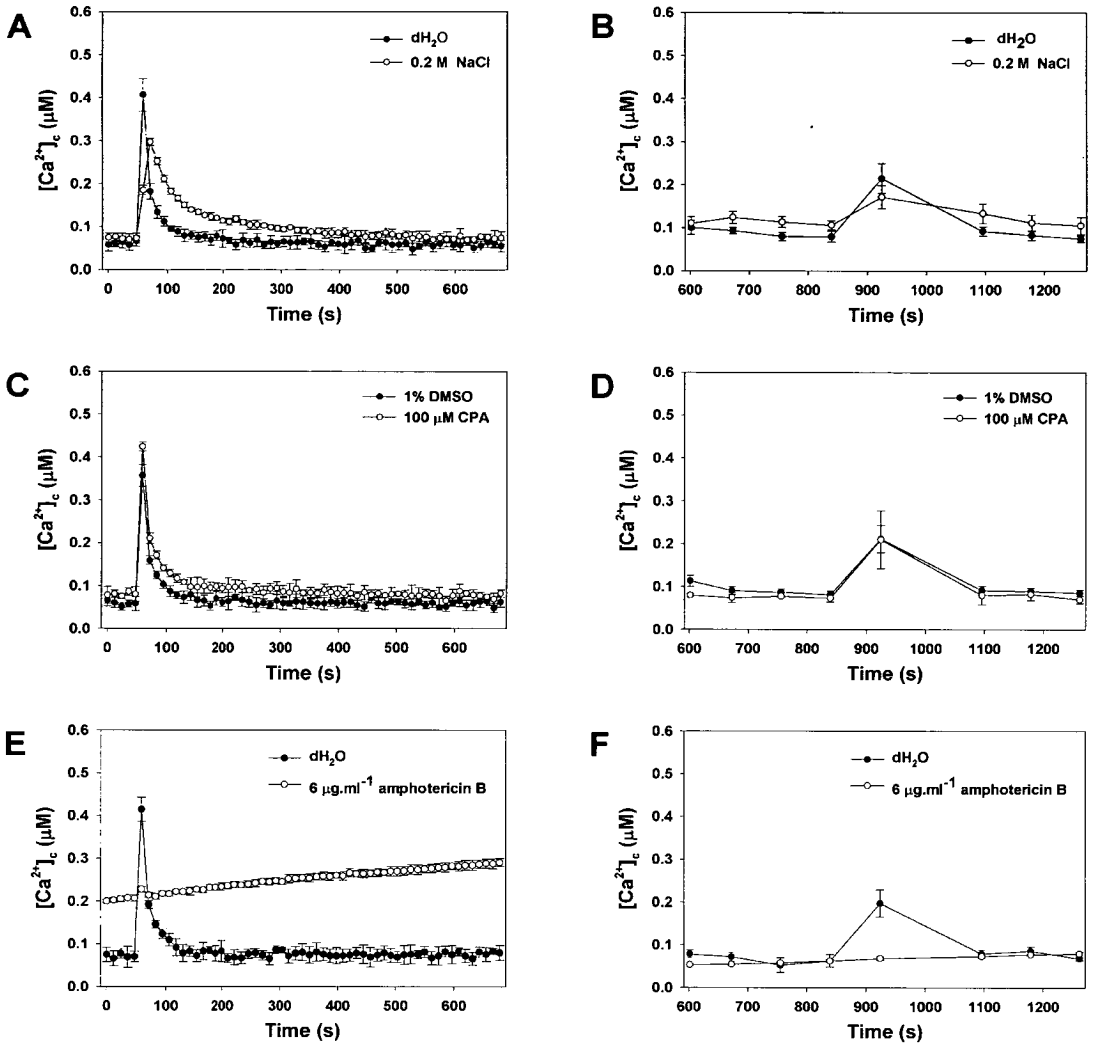

Fig. 6.6. Examples of results obtained by the standard and high throughput $[Ca^{2+}]_c$ assays. **A.** The effects of NaCl in the standard $[Ca^{2+}]_c$ assay. **B.** Effect in NaCl on the high throughput $[Ca^{2+}]_c$ assay. **C.** The effect of CPA in the standard $[Ca^{2+}]_c$ assay. **D.** The effect of CPA in the high throughput assay. **E.** The effect of amphotericin B in the standard $[Ca^{2+}]_c$ assay. **F.** The effect of amphotericin B in the high throughput assay. In relation to table 6.4, **A** and **B.** Example of a "correct result". **C** and **D.** Example of a "missed positive". **E** and **F.** Example of a "false positive" result.

Table 6.4. Definitions of comparison between results obtained by the high throughput and standard $[Ca^{2+}]_c$ assays.

Classification	Definition	Example
Correct	Finding for a sample in the high throughput assay agreed with that of the standard assay	Fig. 6.6 A,B, amplitude and resting $[Ca^{2+}]_c$
Missed positive	An effect detected in the standard assay was not detected by the high throughput assay	Fig. 6.6 C, D, amplitude and resting $[Ca^{2+}]_c$
False positive	An effect detected by the high throughput assay which was not observed in the standard assay	Fig. 6.6 E, F, resting $[Ca^{2+}]_c$

Figures 6.6A and B show a "correct" detection by the high throughput assay in which the effects of NaCl on increasing $[Ca^{2+}]_c$ amplitude and resting $[Ca^{2+}]_c$ were detected. Figure 6.6C and D provide an example of "missed positive" results for both resting $[Ca^{2+}]_c$ and $[Ca^{2+}]_c$ amplitude. The resting $[Ca^{2+}]_c$ in Fig. 6.6 E and F show an example of a "false positive" result.

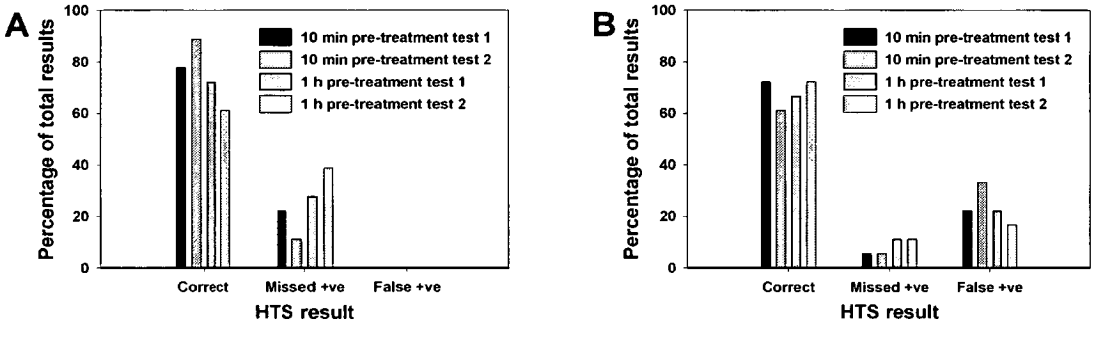

Fig. 6.7 A. Comparison of results obtained with the high throughput $[Ca^{2+}]_c$ assay compared with those obtained using the standard $[Ca^{2+}]_c$ assay. This comparison involved compiling all the results for each assay and classifing them as described in Table 6.4 and Fig. 6.6. **A.** Comparison of the $[Ca^{2+}]_c$ amplitudes. **B.** Comparison of the resting $[Ca^{2+}]_c$ values.

Accuracy for the high throughput assay was defined as the proportion of correct detections across all samples for results involving the measurement of resting $[Ca^{2+}]_c$ and $[Ca^{2+}]_c$ amplitude. The length of pre-treatment had little effect on the accuracy of the high throughput assay and no obvious trends were apparent (Fig. 6.7). For detection of changes in the $[Ca^{2+}]_c$ amplitude, the high throughput assay had an accuracy that varied between 61% and 89% (Fig. 6.7A). All errors in the detection of $[Ca^{2+}]_c$ amplitude changes were missed positives (Fig. 6.7A). Failure to detect changes in $[Ca^{2+}]_c$ amplitude was observed in compounds that caused a small inhibition or elevation of the $[Ca^{2+}]_c$ amplitude or resting level particularly 0.75 mM BAPTA (not detected in 3 out of 4 experiments), 100 μM CPA and 4 μM RsAFP2 (nothing detected in any high throughput assay). A significant level of errors also occurred in the detection of the inhibition of the $[Ca^{2+}]_c$ amplitude by Triton X-100 (inhibition not detected in 2 out of 4 samples) and 6.6% H_2O_2 (inhibition not detected in 3 out of 4 samples). Errors obtained with these compounds may be related to aequorin consumption as > 50% consumption was always observed after adding 6.6% H_2O_2, and frequently observed after adding 0.1% Triton X-100.

The overall level of accuracy for detecting changes in resting $[Ca^{2+}]_c$ (62% to 72%) was slightly greater than for detecting changes in $[Ca^{2+}]_c$ amplitude (61-89%; compare Figs. 6.7A with 6.7B). The detection of large increases in resting $[Ca^{2+}]_c$ was very accurate, and thus increases in $[Ca^{2+}]_c$ were detected for all tests involving treatment with H_2O_2, verapamil, diltiazem, Triton X-100, amphotericin B (60 $\mu g.ml^{-1}$) and RsAFP2. Small increases in resting $[Ca^{2+}]_c$ were less accurately detected especially those caused by CPA (no effect on resting $[Ca^{2+}]_c$ was detected in the high throughput assay) and NaCl (an increased resting $[Ca^{2+}]_c$ was detected in only 2 out of 4 assays). The greatest occurrence of error in the detection of changes in resting $[Ca^{2+}]_c$ was due to false positive results (Fig. 6.7B).

6.3 Discussion

6.3.1 Increase in throughput of the aequorin $[Ca^{2+}]_c$ assay

Development of the standard aequorin $[Ca^{2+}]_c$ assay into a high throughput assay facilitated the measurement of 23 samples per experiment. The time required for setup, experimentation, and $[Ca^{2+}]_c$ calibration of the high throughput assay, was similar to the standard aequorin assay. Despite the large increase in throughput here, many other high throughput screens in drug discovery are capable of considerably more rapid screening. The possibility of increasing the throughput of compounds tested by the use of a 384 well plate was considered. However the capacity of 120 µl per well (compared to 350 µl per well in a 96 well plate) would limit inoculation volume and therefore aequorin luminescence. Reduced levels of aequorin caused by smaller sample volumes would decrease the ratio between background luminescence and signal luminescence thus decreasing the reliability of the $[Ca^{2+}]_c$ assay (Chapter 3). The use of increased coelenterazine concentrations, or coelenterazine derivatives with increased activity, may be advantageous in adapting the assay developed in this chapter for use in a 384 well plate.

Although the aequorin high throughput assay has limited throughput, its specificity may provide benefits for future investigations. In chapters 4 and 5 the effects of defensin plant proteins and the deletion of putative $[Ca^{2+}]_c$ modulating proteins on the $[Ca^{2+}]_c$ responses to mechanical perturbation and hypo-osmotic shock, were described. Insights into the mode of action of the defensin plant proteins may be obtained by treating each of the deletion mutants, compromised in different components of the Ca^{2+} signalling machinery, with them. If the defensin treatment had no effect on the $[Ca^{2+}]_c$ signature of the mutant, this would provide evidence that the protein encoded by the deleted gene may be a target of the defensin. The assay developed in this chapter would represent a rapid and efficient mechanism of screening multiple deletion mutants against defensin proteins.

6.3.2 Sensitivity of the aequorin high throughput assay

Adaptation of the aequorin $[Ca^{2+}]_c$ assay into a high throughput screen required significant reduction in the measurement of RLU values from 59 to 9 measurements over ~ 11 min. This prevented the calculation of FWHM. The higher throughput method developed allowed measurement of the resting $[Ca^{2+}]_c$, amplitude of the $[Ca^{2+}]_c$ response and luminescence from total aequorin in a simple and rapid manner.

Comparison of the high throughput assay with the standard assay for $[Ca^{2+}]_c$ measurement confirmed that the high throughput method provided reasonably reliable identification of increased $[Ca^{2+}]_c$ (62-72% accuracy) and amplitude inhibition (61-89% accuracy). The duration of compound pre-treatment had little effect on the accuracy of the assay. The high throughput screen provided consistent identification of large changes in amplitude or resting $[Ca^{2+}]_c$. Where effects on resting $[Ca^{2+}]_c$ or amplitude were less pronounced, the efficiency of detection was reduced. The smaller changes in the $[Ca^{2+}]_c$ amplitude or resting $[Ca^{2+}]_c$ may be detected in future experiments by increasing the number of wells used for each sample, although this would reduce throughput of samples.

6.3.3 The aequorin $[Ca^{2+}]_c$ assay as a high throughput screen

For an effective and viable high throughput screen a range of characteristics and features are required. The key advantages of the aequorin $[Ca^{2+}]_c$ assay as a high throughput screen are:

- Capable of identifying perturbations in fungal $[Ca^{2+}]_c$ homeostasis (i.e. resting $[Ca^{2+}]_c$).
- Can detect perturbations in a $[Ca^{2+}]_c$ response of physiological significance in *N. crassa*.
- Allows the effects of potential antifungal compounds to be analysed in a living population of cells.
- The assay is based upon an extensively analysed model filamentous fungus

(*N. crassa*), which is well suited for genetic, molecular and physiological studies.

- The assay can be developed to screen for the involvement of specific $[Ca^{2+}]_c$ modulating proteins (e.g. defensins) in antifungal mechanisms of action.

6.4 Summary

The main findings described in this chapter were:

- A high throughput assay for measurement $[Ca^{2+}]_c$ has been developed and optimized for screening large numbers of potential antifungal compounds.
- A proof-of-concept for the use of a high throughput aequorin assay to detect effects of antifungal compounds on Ca^{2+} signalling, and homeostasis, has been provided.

Chapter 7

Summary and future work

In the research described in this thesis I have developed and optimized the existing aequorin $[Ca^{2+}]_c$ assay for fungal mycelia (Nelson *et al.*, 2004; Zelter, 2004) for use with germ tubes of *Neurospora crassa*. This assay was then used to analyse the $[Ca^{2+}]_c$ responses to mechanical perturbation and hypo-osmotic shock, examine the influences of antifungal proteins on these processes, and identify proteins that are involved in generating the $[Ca^{2+}]_c$ responses. The final stage of this work evaluated how the aequorin $[Ca^{2+}]_c$ assay could be developed into a high throughput screen to discover antifungal agents that target Ca^{2+} signalling and/or homeostasis.

Germ tubes of *N. crassa* were selected to provide a more homogenous cell population than the vegetative hyphal cultures previously examined (Zelter, 2004). Optimization of the assay confirmed that germ tubes produced sufficient recombinant aequorin for

accurate $[Ca^{2+}]_c$ measurement in cell populations. The germ tube $[Ca^{2+}]_c$ response was more reproducible than vegetative hyphae when subjected to increasing strengths of mechanical perturbation. The increased reproducibility was most likely due to a more even distribution of the mechanical perturbation stimulus to the germ tubes than can be achieved with the vegetative hyphal cultures. The lack of a hyphal matt may also be advantageous for even and effective distribution of potential $[Ca^{2+}]_c$ modulating compounds added to the germ tubes in this assay. On the basis of these benefits, 6 h germ tubes were selected for further experimentation in subsequent work described in this thesis.

Investigation of the apical hyphal swelling effects of mechanical perturbation on germ tubes identified a morphological response in the form of a transient cessation of apical extension accompanied by apical hyphal swelling that could be quantified. Removal of external Ca^{2+} abolished the $[Ca^{2+}]_c$ response to mechanical perturbation and severely inhibited the swelling response. This established a physiological link between the two responses. Polarized apical extension in *N. crassa* has been reported to require an apical $[Ca^{2+}]_c$ gradient (Levina *et al.*, 1995; Silverman-Gavrila and Lew, 2000; Silverman-Gavrila and Lew, 2003). Ca^{2+} influx in response to mechanical perturbation via stretch activated CPCs in the plasma membrane (Levina *et al.*, 1995) may increase $[Ca^{2+}]_c$ behind the tip. Sub-apical $[Ca^{2+}]_c$ elevation may temporarily disrupt the $[Ca^{2+}]_c$ gradient leading to apical swelling and cessation of extension in germ tubes.

Defensins are an important group of antifungal plant proteins, which may exert antifungal activity by perturbation of Ca^{2+} signalling (Osborn *et al.*, 1995). Despite considerable evidence that defensins increase Ca^{2+} accumulation (Thevissen *et al.*, 1996; De Samblanx *et al.*, 1997; Spelbrink *et al.*, 2004) and inhibit Ca^{2+} channel activity (Spelbrink *et al.*, 2004), their effects on fungal $[Ca^{2+}]_c$ had not been examined. MsDef1, RsAFP2 and MtDef4 were all found to substantially increase resting $[Ca^{2+}]_c$ and exert specific effects on the $[Ca^{2+}]_c$ responses to mechanical perturbation and hypo-osmotic shock. Morphogenic defensins, such as MsDef1 and RsAFP2, inhibit growth by inducing hyperbranching and inhibiting hyphal elongation (Thevissen *et al.*, 1996). Non-morphogenic defensins, such as MtDef4, inhibit hyphal elongation without affecting branching (Ramamoorthy *et al.*, 2007). Although

branching in *N. crassa* has been proposed to be initiated by localized increases in $[Ca^{2+}]_c$ (Silverman-Gavrila *et al.*, 2000), this is not consistent with my finding that MtDef4 increases $[Ca^{2+}]_c$ without inducing branching.

This process of membrane permeabilization may facilitate the defensin targeting CPCs, Ca^{2+} pumps and transporters located on intracellular membranes. My results indicated that the different defensins targeted different components of the Ca^{2+} signalling machinery either directly or indirectly. I obtained evidence for some targeting both CPCs and Ca^{2+} pumps or transporters (MsDef1 and MtDef4) whilst others (RsAFP2 and MtDef2) may only target Ca^{2+} pumps or transporters. A mechanism of action for defensins has been proposed in which they bind specific sites at the plasma membrane where they become inserted into the membrane resulting in pore formation and permeabilization the membrane to Ca^{2+} (Thevissen *et al.*, 2003a). The increased $[Ca^{2+}]_c$ resting level which consistently resulted from treatment with defensins may then have been a non-specific effect of membrane permeabilization.

There is increasing evidence that defensins may also inhibit fungal growth by interaction with intracellular components other than $[Ca^{2+}]_c$ signalling (Lobo *et al.*, 2007; Ramamoorthy *et al.*, 2007). This evidence is supported by my results which showed weak effects of MtDef2 on Ca^{2+} signalling at concentrations capable of inhibiting *N. crassa* growth. Future studies should focus on biochemical assays to analyse the interaction between the defensins and different Ca^{2+} signalling proteins as well as analysing cross talk with other signalling pathways (e.g. MAP kinase signalling, Ramamoorthy *et al.*, 2007) that may also be targets of defensins.

Creation of deletion mutants by the *Neurospora* Genome Project (http://www.dartmouth.edu/~neurosporagenome/index.html) facilitated analysis of predicted $[Ca^{2+}]_c$ modulating proteins in the responses to mechanical perturbation and hypo-osmotic shock. Deletion mutants were selected on the basis of existing genetic and functional evidence (Margolles-Clark *et al.*, 1999; Benito *et al.*, 2000; Zelter *et al.*, 2004), and knock out strains were transformed with codon optimized aequorin. My work found that *N. crassa* MID-1 was essential for the $[Ca^{2+}]_c$ response to mechanical perturbation despite being predicted to be unable to form a functional CPC on its own. MID-1 may act as a mechanosensor and mediate Ca^{2+} influx via

regulation of CCH-1; the two proteins are believed to act cooperatively in both *Saccharomyces cerevisiae* (Paidhungat and Garrett, 1997) and *Candida albicans* (Brand et al., 2007). This theory was supported by my results that showed inhibition of Ca^{2+} influx by L-type Ca^{2+} channel blockers which are predicted to inhibit CCH-1 activity.

Future work will need to examine whether the reintroduction of the *mid-1* gene in the aequorin expressing Δ*mid-1* strain can restore the $[Ca^{2+}]_c$ response. GFP localization of MID-1 would also be useful to determine whether MID-1 is localized in the germ tube tip (where swelling occurs).

Work with the deletion mutants also revealed the involvement of multiple ATPases in the reduction of $[Ca^{2+}]_c$ following its transient increase after mechanical perturbation and hypo-osmotic shock. *N. crassa* possesses 18 proteins that are predicted to remove Ca^{2+} from the cytoplasm (Zelter *et al.*, 2004). These proteins include predicted ATPases, Ca^{2+}/H^+ exchangers and Ca^{2+}/Na^+ exchangers. Deletion mutants are now available from the FGSC (www.fgsc.net) for 14 of these proteins. However, the remaining deletion mutants, along with the putative CCH-1 protein, were ascospore lethal. Ascospore lethal deletion mutants are available as heterokaryons which have not been put through a sexual cross and thus contain both antibiotic selection markers for *N. crassa* used in this study (hygromycin and ignite resistance, see section 1.3.2). In order to complete the analysis of Ca^{2+} signalling in response to mechanical perturbation and hypo-osmotic shock recombinant aequorin must be expressed in these strains. A potential third selection marker which could be used to select for aequorin expressing transformants of these strains is histidine auxotrophy.

In future work it will be important to identify the location of different components of the Ca^{2+} signalling machinery by using GFP labelling. The roles of different Ca^{2+} storage organelles (e.g. vacuoles, ER, mitochondria and Golgi) should also be analysed by targeting aequorin to these organelles in order to measure organellar free Ca^{2+} changes following stimulation. The targeting of aequorin to subcellular organelles was been developed in mammalian cells (e.g. Brini *et al.*, 1999) and aequorin has since been targeted to ER in *S. cerevisiae* (Strayle *et al.*, 1999) and mitochondria in *Aspergillus nidulans* (Greene *et al.*, 2002).

Despite the considerable progress made with the aequorin method in this work, investigation of Ca^{2+} signalling in filamentous fungi is still limited by the inability to reliably image $[Ca^{2+}]_c$ in single, living fungal cells. At present there are major problems because the Ca^{2+}-sensitive dyes do not work (see section 1.4.1).

The final section of my work examined how the aequorin $[Ca^{2+}]_c$ assay could be adapted and optimized for use for a high throughput screen to discover antifungal agents that target Ca^{2+} signalling and/or homeostasis. Assay protocols were designed, and optimized. Although the high throughput assay displayed reduced accuracy and resolution of the Ca^{2+} signal compared with the standard assay, the level of throughput was substantially increased.

Appendix A

Media and Solutions

A-1 *E. coli* growth media

A-1.1 Luria-Bertani (LB) medium

Ingredient	Amount
Bacto Tryptone	10 g
Bacto Yeast Extract	5 g
NaCl	10 g
dH_20	to 1 litre
Oxoid Agar (for solid media)	15 $mgml^{-1}$

A-2 *Neurospora crassa* growth media

A-2.1 Vogel's Medium

A-2.1.1 Vogel's 50× stock solution

Ingredient	Amount
Na_3 citrate.$2H_2O$	126.7 g
KH_2PO_4	250 g
NH_4NO_3	100 g
$MgSO_4.7H_2O$	10 g
$CaCl_2.2H_2O$	5 g
D-Biotin solution	5 ml
Trace element solution	5 ml
dH_2O	to 1 litre

Chloroform was added as a preservative and the solution was stored in the dark at room temperature. Biotin solution - 5 mg of D-biotin dissolved in 100 ml of 50 % v/v ethanol (EtOH) and was stored at 4 °C.

A-2.1.2 Biotin Stock Solution

Dissolve 5 mg Biotin in 100 ml 50% ethanol, filter sterilize and store at 4 °C.

A-2.1.3 Vogels Medium Trace Element Solution

Ingredient	Amount
citric acid.$1H_2O$	5.0 g
$ZnSO_4.7H_2O$	5.0 g
$Fe(NH_4)2(SO_4)2.6H_2O$	1.0 g
$CuSO_4.5H_2O$	0.25 g
$MnSO_4.1H_2O$	0.05 g
H_3BO_3	0.05 g
$Na_2MoO_4.2H_20$	0.05 g
dH_2O	to 100 ml

Chloroform (1 ml) was added as a preservative and the solution was stored at room temperature.

A-2.1.4 Vogel's medium (complete)

Ingredient	Amount
Vogels 50× stock solution	20 ml
Sucrose	15 g
Agar	18 g
dH_2O	to 1 litre

A-2.2 *Neurospora crassa* transformation media

A-2.2.1 10× Fructose Sucrose Sorbose solution (FGS)

Ingredient	Amount
Sorbose	100 g
Fructose	2.5 g
Glucose	2.5 g
dH_2O	to 500 ml

A-2.2.2 Bottom agar

Ingredient	Amount
50× Nitrogen free Vogels stock solution	10 ml
Bacto Agar	7.5 g
L-Arginine hydrochloride	1.5 g
dH_2O	to 450 ml

Autoclave then add 50 ml 10× FIGS. Cool to 50 – 60 °C then add antibiotic for selection.

A-2.2.3 Top agar for hygromycin B selection

Ingredient	Amount
50x Vogels stock solution	10 ml
Sorbitol	91 g
Oxoid agar	5 g
dH_2O	to 450 ml

Autoclave then add 50 ml 10× FIGS.

A-2.2.4 Top agar for ignite selection

Ingredient	Amount
Sorbitol	91 g
Oxoid agar	5 g
dH_2O	to 450 ml

Autoclave then add 50 ml 10× FIGS. Cool to 50 – 60 °C then add ignite.

Appendix B

Plasmid Maps

B-1 pAZ6

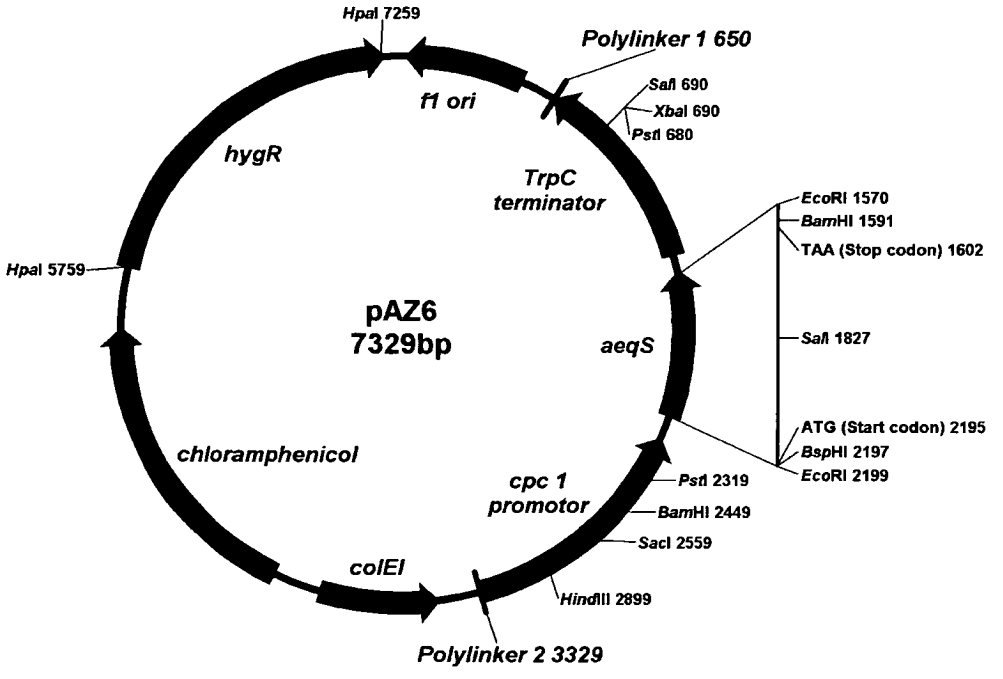

Fig B.1 The pAZ6 plasmid (from Zelter, 2004). Polylinker 1:T7.*Kpn*I.*Apa*I.*Xho*I.*Sal*I.*Cla*I. *Hind*III. Polylinker 2: *Xba*I.*Not*I.*Sac*I.T3.

B-2 pBARGRG1

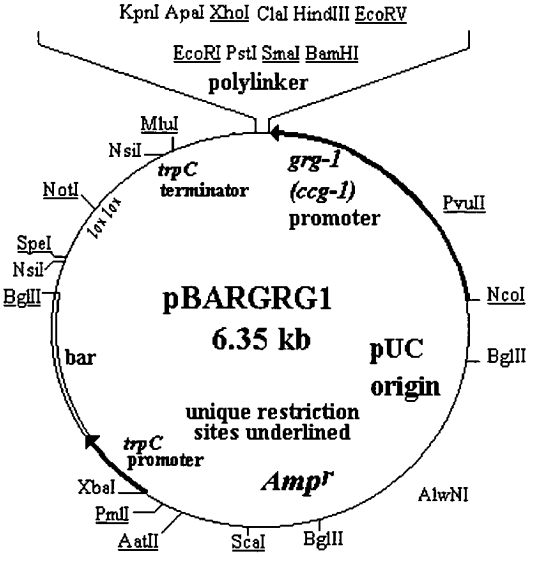

Fig B.2. The pBARGRG1 plasmid. Figure from Pall and Brunelli (1994).

B-3 pAB19

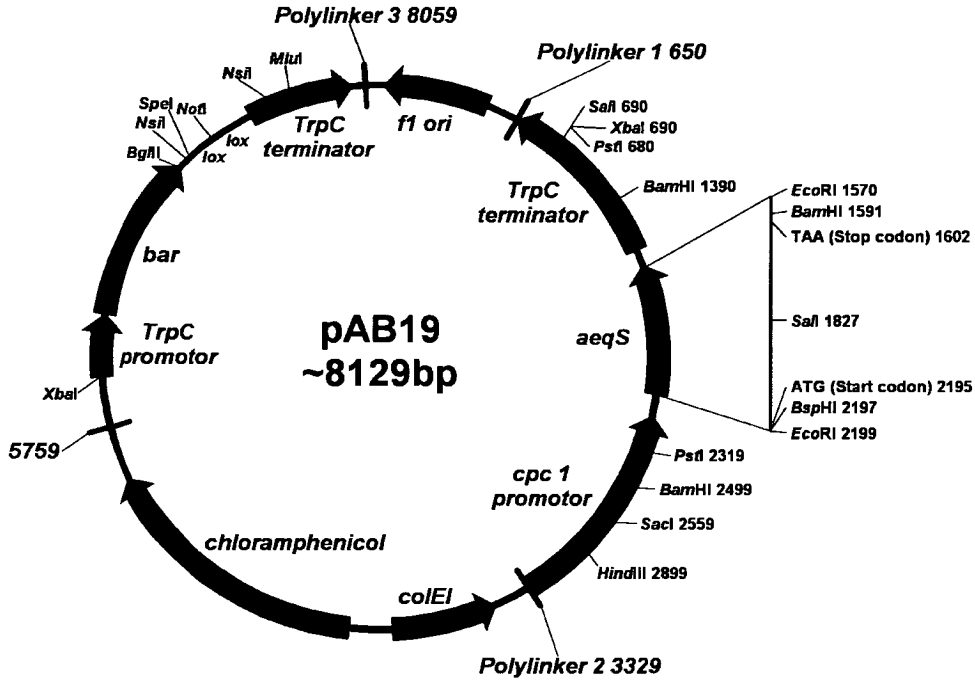

Fig B.3. The pAB19 plasmid. Polylinker 1: T7.*Kpn*I.*Apa*I.*Xho*I.*Sal*I.*Cla*I.*Hind*III; Polylinker 2: *Xba*I.*Not*I.*Sac*I.T3; Polylinker 3: *Kpn*I.*Apa*I.*Xho*I.*Cla*I.*Hind*III.

Bibliography

Adamikova, L., Straube, A., Schulz, I., Steinberg, G., 2004. Calcium signalling is involved in dynein-dependent microtubule organization. Mol. Biol. Cell 15, 1969-1980.

Ansari, K., Martin, S., Farkasovsky, M., Ehbrecht, I.M., Kuntzel, H., 1999. Phospholipase C binds to the receptor-like GPR1 protein and controls pseudohyphal differentiation in Saccharomyces cerevisiae. J. Biol. Chem. 274, 30052-30058.

Antebi, A., Fink, G.R., 1992. The yeast Ca^{2+}-ATPase homologue, PMR1, is required for normal Golgi function and localizes in a novel Golgi-like distribution. Mol. Biol. Cell 3, 633-654.

Baniecki, M.L., Wirth, D.F., Clardy, J., 2007. High-throughput Plasmodium falciparum growth assay for malaria drug discovery. Antimicrob. Agents Chemother. 51, 716-723.

Batiza, A.F., Schulz, T., Masson, P.H., 1996. Yeast respond to hypotonic shock with a calcium pulse. J. Biol. Chem. 271, 23357-23362.

Bencina, M., Legisa, M., Read, N.D., 2005. Cross-talk between cAMP and calcium signalling in *Aspergillus niger*. Mol. Microbiol. 56, 268-281.

Benito, B., Garciadeblas, B., Rodriguez-Navarro, A., 2000. Molecular cloning of the calcium and sodium ATPases in *Neurospora crassa*. Mol. Microbiol. 35, 1079-1088.

Berridge, M.J., 2006. Calcium microdomains: organization and function. Cell Calcium 40, 405-412.

Berridge, M.J., Bootman, M.D., Roderick, H.L., 2003. Calcium signalling: dynamics, homeostasis and remodelling. Nat. Rev. Mol. Cell Biol. 4, 517-529.

Berridge, M.J., Lipp, P., Bootman, M.D., 2000. The versatility and universality of calcium signalling. Nat. Rev. Mol. Cell Biol. 1, 11-21.

Bibikova, T.N., Zhigilei, A., Gilroy, S., 1997. Root hair growth in *Arabidopsis thaliana* is directed by calcium and an endogenous polarity. Planta 203, 495-505.

Bok, J.W., Sone, T., Silverman-Gavrila, L.B., Lew, R.R., Bowring, F.J., Catcheside, D.E., Griffiths, A.J., 2001. Structure and function analysis of the calcium-related gene spray in *Neurospora crassa*. Fun. Genet. Biol. 32, 145-158.

Bonilla, M., Cunningham, K.W., 2003. Mitogen-activated protein kinase stimulation of Ca^{2+} signalling is required for survival of endoplasmic reticulum stress in yeast. Mol. Biol. Cell 14, 4296-4305.

Bonilla, M., Nastase, K.K., Cunningham, K.W., 2002. Essential role of calcineurin in response to endoplasmic reticulum stress. EMBO J. 21, 2343-2353.

Bootman, M.D., Thomas, D., Tovey, S.C., Berridge, M.J., Lipp, P., 2000. Nuclear calcium signalling. Cell Mol. Life Sci. 57, 371-378.

Borisy, A.A., Elliott, P.J., Hurst, N.W., Lee, M.S., Lehar, J., Price, E.R., Serbedzija, G., Zimmermann, G.R., Foley, M.A., Stockwell, B.R., Keith, C.T., 2003. Systematic discovery of multicomponent therapeutics. Proc. Natl. Acad. Sci. U. S. A 100, 7977-7982.

Borkovich, K.A., Alex, L.A., Yarden, O., Freitag, M., Turner, G.E., Read, N.D., Seiler, S., Bell-Pedersen, D., Paietta, J., Plesofsky, N., Plamann, M., Goodrich-Tanrikulu, M., Schulte, U., Mannhaupt, G., Nargang, F.E., Radford, A., Selitrennikoff, C., Galagan, J.E., Dunlap, J.C., Loros, J.J., Catcheside, D., Inoue, H., Aramayo, R., Polymenis, M., Selker, E.U., Sachs, M.S., Marzluf, G.A., Paulsen, I., Davis, R., Ebbole, D.J., Zelter, A., Kalkman, E.R., O'Rourke, R., Bowring, F., Yeadon, J., Ishii, C., Suzuki, K., Sakai, W., Pratt, R., 2004. Lessons from the genome sequence of *Neurospora crassa*: tracing the path from genomic blueprint to multicellular organism. Microbiol. Mol. Biol. Rev. 68, 1-108, table.

Bowman, E.J., O'Neill, F.J., Bowman, B.J., 1997. Mutations of pma-1, the gene encoding the plasma membrane H^+-ATPase of *Neurospora crassa*, suppress inhibition of growth by concanamycin A, a specific inhibitor of vacuolar ATPases. J. Biol. Chem. 272, 14776-14786.

Braam, J., Davis, R.W., 1990. Rain-, wind-, and touch-induced expression of calmodulin and calmodulin-related genes in *Arabidopsis*. Cell 60, 357-364.

Brand, A., Shanks, S., Duncan, V.M., Yang, M., Mackenzie, K., Gow, N.A., 2007. Hyphal orientation of *Candida albicans* is regulated by a calcium-dependent mechanism. Curr. Biol. 17, 347-352.

Brini, M., Pinton, P., Pozzan, T., and Rizzuto, R. Targeted Recombinant Aequorins: Tools for monitoring $[Ca^{2+}]$ in the Various Compartments of a Living Cell. Micro. Res. and Tech. 46, 380-389.

Brini, M., Carafoli, E., 2000. Calcium signalling: a historical account, recent developments and future perspectives. Cell Mol. Life Sci. 57, 354-370.

Broekaert, W.F., Terras, F.R., Cammue, B.P., Osborn, R.W., 1995. Plant defensins: novel antimicrobial peptides as components of the host defence system. Plant Physiol. 108, 1353-1358.

Capelli, N., Barja, F., van, T.D., Monnat, J., Turian, G., Ortega, P.R., 1997. Purification of a 47-kDa calmodulin-binding polypeptide as an actin-binding protein from *Neurospora crassa*. FEMS Microbiol. Lett. 147, 215-220.

Catty, P., de Kerchove, d.A., Goffeau, A., 1997. The complete inventory of the yeast *Saccharomyces cerevisiae* P-type transport ATPases. FEBS Lett. 409, 325-332.

Catty, P., Goffeau, A., 1996. Identification and phylogenetic classification of eleven putative P-type calcium transport ATPase genes in the yeasts *Saccharomyces cerevisiae* and *Schizosaccharomyces pombe*. Biosci. Rep. 16, 75-85.

Chen, T.H., Hsu, C.S., Tsai, P.J., Ho, Y.F., Lin, N.S., 2001. Heterotrimeric G-protein and signal transduction in the nematode-trapping fungus *Arthrobotrys dactyloides*. Planta 212, 858-863.

Coccetti, P., Tisi, R., Martegani, E., Souza, T.L., Lopes, B.R., de, M.C., I, Thevelein, J.M., 1998. The PLC1 encoded phospholipase C in the yeast *Saccharomyces cerevisiae* is essential for glucose-induced phosphatidylinositol turnover and activation of plasma membrane H^+-ATPase. Biochim. Biophys. Acta 1405, 147-154.

Collins, T.J., Read, N.D., 1997. Appressorium induction by topographical signals in six cereal rusts. Physiological and Mol. Plant Path. 51, 169-179.

Colot, H.V., Park, G., Turner, G.E., Ringelberg, C., Crew, C.M., Litvinkova, L., Weiss, R.L., Borkovich, K.A., Dunlap, J.C., 2006. A high-throughput gene knockout procedure

for *Neurospora* reveals functions for multiple transcription factors. Proc. Natl. Acad. Sci. U.S.A. 103, 10352-10357.

Cornelius, G., Gebauer, G., Techel, D., 1989. Inositol trisphosphate induces calcium release from *Neurospora crassa* vacuoles. Biochem. Biophys. Res. Commun. 162, 852-856.

Cornelius, G., Nakashima, H., 1987. Vacuoles play a decisive role in calcium homeostasis in *Neurospora crassa*. J. of Gen. Micro. 133, 2341-2347.

Corrêa, A., Staples, R.C., Hoch, H.C. Inhibition of thigmostimulated cell differentiation with RGD-peptides in *Uromyces* germlings. Protoplasma 194, 91-102. 1996.

Courchesne, W.E., Ozturk, S., 2003. Amiodarone induces a caffeine-inhibited, MID1-depedent rise in free cytoplasmic calcium in *Saccharomyces cerevisiae*. Mol. Microbiol. 47, 223-234.

Cronin, S.R., Rao, R., Hampton, R.Y., 2002. Cod1p/Spf1p is a P-type ATPase involved in ER function and Ca^{2+} homeostasis. J. Cell Biol. 157, 1017-1028.

Cruz, M.C., Fox, D.S., Heitman, J., 2001. Calcineurin is required for hyphal elongation during mating and haploid fruiting in *Cryptococcus neoformans*. EMBO J. 20, 1020-1032.

Cruzalegui, F.H., Bading, H., 2000. Calcium-regulated protein kinase cascades and their transcription factor targets. Cell Mol. Life Sci. 57, 402-410.

Cunningham, K.W., Fink, G.R., 1994. Calcineurin-dependent growth control in *Saccharomyces cerevisiae* mutants lacking *PMC1*, a homolog of plasma membrane Ca^{2+} ATPases. J. Cell Biol. 124, 351-363.

Cunningham, K.W., Fink, G.R., 1996. Calcineurin inhibits VCX1-dependent H^+/Ca^{2+} exchange and induces Ca^{2+} ATPases in *Saccharomyces cerevisiae*. Mol. Cell Biol. 16, 2226-2237.

Cyert, M.S., 2001. Genetic analysis of calmodulin and its targets in *Saccharomyces cerevisiae*. Annu. Rev. Genet. 35, 647-672.

Cyert, M.S., Kunisawa, R., Kaim, D., Thorner, J., 1991. Yeast has homologs (CNA1 and CNA2 gene products) of mammalian calcineurin, a calmodulin-regulated phosphoprotein phosphatase. Proc. Natl. Acad. Sci. U.S.A. 88, 7376-7380.

d'Enfert, C., Bonini, B.M., Zapella, P.D., Fontaine, T., da Silva, A.M., Terenzi, H.F., 1999. Neutral trehalases catalyse intracellular trehalose breakdown in the filamentous fungi *Aspergillus nidulans* and *Neurospora crassa*. Mol. Microbiol. 32, 471-483.

Davidson, S.M., Duchen, M.R., 2006. Calcium microdomains and oxidative stress. Cell Calcium 40, 561-574.

Davis, T.N., Urdea, M.S., Masiarz, F.R., Thorner, J., 1986. Isolation of the yeast calmodulin gene: calmodulin is an essential protein. Cell 47, 423-431.

de Groot, P.W., Hellingwerf, K.J., Klis, F.M., 2003. Genome-wide identification of fungal GPI proteins. Yeast 20, 781-796.

De Virgilio, V.C., Burckert, N., Neuhaus, J.M., Boller, T., Wiemken, A., 1993. CNE1, a Saccharomyces cerevisiae homologue of the genes encoding mammalian calnexin and calreticulin. Yeast 9, 185-188.

Denis, V., Cyert, M.S., 2002. Internal Ca^{2+} release in yeast is triggered by hypertonic shock and mediated by a TRP channel homologue. J. Cell Biol. 156, 29-34.

De Samblanx, G.W., Goderis, I.J., Thevissen, K., Raemaekers, R., Fant, F., Borremans, F., Acland, D.P., Osborn, R.W., Patel, S., Broekaert, W.F., 1997. Mutational analysis of a plant defensin from radish (Raphanus sativus L.) reveals two adjacent sites important for antifungal activity. J. Biol. Chem. 272, 1171-1179.

Diaz, M.R., Fell, J.W., 2004. High-throughput detection of pathogenic yeasts of the genus trichosporon. J. Clin. Microbiol. 42, 3696-3706.

Dolman, N.J., Tepikin, A.V., 2006. Calcium gradients and the Golgi. Cell Calcium 40, 505-512.

Dominguez, D.C., 2004. Calcium signalling in bacteria. Mol. Microbiol. 54, 291-297.

Dunlap, J.C., Borkovich, K.A., Henn, M.R., Turner, G.E., Sachs, M.S., Glass, N.L., McCluskey, K., Plamann, M., Galagan, J.E., Birren, B.W., Weiss, R.L., Townsend, J.P., Loros, J.J., Nelson, M.A., Lambreghts, R., Colot, H.V., Park, G., Collopy, P., Ringelberg, C., Crew, C., Litvinkova, L., DeCaprio, D., Hood, H.M., Curilla, S., Shi, M., Crawford, M., Koerhsen, M., Montgomery, P., Larson, L., Pearson, M., Kasuga, T., Tian, C., Basturkmen, M., Altamirano, L., Xu, J., 2007. Enabling a community to dissect an organism: overview of the *Neurospora* functional genomics project. Adv. Genet. 57, 49-96.

Durr, G., Strayle, J., Plemper, R., Elbs, S., Klee, S.K., Catty, P., Wolf, D.H., Rudolph, H.K., 1998. The medial-Golgi ion pump Pmr1 supplies the yeast secretory pathway with Ca^{2+} and Mn^{2+} required for glycosylation, sorting, and endoplasmic reticulum-associated protein degradation. Mol. Biol. Cell 9, 1149-1162.

Edlind, T., Smith, L., Henry, K., Katiyar, S., Nickels, J., 2002. Antifungal activity in *Saccharomyces cerevisiae* is modulated by calcium signalling. Mol. Microbiol. 46, 257-268.

Fischer, M., Schnell, N., Chattaway, J., Davies, P., Dixon, G., Sanders, D., 1997. The *Saccharomyces cerevisiae* CCH1 gene is involved in calcium influx and mating. FEBS Lett. 419, 259-262.

Flick, J.S., Thorner, J., 1993. Genetic and biochemical characterization of a phosphatidylinositol-specific phospholipase C in *Saccharomyces cerevisiae*. Mol. Cell Biol. 13, 5861-5876.

Flick, J.S., Thorner, J., 1998. An essential function of a phosphoinositide-specific phospholipase C is relieved by inhibition of a cyclin-dependent protein kinase in the yeast *Saccharomyces cerevisiae*. Genetics 148, 33-47.

Forster, C., Kane, P.M., 2000. Cytosolic Ca^{2+} homeostasis is a constitutive function of the V-ATPase in *Saccharomyces cerevisiae*. J. Biol. Chem. 275, 38245-38253.

Fox, D.S., Cruz, M.C., Sia, R.A., Ke, H., Cox, G.M., Cardenas, M.E., Heitman, J., 2001. Calcineurin regulatory subunit is essential for virulence and mediates interactions with FKBP12-FK506 in *Cryptococcus neoformans*. Mol. Microbiol. 39, 835-849.

Fox, D.S., Heitman, J., 2002. Good fungi gone bad: the corruption of calcineurin. Bioessays 24, 894-903.

Fox, D.S., Heitman, J., 2005. Calcineurin-binding protein Cbp1 directs the specificity of calcineurin-dependent hyphal elongation during mating in *Cryptococcus neoformans*. Euk. Cell 4, 1526-1538.

Fricker, M.D., Pleith, C., Knight, H., Blancaflor, E., Knight, M., White, N.S., Gilroy, S., 1999. Fluorescence and luminescence techniques to probe ion activities in living plant cells. In: Mason, W.T. (Ed.), Fluorescent and Luminescent Probes for Biological Activity Academic Press, pp. 569-596.

Gage, M.J., Bruenn, J., Fischer, M., Sanders, D., Smith, T.J., 2001. KP4 fungal toxin inhibits growth in *Ustilago maydis* by blocking calcium uptake. Mol. Microbiol. 41, 775-785.

Galagan, J.E., Calvo, S.E., Borkovich, K.A., Selker, E.U., Read, N.D., Jaffe, D., FitzHugh, W., Ma, L.J., Smirnov, S., Purcell, S., Rehman, B., Elkins, T., Engels, R., Wang, S., Nielsen, C.B., Butler, J., Endrizzi, M., Qui, D., Ianakiev, P., Bell-Pedersen, D., Nelson, M.A., Werner-Washburne, M., Selitrennikoff, C.P., Kinsey, J.A., Braun, E.L., Zelter, A., Schulte, U., Kothe, G.O., Jedd, G., Mewes, W., Staben, C., Marcotte, E., Greenberg, D., Roy, A., Foley, K., Naylor, J., Stange-Thomann, N., Barrett, R., Gnerre, S., Kamal, M., Kamvysselis, M., Mauceli, E., Bielke, C., Rudd, S., Frishman, D., Krystofova, S., Rasmussen, C., Metzenberg, R.L., Perkins, D.D., Kroken, S., Cogoni, C., Macino, G., Catcheside, D., Li, W., Pratt, R.J., Osmani, S.A., DeSouza, C.P., Glass, L., Orbach, M.J., Berglund, J.A., Voelker, R., Yarden, O., Plamann, M., Seiler, S., Dunlap, J., Radford, A., Aramayo, R., Natvig, D.O., Alex, L.A., Mannhaupt, G., Ebbole, D.J., Freitag, M., Paulsen, I., Sachs, M.S., Lander, E.S., Nusbaum, C., Birren, B., 2003. The genome sequence of the filamentous fungus *Neurospora crassa*. Nature 422, 859-868.

Garrill, A., Jackson, S.L., Lew, R.R., Heath, I.B., 1993. Ion channel activity and tip growth: tip-localized stretch-activated channels generate an essential Ca^{2+} gradient in the oomycete *Saprolegnia ferax*. Eur. J. Cell Biol. 60, 358-365.

Gorlach, J., Fox, D.S., Cutler, N.S., Cox, G.M., Perfect, J.R., Heitman, J., 2000. Identification and characterization of a highly conserved calcineurin binding protein, CBP1/calcipressin, in *Cryptococcus neoformans*. EMBO J. 19, 3618-3629.

Gorovits, R., Propheta, O., Kolot, M., Dombradi, V., Yarden, O., 1999. A mutation within the catalytic domain of COT1 kinase confers changes in the presence of two COT1 isoforms and in Ser/Thr protein kinase and phosphatase activities in *Neurospora crassa*. Fun. Genet. Biol. 27, 264-274.

Greene, V., Cao, H., Schanne, F.A., Bartelt, D.C., 2002. Oxidative stress-induced calcium signalling in *Aspergillus nidulans*. Cell Signal. 14, 437-443.

Gu, F., Khimani, A., Rane, S.G., Flurkey, W.H., Bozarth, R.F., Smith, T.J., 1995. Structure and function of a virally encoded fungal toxin from *Ustilago maydis*: a fungal and mammalian Ca^{2+} channel inhibitor. Structure. 3, 805-814.

H.C.Hoch, Staples, R.C., Whitehead, B., Comeau, J., Wolf, E.D., 1987. Signalling for growth orientation and cell differentiation by surface topography in *Uromyces*. Science 235, 1659-1662.

Haley, A., Russell, A.J., Wood, N., Allan, A.C., Knight, M., Campbell, A.K., Trewavas, A.J., 1995. Effects of mechanical signalling on plant cell cytosolic calcium. Proc. Natl. Acad. Sci. U.S.A. 92, 4124-4128.

Hashido, M., Hayashi, K., Hirose, K., Iino, M., 2006. Ca^{2+} lightning conveys cell-cell contact information inside the cells. EMBO Rep. 7, 1117-1123.

Hays, S., Selker, E.U., 2000. Making the selectable marker *bar* tighter and more economical. F. G. N. 47, 107.

Hetherington, A.M., Brownlee, C., 2004. The generation of Ca^{2+} signals in plants. Annu. Rev. Plant Biol. 55, 401-427.

Hickey, P.C., Swift, S.R., Roca, M.G., Read, N.D., 2005. Live-cell Imaging of Filamentous Fungi Using Vital Fluorescent Dyes and Confocal Microscopy. Methods in Microbiology Elsevier: Amsterdam, pp. 63-87.

Higuchi, S., Tamura, J., Giri, P.R., Polli, J.W., Kincaid, R.L., 1991. Calmodulin-dependent protein phosphatase from *Neurospora crassa*. Molecular cloning and expression of recombinant catalytic subunit. J. Biol. Chem. 266, 18104-18112.

Hosking, S.L., Robson, G.D., Trinci, A.P.J., 1995. Phosphoinositides Play a Role in Hyphal Extension and Branching in *Neurospora crassa*. Exper. Mycol. 19, 71-80.

Hudecova, D., Varecka, L., Vollek, V., Betina, V., 1994. Growth and morphogenesis of *Botrytis cinera*. Effects of exogenous calcium ions, calcium channel blockers and cyclosporin A. Folia Microbiol. 39, 269-275.

Iida, H., Nakamura, H., Ono, T., Okumura, M.S., Anraku, Y., 1994. MID1, a novel *Saccharomyces cerevisiae* gene encoding a plasma membrane protein, is required for Ca^{2+} influx and mating. Mol. Cell Biol. 14, 8259-8271.

Iida, K., Tada, T., Iida, H., 2004. Molecular cloning in yeast by in vivo homologous recombination of the yeast putative alpha1 subunit of the voltage-gated calcium channel. FEBS Lett. 576, 291-296.

Inglese, J., Auld, D.S., Jadhav, A., Johnson, R.L., Simeonov, A., Yasgar, A., Zheng, W., Austin, C.P., 2006. Quantitative high-throughput screening: a titration-based approach that efficiently identifies biological activities in large chemical libraries. Proc. Natl. Acad. Sci. U.S.A. 103, 11473-11478.

Inouye, S., Noguchi, M., Sakaki, Y., Takagi, Y., Miyata, T., Iwanaga, S., Miyata, T., Tsuji, F.I., 1985. Cloning and sequence analysis of cDNA for the luminescent protein aequorin. Proc. Natl. Acad. Sci. U.S.A. 82, 3154-3158.

Iqbal, J., Zaidi, M., 2005. Molecular regulation of mechanotransduction. Biochem. Biophys. Res. Commun. 328, 751-755.

Joseph, J.D., Means, A.R., 2000. Identification and characterization of two Ca^{2+}/CaM-dependent protein kinases required for normal nuclear division in *Aspergillus nidulans*. J. Biol. Chem. 275, 38230-38238.

Jung, O.J., Lee, E.J., Kim, J.W., Chung, Y.R., Lee, C.W., 1997. Identification of putative phosphoinositide-specific phospholipase C genes in filamentous fungi. Mol. Cell. 7, 192-199.

Juvvadi, P.R., Arioka, M., Nakajima, H., Kitamoto, K., 2001. Cloning and sequence analysis of cnaA gene encoding the catalytic subunit of calcineurin from *Aspergillus oryzae*. FEMS Microbiol. Lett. 204, 169-174.

Kafadar, K.A., Cyert, M.S., 2004. Integration of stress responses: modulation of calcineurin signalling in *Saccharomyces cerevisiae* by protein kinase A. Euk. Cell 3, 1147-1153.

Kafadar, K.A., Zhu, H., Snyder, M., Cyert, M.S., 2003. Negative regulation of calcineurin signalling by Hrr25p, a yeast homolog of casein kinase I. Genes Dev. 17, 2698-2708.

Kallies, A., Gebauer, G., Rensing, L., 1998. Heat shock effects on second messenger systems of *Neurospora crassa*. Arch. Microbiol. 170, 191-200.

Kanzaki, M., Nagasawa, M., Kojima, I., Sato, C., Naruse, K., Sokabe, M., Iida, H., 1999. Molecular identification of a eukaryotic, stretch-activated nonselective cation channel. Science 285, 882-886.

Kellermayer, R., Szigeti, R., Kellermayer, M., Miseta, A., 2004. The intracellular dissipation of cytosolic calcium following glucose re-addition to carbohydrate depleted *Saccharomyces cerevisiae*. FEBS Lett. 571, 55-60.

Kim, Y.K., Li, D., Kolattukudy, P.E., 1998. Induction of Ca^{2+}-calmodulin signalling by hard-surface contact primes *Colletotrichum gloeosporioides* conidia to germinate and form appressoria. J. Bacteriol. 180, 5144-5150.

Kingsbury, T.J., Cunningham, K.W., 2000. A conserved family of calcineurin regulators. Genes Dev. 14, 1595-1604.

Knight, M.R., Campbell, A.K., Smith, S.M., Trewavas, A.J., 1991. Transgenic plant aequorin reports the effects of touch and cold-shock and elicitors on cytoplasmic calcium. Nature 352, 524-526.

Knight, M.R., Read, N.D., Campbell, A.K., Trewavas, A.J., 1993. Imaging calcium dynamics in living plants using semi-synthetic recombinant aequorins. J. Cell Biol. 121, 83-90.

Knight, M.R., Smith, S.M., Trewavas, A.J., 1992. Wind-induced plant motion immediately increases cytosolic calcium. Proc. Natl. Acad. Sci. U.S.A. 89, 4967-4971.

Kornstein, L.B., Gaiso, M.L., Hammell, R.L., Bartelt, D.C., 1992. Cloning and sequence determination of a cDNA encoding *Aspergillus nidulans* calmodulin-dependent multifunctional protein kinase. Gene 113, 75-82.

Kothe, G.O., Free, S.J., 1998. Calcineurin subunit B is required for normal vegetative growth in *Neurospora crassa*. Fun. Genet. Biol. 23, 248-258.

Kozlova-Zwinderman, O., 2002. Calcium Measurement in Living Filamentous Fungi Expressing Codon-Optimized Aequorin. PhD Thesis, University of Edinburgh.

Kraus, P.R., Nichols, C.B., Heitman, J., 2005. Calcium- and calcineurin-independent roles for calmodulin in *Cryptococcus neoformans* morphogenesis and high-temperature growth. Euk. Cell 4, 1079-1087.

Kuno, T., Tanaka, H., Mukai, H., Chang, C.D., Hiraga, K., Miyakawa, T., Tanaka, C., 1991. cDNA cloning of a calcineurin B homolog in *Saccharomyces cerevisiae*. Biochem. Biophys. Res. Commun. 180, 1159-1163.

Kwon, S.-I., van Dohlon, C.D., Anderson, A.J., 2001. Gene sequence analysis of an opportunistic wheat pathogen, an isolate of *Fusarium proliferatum*. Can. J. Bot. 79, 1115-1121.

Legue, V., Blancaflor, E., Wymer, C., Perbal, G., Fantin, D., Gilroy, S., 1997. Cytoplasmic free Ca^{2+} in *Arabidopsis* roots changes in response to touch but not gravity. Plant Physiol. 114, 789-800.

Leinberger, D.M., Schumacher, U., Autenrieth, I.B., Bachmann, T.T., 2005. Development of a DNA microarray for detection and identification of fungal pathogens involved in invasive mycoses. J. Clin. Microbiol. 43, 4943-4953.

Levina, N.N., Lew, R.R., 2006. The role of tip-localized mitochondria in hyphal growth. Fun. Genet. Biol. 43, 65-74.

Levina, N.N., Lew, R.R., Hyde, G.J., Heath, I.B., 1995. The roles of Ca^{2+} and plasma membrane ion channels in hyphal tip growth of *Neurospora crassa*. J. Cell Sci. 108, 3405-3417.

Lew, R.R., 1999. Comparative analysis of Ca^{2+} and H^{+} flux magnitude and location along growing hyphae of *Saprolegnia ferax* and *Neurospora crassa*. Eur. J. Cell Biol. 78, 892-902.

Lew, R.R., Levina, N.N., 2004. Oxygen flux magnitude and location along growing hyphae of *Neurospora crassa*. FEMS Microbiol. Lett. 233, 125-130.

Lobo, D.S., Pereira, I.B., Fragel-Madeira, L., Medeiros, L.N., Cabral, L.M., Faria, J., Bellio, M., Campos, R.C., Linden, R., Kurtenbach, E., 2007. Antifungal Pisum sativum defensin 1 interacts with *Neurospora crassa* cyclin F related to the cell cycle. Biochemistry 46, 987-996.

Locke, E.G., Bonilla, M., Liang, L., Takita, Y., Cunningham, K.W., 2000a. A homolog of voltage-gated Ca^{2+} channels stimulated by depletion of secretory Ca^{2+} in yeast. Mol. Cell Biol. 20, 6686-6694.

Loukin, S.H., Kung, C., Saimi, Y., 2007. Lipid perturbations sensitize osmotic down-shock activated Ca^{2+} influx, a yeast "deletome" analysis. FASEB J.

Magalhaes, B.P., Wayne, R., Humber, R.A., Shields, E.J., Roberts, D.W. Calcium-regulated appressorium formation of the entomopathic fungus *Zoophthora radicans*. Protoplasma , 77-88. 1991.

Mahlo, R., Moutinho, A., van der Luit, A., Trewavas, A.J. Spatial characteristics of calcium signalling: the calcium wave as a basic unit in plant cell calcium signalling. Phil. Trans. R.Soc. Lond. 353, 1463-1473. 1998.

Marchi, V., Sorin, A., Wei, Y., Rao, R., 1999. Induction of vacuolar Ca^{2+}-ATPase and H^{+}/Ca^{2+} exchange activity in yeast mutants lacking Pmr1, the Golgi Ca^{2+}-ATPase. FEBS Lett. 454, 181-186.

Margolles-Clark, E.E., Abreu, S., Bowman, B.J., 1999. Characterization of a vacuolar Ca^{2+}/H^{+} exchanger (CAX) of *Neurospora crassa*. F. G. N. 46 (Supplementary), 37.

Matheos, D.P., Kingsbury, T.J., Ahsan, U.S., Cunningham, K.W., 1997. Tcn1p/Crz1p, a calcineurin-dependent transcription factor that differentially regulates gene expression in *Saccharomyces cerevisiae*. Genes Dev. 11, 3445-3458.

Matsumoto, T.K., Ellsmore, A.J., Cessna, S.G., Low, P.S., Pardo, J.M., Bressan, R.A., Hasegawa, P.M., 2002. An osmotically induced cytosolic Ca^{2+} transient activates calcineurin signalling to mediate ion homeostasis and salt tolerance of *Saccharomyces cerevisiae*. J. Biol. Chem. 277, 33075-33080.

Mendoza, I., Quintero, F.J., Bressan, R.A., Hasegawa, P.M., Pardo, J.M., 1996. Activated calcineurin confers high tolerance to ion stress and alters the budding pattern and cell morphology of yeast cells. J. Biol. Chem. 271, 23061-23067.

Mikuni-Takagaki, Y., 1999. Mechanical responses and signal transduction pathways in stretched osteocytes. J. Bone Miner. Metab 17, 57-60.

Miller, A.J., Vogg, G., Sanders, D., 1990. Cytosolic calcium homeostasis in fungi: roles of plasma membrane transport and intracellular sequestration of calcium. Proc. Natl. Acad. Sci. U.S.A. 87, 9348-9352.

Miseta, A., Fu, L., Kellermayer, R., Buckley, J., Bedwell, D.M., 1999a. The Golgi apparatus plays a significant role in the maintenance of Ca^{2+} homeostasis in the vps33Delta vacuolar biogenesis mutant of *Saccharomyces cerevisiae*. J. Biol. Chem. 274, 5939-5947.

Miseta, A., Kellermayer, R., Aiello, D.P., Fu, L., Bedwell, D.M., 1999b. The vacuolar Ca^{2+}/H^{+} exchanger Vcx1p/Hum1p tightly controls cytosolic Ca^{2+} levels in *S. cerevisiae*. FEBS Lett. 451, 132-136.

Mori, I.C., Iida, H., Tsuji, F.I., Isobe, M., Uozumi, N., Muto, S., 1998. Salicylic acid induces a cytosolic Ca^{2+} elevation in yeast. Biosci. Biotechnol. Biochem. 62, 986-989.

Muller, E.M., Locke, E.G., Cunningham, K.W., 2001. Differential regulation of two Ca^{2+} influx systems by pheromone signalling in Saccharomyces cerevisiae. Genetics 159, 1527-1538.

Muller, E.M., Mackin, N.A., Erdman, S.E., Cunningham, K.W., 2003. Fig1p facilitates Ca^{2+} influx and cell fusion during mating of *Saccharomyces cerevisiae*. J. Biol. Chem. 278, 38461-38469.

Nakagawa, Y., Katagiri, T., Shinozaki, K., Qi, Z., Tatsumi, H., Furuichi, T., Kishigami, A., Sokabe, M., Kojima, I., Sato, S., Kato, T., Tabata, S., Iida, K., Terashima, A., Nakano, M., Ikeda, M., Yamanaka, T., Iida, H., 2007. *Arabidopsis* plasma membrane protein crucial for Ca^{2+} influx and touch sensing in roots. Proc. Natl. Acad. Sci. U.S.A. 104, 3639-3644.

Nakajima-Shimada, J., Iida, H., Tsuji, F.I., Anraku, Y., 1991. Monitoring of intracellular calcium in *Saccharomyces cerevisiae* with an apoaequorin cDNA expression system. Proc. Natl. Acad. Sci. U.S.A. 88, 6878-6882.

Nelson, G., 1999. Development of the Recombinant Aequorin Method and its Evaluation for Calcium Measurement in Filamentous Fungi. PhD Thesis, University of Edinburgh.

Nelson, G., Kozlova-Zwinderman, O., Collis, A.J., Knight, M.R., Fincham, J.R., Stanger, C.P., Renwick, A., Hessing, J.G., Punt, P.J., van den Hondel, C.A., Read, N.D., 2004. Calcium measurement in living filamentous fungi expressing codon-optimized aequorin. Mol. Microbiol. 52, 1437-1450.

Ng, C.K., McAinsh, M.R., 2003. Encoding specificity in plant calcium signalling: hot-spotting the ups and downs and waves. Ann. Bot. 92, 477-485.

Ninomiya, Y., Suzuki, K., Ishii, C., Inoue, H., 2004. Highly efficient gene replacements in *Neurospora* strains deficient for nonhomologous end-joining. Proc. Natl. Acad. Sci. U.S.A. 101, 12248-12253.

Odom, A., Muir, S., Lim, E., Toffaletti, D.L., Perfect, J., Heitman, J., 1997. Calcineurin is required for virulence of *Cryptococcus neoformans*. EMBO J. 16, 2576-2589.

Ohsumi, Y., Anraku, Y., 1983. Calcium transport driven by a proton motive force in vacuolar membrane vesicles of *Saccharomyces cerevisiae*. J. Biol. Chem. 258, 5614-5617.

Ohya, Y., Umemoto, N., Tanida, I., Ohta, A., Iida, H., Anraku, Y., 1991. Calcium-sensitive cls mutants of *Saccharomyces cerevisiae* showing a Pet- phenotype are ascribable to defects of vacuolar membrane H^+-ATPase activity. J. Biol. Chem. 266, 13971-13977.

Okorokov, L.A., Silva, F.E., Okorokova Facanha, A.L., 2001. Ca^{2+} and H^+ homeostasis in fission yeast: a role of Ca^{2+}/H^+ exchange and distinct V-H^+-ATPases of the secretory pathway organelles. FEBS Lett. 505, 321-324.

Osborn, R.W., De Samblanx, G.W., Thevissen, K., Goderis, I., Torrekens, S., Van, L.F., Attenborough, S., Rees, S.B., Broekaert, W.F., 1995. Isolation and characterisation of plant defensins from seeds of *Asteraceae*, *Fabaceae*, *Hippocastanaceae* and *Saxifragaceae*. FEBS Lett. 368, 257-262.

Ozeki-Miyawaki, C., Moriya, Y., Tatsumi, H., Iida, H., Sokabe, M., 2005. Identification of functional domains of Mid1, a stretch-activated channel component, necessary for localization to the plasma membrane and Ca^{2+} permeation. Exp. Cell Res. 311, 84-95.

Paidhungat, M., Garrett, S., 1997. A homolog of mammalian, voltage-gated calcium channels mediates yeast pheromone-stimulated Ca^{2+} uptake and exacerbates the cdc1(Ts) growth defect. Mol. Cell Biol. 17, 6339-6347.

Pall, M.L., 1993. The use of Ignite (Basta; glufosinate; phosphinothricin) to select transformants of bar-containing plasmids in *Neurospora crassa*. F. G. N. 40, 58.

Pall, M.L., Brunelli, J.P., 1994. New plasmid and lambda/plasmid hybrid vectors and a *Neurospora crassa* genomic library containing the bar selectable marker and the Cre/lox site-specific recombination system for use in filamentous fungi. F. G. N. 41, 63-65.

Palmer, C.P., Zhou, X.L., Lin, J., Loukin, S.H., Kung, C., Saimi, Y., 2001. A TRP homolog in *Saccharomyces cerevisiae* forms an intracellular Ca^{2+}-permeable channel in the yeast vacuolar membrane. Proc. Natl. Acad. Sci. U.S.A. 98, 7801-7805.

Pauly, N., Knight, M.R., Thuleau, P., Graziana, A., Muto, S., Ranjeva, R., Mazars, C., 2001. The nucleus together with the cytosol generates patterns of specific cellular calcium signatures in tobacco suspension culture cells. Cell Calcium 30, 413-421.

Payne, W.E., Fitzgerald-Hayes, M., 1993. A mutation in PLC1, a candidate phosphoinositide-specific phospholipase C gene from *Saccharomyces cerevisiae*, causes aberrant mitotic chromosome segregation. Mol. Cell Biol. 13, 4351-4364.

Peiter, E., Fischer, M., Sidaway, K., Roberts, S.K., Sanders, D., 2005. The *Saccharomyces cerevisiae* Ca^{2+} channel Cch1pMid1p is essential for tolerance to cold stress and iron toxicity. FEBS Lett. 579, 5697-5703.

Petersen, O.H., Michalak, M., Verkhratsky, A., 2005. Calcium signalling: past, present and future. Cell Calcium 38, 161-169.

Pozos, T.C., Sekler, I., Cyert, M.S., 1996. The product of HUM1, a novel yeast gene, is required for vacuolar Ca^{2+}/H^{+} exchange and is related to mammalian Na^{+}/Ca^{2+} exchangers. Mol. Cell Biol. 16, 3730-3741.

Pozzan, T., Magalhaes, P., Rizzuto, R., 2000. The comeback of mitochondria to calcium signalling. Cell Calcium 28, 279-283.

Prasher, D., McCann, R.O., Cormier, M.J., 1985. Cloning and expression of the cDNA coding for aequorin, a bioluminescent calcium-binding protein. Biochem. Biophys. Res. Commun. 126, 1259-1268.

Price, A.H., Taylor, A., Ripley, S.J. Griffiths, A., Trewavas, A.J., Knight, M.R. 1994 Oxidative Signals in Tobacco Increase Cytosolic Calcium. The Plant Cell. 6, 1301-1310.

Prokisch, H., Yarden, O., Dieminger, M., Tropschug, M., Barthelmess, I.B., 1997. Impairment of calcineurin function in *Neurospora crassa* reveals its essential role in hyphal growth, morphology and maintenance of the apical Ca^{2+} gradient. Mol. Gen. Genet. 256, 104-114.

Ramage, G., Vande, W.K., Wickes, B.L., Lopez-Ribot, J.L., 2001. Standardized method for in vitro antifungal susceptibility testing of *Candida albicans* biofilms. Antimicrob. Agents Chemother. 45, 2475-2479.

Ramamoorthy, V., Zhao, X., Snyder, A.K., Xu, J.R., Shah, D.M., 2007. Two mitogen-activated protein kinase signalling cascades mediate basal resistance to antifungal plant defensins in *Fusarium graminearum*. Cell Microbiol. 9, 1491-1506.

Rao, J.P., Reena, G., Subramanyam, C., 1997. Calmodulin-dependent protein phosphorylation during conidial germination and growth of *Neurospora crassa*. Mycol. Res. 101, 1484-1488.

Rasmussen, C., Garen, C., Brining, S., Kincaid, R.L., Means, R.L., Means, A.R., 1994. The calmodulin-dependent protein phosphatase catalytic subunit (calcineurin A) is an essential gene in *Aspergillus nidulans*. EMBO J. 13, 3917-3924.

Rasmussen, C.D., Means, R.L., Lu, K.P., May, G.S., Means, A.R., 1990. Characterization and expression of the unique calmodulin gene of *Aspergillus nidulans*. J. Biol. Chem. 265, 13767-13775.

Read, N.D., Kellock, L.J., Collins, T.J., Gundlach, A.M., 1997. Role of topography sensing for infection-structure differentiation in cereal rust fungi. Planta 202, 163-170.

Read, N.D., Shacklock, P.S., Knight, M.R., Trewavas, A.J., 1993. Imaging calcium dynamics in living plant cells and tissues. Cell Bio. Intern. 17, 111-125.

Reig, J.A., Tellez-Inon, M.T., Flawia, M.M., Torres, H.N., 1984. Activation of *Neurospora crassa* soluble adenylate cyclase by calmodulin. Biochem. J. 221, 541-543.

Reissig, J.L., Kinney, S.G., 1983. Calcium as a branching signal in *Neurospora crassa*. J. Bacteriol. 154, 1397-1402.

Robson, G.D., Wiebe, M.G., Trinici, P.J., 1991a. Involvement of Ca^{2+} in the regulation of hyphal extension and branching in *Fusarium graminearum*. Exper. Mycol. 15, 263-272.

Robson, G.D., Wiebe, M.G., Trinici, P.J., 1991b. Low calcium concentrations induce increased branching in *Fusarium graminearum*. Mycol. Res. 95, 561-565.

Rudolph, H.K., Antebi, A., Fink, G.R., Buckley, C.M., Dorman, T.E., LeVitre, J., Davidow, L.S., Mao, J.I., Moir, D.T., 1989. The yeast secretory pathway is perturbed by mutations in PMR1, a member of a Ca^{2+} ATPase family. Cell 58, 133-145.

Sadakane, Y., Nakashima, H., 1996. Light-induced phase shifting of the circadian conidiation rhythm is inhibited by calmodulin antagonists in *Neurospora crassa*. J. Biol. Rhythms 11, 234-240.

Sambrook, J., Russell, D.W., 2001. Molecular Cloning: A laboratory manual. Cold Spring Harbour Press, Cold Spring Harbor, New York, United States.

Sanders, D., Brownlee, C., Harper, J.F., 1999. Communicating with calcium. Plant Cell 11, 691-706.

Sanders, D., Pelloux, J., Brownlee, C., Harper, J.F., 2002. Calcium at the crossroads of signalling. Plant Cell 14, S401-S417.

Schultz, C., Gebauer, G., Metschies, T., Rensing, L., Jastorff, B., 1990. cis,cis-cyclohexane 1,3,5-triol polyphosphates release calcium from *Neurospora crassa* via an unspecific Ins 1,4,5-P_3 receptor. Biochem. Biophys. Res. Commun. 166, 1319-1327.

Scrase-Field, S.A., Knight, M.R., 2003. Calcium: just a chemical switch? Curr. Opin. Plant Biol. 6, 500-506.

Serrano, R., Ruiz, A., Bernal, D., Chambers, J.R., Arino, J., 2002. The transcriptional response to alkaline pH in *Saccharomyces cerevisiae*: evidence for calcium-mediated signalling. Mol. Microbiol. 46, 1319-1333.

Shaw, B.D., Hoch, H.C., 2000. Ca^{2+} regulation of *Phyllosticta ampelicida* pycnidiospore germination and appressorium Formation. Fun. Genet. Biol. 31, 43-53.

Silverman-Gavrila, L.B., Lew, R.R., 2000. Calcium and tip growth in *Neurospora crassa.* Protoplasma 213, 203-217.

Silverman-Gavrila, L.B., Lew, R.R., 2001. Regulation of the tip-high [Ca^{2+}] gradient in growing hyphae of the fungus *Neurospora crassa.* Eur. J. Cell Biol. 80, 379-390.

Silverman-Gavrila, L.B., Lew, R.R., 2002. An IP_3-activated Ca^{2+} channel regulates fungal tip growth. J. Cell Sci. 115, 5013-5025.

Silverman-Gavrila, L.B., Lew, R.R., 2003. Calcium gradient dependence of *Neurospora crassa* hyphal growth. Microbiology 149, 2475-2485.

Solomon, P.S., Rybak, K., Trengove, R.D., Oliver, R.P., 2006. Investigating the role of calcium/calmodulin-dependent protein kinases in *Stagonospora nodorum.* Mol. Microbiol. 62, 367-381.

Sone, T., Griffiths, A.J., 1999. The frost gene of *Neurospora crassa* is a homolog of yeast cdc1 and affects hyphal branching via manganese homeostasis. Fun. Genet. Biol. 28, 227-237.

Sorin, A., Rosas, G., Rao, R., 1997. PMR1, a Ca^{2+}-ATPase in yeast Golgi, has properties distinct from sarco/endoplasmic reticulum and plasma membrane calcium pumps. J. Biol. Chem. 272, 9895-9901.

Spelbrink, R.G., Dilmac, N., Allen, A., Smith, T.J., Shah, D.M., Hockerman, G.H., 2004. Differential antifungal and calcium channel-blocking activity among structurally related plant defensins. Plant Physiol 135, 2055-2067.

Stathopoulos, A.M., Cyert, M.S., 1997. Calcineurin acts through the CRZ1/TCN1-encoded transcription factor to regulate gene expression in yeast. Genes Dev. 11, 3432-3444.

Stathopoulos-Gerontides, A., Guo, J.J., Cyert, M.S., 1999. Yeast calcineurin regulates nuclear localization of the Crz1p transcription factor through dephosphorylation. Genes Dev. 13, 798-803.

Strayle, J., Pozzan, T., Rudolph, H.K., 1999. Steady-state free Ca^{2+} in the yeast endoplasmic reticulum reaches only 10 microM and is mainly controlled by the secretory pathway pump pmr1. EMBO J. 18, 4733-4743.

Stroobant, P., Scarborough, G.A., 1979. Active transport of calcium in *Neurospora plasma* membrane vesicles. Proc. Natl. Acad. Sci. U.S.A. 76, 3102-3106.

Stryer, L., 1997. Signal Transduction Cascades. Biochemistry W. H. Freeman and Company New York, pp. 325-360.

Takahashi, K., Isobe, M., Knight, M.R., Trewavas, A.J., Muto, S., 1997. Hypoosmotic Shock Induces Increases in Cytosolic Ca^{2+} in Tobacco Suspension-Culture Cells. Plant Physiol. 113, 587-594.

Takeuchi, Y., Schmid, J., Caldwell, J.H., Harold, F.M., 1988. Transcellular ion currents and extension of *Neurospora crassa* hyphae. J. Membr. Biol. 101, 33-41.

Taylor, A.R., Manison, N., Fernandez, C., Wood, J., Brownlee, C., 1996. Spatial Organization of Calcium Signalling Involved in Cell Volume Control in the Fucus Rhizoid. Plant Cell 8, 2015-2031.

Techel, D., Gebauer, G., Kohler, W., Braumann, T., Jastorff, B., Rensing, L., 1990. On the role of Ca^{2+}-calmodulin-dependent and cAMP-dependent protein phosphorylation in the circadian rhythm of Neurospora crassa. J. Comp Physiol [B] 159, 695-706.

Tellez-Inon, M.T., Ulloa, R.M., Glikin, G.C., Torres, H.N., 1985. Characterization of *Neurospora crassa* cyclic AMP phosphodiesterase activated by calmodulin. Biochem. J. 232, 425-430.

Thevissen, K., Ghazi, A., De Samblanx, G.W., Brownlee, C., Osborn, R.W., Broekaert, W.F., 1996. Fungal membrane responses induced by plant defensins and thionins. J. Biol. Chem. 271, 15018-15025.

Thevissen, K., Osborn, R.W., Acland, D.P., Broekaert, W.F., 1997. Specific, high affinity binding sites for an antifungal plant defensin on *Neurospora crassa* hyphae and microsomal membranes. J. Biol. Chem. 272, 32176-32181.

Thevissen, K., Terras, F.R., Broekaert, W.F., 1999. Permeabilization of fungal membranes by plant defensins inhibits fungal growth. Appl. Environ. Microbiol. 65, 5451-5458.

Thevissen, K., Osborn, R.W., Acland, D.P., Broekaert, W.F., 2000. Specific binding sites for an antifungal plant defensin from *Dahlia* (*Dahlia merckii*) on fungal cells are required for antifungal activity. Mol. Plant Microbe Interact. 13, 54-61.

Thevissen, K., Ferket, K.K., Francois, I.E., Cammue, B.P., 2003a. Interactions of antifungal plant defensins with fungal membrane components. Peptides 24, 1705-1712.

Thevissen, K., Francois, I.E., Takemoto, J.Y., Ferket, K.K., Meert, E.M., Cammue, B.P., 2003b. DmAMP1, an antifungal plant defensin from *dahlia* (*Dahlia merckii*), interacts with sphingolipids from *Saccharomyces cerevisiae.* FEMS Microbiol. Lett. 226, 169-173.

Thevissen, K., Warnecke, D.C., Francois, I.E., Leipelt, M., Heinz, E., Ott, C., Zahringer, U., Thomma, B.P., Ferket, K.K., Cammue, B.P., 2004. Defensins from insects and plants interact with fungal glucosylceramides. J. Biol. Chem. 279, 3900-3905.

Thomma, B.P., Cammue, B.P., Thevissen, K., 2003. Mode of action of plant defensins suggests therapeutic potential. Curr. Drug Targets. Infect. Disord. 3, 1-8.

Tisi, R., Baldassa, S., Belotti, F., Martegani, E., 2002. Phospholipase C is required for glucose-induced calcium influx in budding yeast. FEBS Lett. 520, 133-138.

Tisi, R., Belotti, F., Wera, S., Winderickx, J., Thevelein, J.M., Martegani, E., 2004. Evidence for inositol triphosphate as a second messenger for glucose-induced calcium signalling in budding yeast. Curr. Genet. 45, 83-89.

Tokes-Fuzesi, M., Bedwell, D.M., Repa, I., Sipos, K., Sumegi, B., Rab, A., Miseta, A., 2002. Hexose phosphorylation and the putative calcium channel component Mid1p are required for the hexose-induced transient elevation of cytosolic calcium response in *Saccharomyces cerevisiae.* Mol. Microbiol. 44, 1299-1308.

Torralba, S., Heath, I.B., Ottensmeyer, F.P., 2001. Ca^{2+} shuttling in vesicles during tip growth in *Neurospora crassa*. Fun. Genet. Biol. 33, 181-193.

Tropia, M.J., Cardoso, A.S., Tisi, R., Fietto, L.G., Fietto, J.L., Martegani, E., Castro, I.M., Brandao, R.L., 2006. Calcium signalling and sugar-induced activation of plasma membrane H^+-ATPase in *Saccharomyces cerevisiae* cells. Biochem. Biophys. Res. Commun. 343, 1234-1243.

Tsai, P.J., Tu, J., Chen, T.H., 2002. Cloning of a Ca^{2+}/calmodulin-dependent protein kinase gene from the filamentous fungus *Arthrobotrys dactyloides*. FEMS Microbiol. Lett. 212, 7-13.

Viladevall, L., Serrano, R., Ruiz, A., Domenech, G., Giraldo, J., Barcelo, A., Arino, J., 2004. Characterization of the calcium-mediated response to alkaline stress in *Saccharomyces cerevisiae*. J. Biol. Chem. 279, 43614-43624.

Vogt, K., Bhabhra, R., Rhodes, J.C., Askew, D.S., 2005. Doxycycline-regulated gene expression in the opportunistic fungal pathogen *Aspergillus fumigatus*. BMC. Microbiol. 5, 1.

Vougel, H.J.A., 1956. Convenient growth medium for *Neurospora* (Medium N). Micro. Gen. Bulletin 13, 42-43.

Watts, H.J., Very, A.A., Perera, T.H., Davies, J.M., Gow, N.A., 1998. Thigmotropism and stretch-activated channels in the pathogenic fungus *Candida albicans*. Microbiology 144, 689-695.

Wera, S., Bergsma, J.C., Thevelein, J.M., 2001. Phosphoinositides in yeast: genetically tractable signalling. FEMS Yeast Res. 1, 9-13.

Wright, G.D., Arlt, J., Poon, W.C., Read, N.D., 2007. Optical tweezer micromanipulation of filamentous fungi. Fun. Genet. Biol. 44, 1-13.

Xiong, T.C., Bourque, S., Lecourieux, D., Amelot, N., Grat, S., Briere, C., Mazars, C., Pugin, A., Ranjeva, R., 2006. Calcium signalling in plant cell organelles delimited by a double membrane. Biochim. Biophys. Acta 1763, 1209-1215.

Yang, J., Kang, H.A., Ko, S.M., Chae, S.K., Ryu, D.D., Kim, J.Y., 2001a. Cloning of the *Aspergillus niger* pmrA gene, a homologue of yeast PMR1, and characterization of a pmrA null mutant. FEMS Microbiol. Lett. 199, 97-102.

Yang, Y., Cheng, P., Zhi, G., Liu, Y., 2001b. Identification of a calcium/calmodulin-dependent protein kinase that phosphorylates the *Neurospora* circadian clock protein FREQUENCY. J. Biol. Chem. 276, 41064-41072.

Yoko-o T, Matsui, Y., Yagisawa, H., Nojima, H., Uno, I., Toh-e A, 1993. The putative phosphoinositide-specific phospholipase C gene, PLC1, of the yeast *Saccharomyces cerevisiae* is important for cell growth. Proc. Natl. Acad. Sci. U. S. A. 90, 1804-1808.

Yokoyama, H., Mizunuma, M., Okamoto, M., Yamamoto, J., Hirata, D., Miyakawa, T., 2006. Involvement of calcineurin-dependent degradation of Yap1p in Ca^{2+}-induced G2 cell-cycle regulation in *Saccharomyces cerevisiae*. EMBO Rep. 7, 519-524.

Yoshimoto, H., Saltsman, K., Gasch, A.P., Li, H.X., Ogawa, N., Botstein, D., Brown, P.O., Cyert, M.S., 2002. Genome-wide analysis of gene expression regulated by the calcineurin/Crz1p signalling pathway in *Saccharomyces cerevisiae*. J. Biol. Chem. 277, 31079-31088.

Yoshimura, H., Tada, T., Iida, H., 2004. Subcellular localization and oligomeric structure of the yeast putative stretch-activated Ca^{2+} channel component Mid1. Exp. Cell Res. 293, 185-195.

Zelter, A. Quantitative Measurement of the Calcium Signature in Living Hyphae of *Neurospora crassa*, and a Genomic Analysis of Calcium Signalling Machinery in Filamentous Fungi. PhD Thesis, University of Edinburgh. 2004.

Zelter, A., Bencina, M., Bowman, B.J., Yarden, O., Read, N.D., 2004. A comparative genomic analysis of the calcium signalling machinery in *Neurospora crassa*, *Magnaporthe grisea*, and *Saccharomyces cerevisiae*. Fun. Genet. Biol. 41, 827-841.

Zhang, J.H., Chung, T.D., Oldenburg, K.R., 1999. A Simple Statistical Parameter for Use in Evaluation and Validation of High Throughput Screening Assays. J. Biomol. Screen. 4, 67-73.

Zhou, X.L., Batiza, A.F., Loukin, S.H., Palmer, C.P., Kung, C., Saimi, Y., 2003. The transient receptor potential channel on the yeast vacuole is mechanosensitive. Proc. Natl. Acad. Sci. U.S.A. 100, 7105-7110.

Ziegelbauer, K., Grusdat, G., Schade, A., Paffhausen, W., 1999. High throughput assay to detect compounds that enhance the proton permeability of *Candida albicans* membranes. Biosci. Biotechnol. Biochem. 63, 1246-1252.